Master Thesis in Geosciences

Delta-influenced Palaeogene depositional environments of the Frysjaodden and Hollendardalen formations in central Spitsbergen

Denise Christina Rüther

UNIVERSITY OF OSLO

FACULTY OF MATHEMATICS AND NATURAL SCIENCES

Delta-influenced Palaeogene depositional environments of the Frysjaodden and Hollendardalen formations in central Spitsbergen

Denise Christina Rüther

Master Thesis in Geosciences

Discipline: Environmental Geology and Geohazards

Department of Geosciences

Faculty of Mathematics and Natural Sciences

UNIVERSITY OF OSLO

November 30th, 2007

ABSTRACT

In this study of the Central Spitsbergen Palaeogene, depositional environments and transgressive-regressive developments of the Frysjaodden and Hollendardalen formations have been reconstructed with combined evidence from sedimentary field data, geochemical parameters, and detailed analyses of benthic foraminifera.

The Palaeogene succession referred to here has been deposited during the formation of a foreland basin in connection to the West Spitsbergen Orogeny. Identified lithofacies include shelf deposits of Marstranderbreen Member, followed by the progradational Hollendardalen Formation consisting of offshore transition to shoreface, foreshore, coastal marsh deposits, and transgressive sands as well as shelf deposits of the basal Gilsonryggen Member. Distal and proximal prodelta settings in Marstranderbreen shales, lagoonal deposits in upper Hollendardalen Formation and prodelta shelf deposits in basal Gilsonryggen Member could be distinguished based on biofacies analysis. The foraminiferal assemblages are entirely agglutinated and show low diversities. Their divergence from normal marine assemblages are explained partly by the regional effects of the Boreal realm, and partly by local effects of delta influence.

The lowermost part of the succession consists of retrogradational parasequences, and maximum flooding occurs in the upper third of Marstranderbreen Member. The subsequent regressive development of Hollendardalen Formation is accompanied by a short parasequential episode. The coal bearing coastal marsh deposits are interpreted as the maximum regressive surfaces, while overlying transgressive sands indicate another parasequence during general relative sea level rise. Furthermore, this study locates the interval of maximum flooding in the basal Gilsonryggen Member shales.

Keywords: Palaeogene, Svalbard, lithofacies, biofacies, benthic foraminifera

TABLE OF CONTENT

1 INTRODUCTION

This master study forms part of the Worldwide Universities Network (WUN) initiative Paleo Arctic Climates& Environments (pACE) where teams from seven different Universities work together in analysing the Palaeocene and Eocene of Svalbard from outcrop and well material. The objective of pACE is to develop a more thorough understanding of the Palaeogene transition from a greenhouse to an icehouse state of the Earth. Of particular interest is the Palaeocene/Eocene Thermal Maximum (PETM) – seemingly one of the most prominent and abrupt climate anomalies in Earth's history.

As part of the pACE interdisciplinary group the University of Oslo participants focus on sedimentological, stratigraphical, mineralogical and micropalaeontological analysis of the prodelta to delta top facies which are represented by the Frysjaodden and Hollendardalen formations.

This master thesis draws upon sedimentological as well as micropalaeontological evidence in order to reconstruct the depositional environments of the succession exposed in onshore sections in Central Spitsbergen. Associated field work took place in August 2007 in the context of a pACE exploratory field trip to localities around Longyearbyen, Svalbard. Detailed sedimentological field logs from outcrop have been realised jointly with master student Florin Burca. Besides the field logs, parameters like boron, total organic carbon (TOC), and calcium carbonate content form the basis of our studies. Florin Burca's thesis, to be handed in June 2008, will additionally focus on the mineralogy of the studied succession. The fundamental part of this master thesis is the analyses of benthic foraminiferal assemblages which support and complement environmental reconstructions based on the sedimentology.

With respect to the context of this master project, the theoretical part includes literature reviews on the geological as well as the climatic background of the Svalbard Palaeogene. Results are presented in two seperate chapters on the sedimentary and geochemical stratigraphy as well as the foraminiferal stratigraphy. In the chapter depositional environments evidence from all employed methods is drawn upon in order to interpret litho- and biofacies and transgressive-regressive developments, while the conclusions underline the most important interpretations.

2 GEOLOGICAL BACKGROUND

The studied section is located within the Palaeogene Central Basin succession of Spitsbergen and belongs to the Van Mijenfjorden Group. This chapter aims at placing the particular locality in a broader geological framework through referring to the general Tertiary Lithostratigraphy (chapter 2.1), to stratigraphic subdivisions of the Van Mijenfjorden Group (chapter 2.2), and associated age determinations (chapter 2.3). The focus will further rest upon the Van Mijenfjorden Group deposits through summaries of their palaeotectonic regime (chapter 2.4), environmental and sequence stratigraphic interpretations (chapter 2.5) and suggested depositional models (chapter 2.6).

2.1 LITHOSTRATIGRAPHIC SETTING OF THE STUDIED SUCCESSION IN THE SPITSBERGEN TERTIARY

According to Dallmann et al. (1999) the deposition of the Tertiary succession of Svalbard is confined to several basins (columns in Figure 2-1). One igneous rock formation and a poorly age-constrained formation are also amongst the described Tertiary rocks:

(1) Central Tertiary Basin/ Palaeogene Central Basin

The largest and most prominent basin developed during the Palaeogene, referred to as Central Tertiary Basin by Dallmann et al. (1999) will be denoted Palaeogene Central Basin hereafter. The Central Basin comprises seven formations which are grouped under the name Van Mijenfjorden Group. Large areas of southern and central Spitsbergen including the studied sedimentary succession, encompassing Palaeocene to Eocene age belong to this group deposited in connection with the West Spitsbergen Orogeny. The Ny-Ålesund Subgroup from the Kongsfjorden area in northwestern Spitsbergen has with great probability been correlated with Central Basin strata and has been included in the Van Mijenfjorden Group.

(2) Forlandsundet Graben

Eocene to Oligocene strata of a separate basin is found on western Spitsbergen and Prins Karls Forland which has been deposited over an older, syn-depositional structure. Due to the usage of Forlandsundet as expression for the post-sedimentary graben-structure, this group is named Buchananisen Group.

(3) Bellsund

Two formations preserved in the Renardodden area at Bellsund, southwestern

Spitsbergen, form the Calypsostranda Group. A connection of this depositional basin with the Buchananisen Group is believed to be likely.

(4) Igneous rocks on northern Spitsbergen

The Seidfjellet Formation contains Miocene to Pliocene volcanic flow deposits that occur on mountain tops of northern Spitsbergen, but are not assigned to any stratigraphic group.

(5) Conglomerate on northwestern Prins Karls Forland

The age question for the Sutorfjella conglomerate on northwestern Prins Karls Forland is not solved yet, and ages from Precambrian over Devonian to Tertiary are possible. It is therefore not included in any superior lithostratigraphic unit.

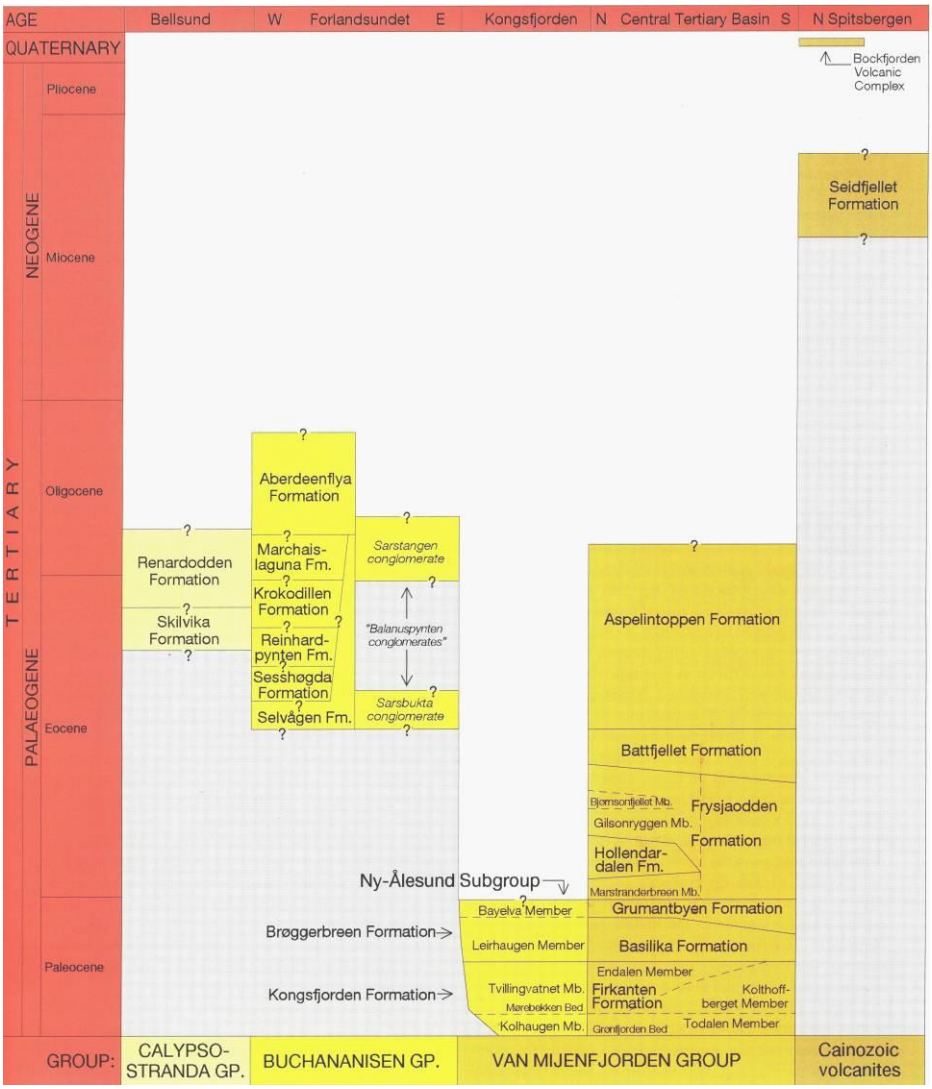

Figure 2-1: Lithostratigraphic scheme for the Tertiary of Svalbard as proposed by Dallmann et al. (1999); member and bed names in italics represent informal units.

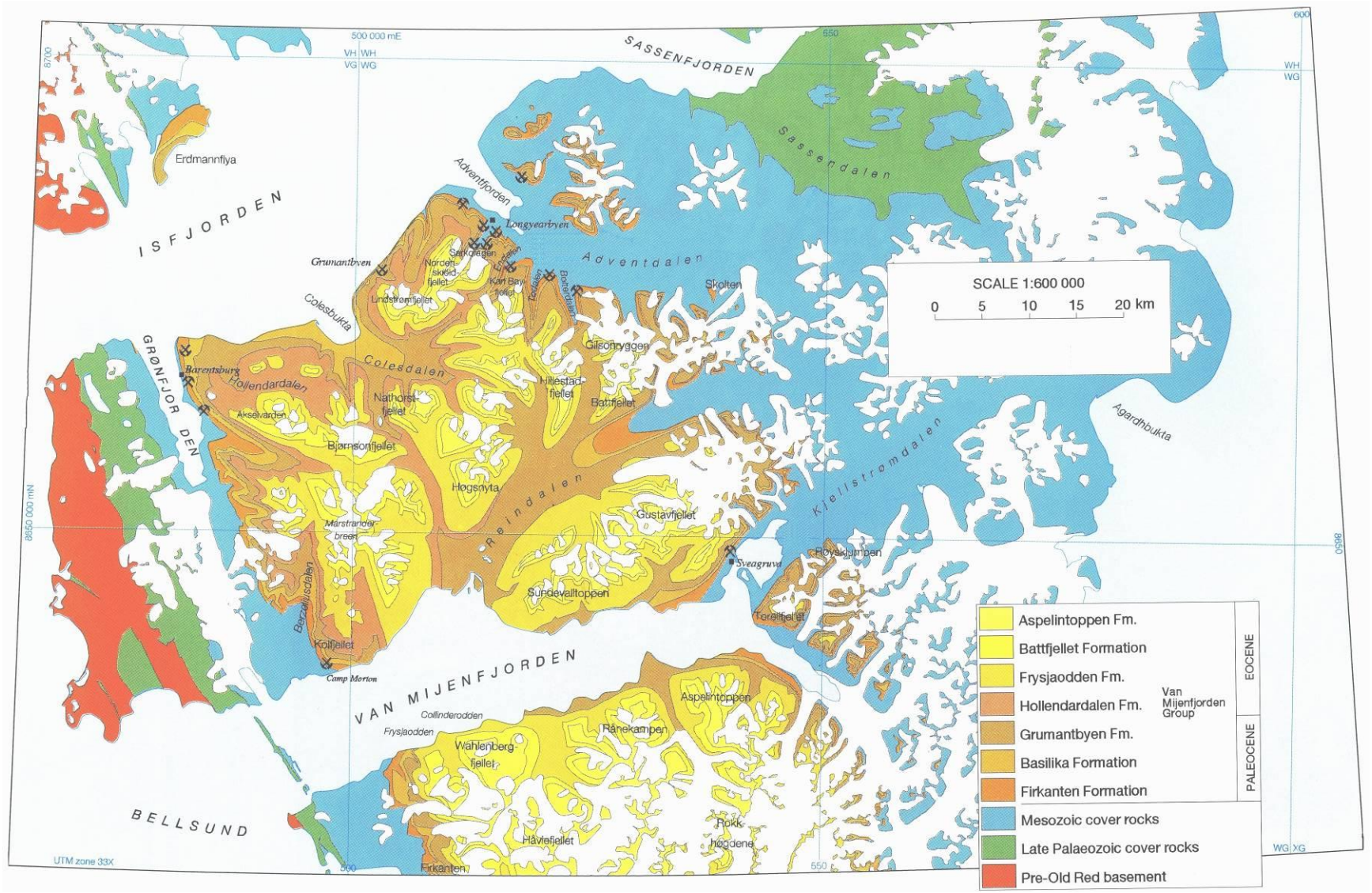

Figure 2-2 : Distribution of rock units in the northern part of the Palaeogene Central Basin. Modified from Dallmann et al. (1999).

2.2 STRATIGRAPHIC SUBDIVISIONS OF THE VAN MIJENFJORDEN GROUP

In their revision of the nomenclature of the Svalbard Tertiary Dallmann et al. (1999) propose the usage of the Norwegian scheme in the lower (Firkanten Formation, Basilika Formation) and upper parts (Battfjellet Formation, Aspelintoppen Formation), and of the Russian scheme in the middle part (Grumantbyen Formation, Hollendardalen Formation, Frysjaodden Formation) due to de facto contemporary publishing of stratigraphic subdivisions by Major and Nagy (1964; 1972) and Livšic (1967; 1974). The alternations of shale and sandstone dominance are reflected in these formational subdivisions of the Palaeogene Central Basin (see Figure 2-2 for geographic distribution of present day exposure).

The sedimentary section studied by our project encompasses clastic basin infill from the uppermost Grumantbyen Formation (sandstones), overlain by Marstranderbreen Member shales (of the Frysjaodden Formation), Hollendardalen Formation sandstone wedge and the lowermost Gilsonryggen Member shales (of the Frysjaodden Formation).

2.3 AGE DETERMINATION FOR THE VAN MIJENFJORDEN GROUP

The age relationships in the group are to the present still not entirely resolved, however, the contribution by Manum and Throndsen (1986) was the benchmark for the last decades. Application of biostratigraphy is restricted by seemingly low fossil content and poor preservation. Out of hundreds of processed samples only few have yielded diagnostic palynomorphs in Manum and Throndsen's work. In addition to restrictions with respect to productivity and preservation, the Palaeogene palaeogeographic configuration (Figure 2-3) hampered water circulation between the open Atlantic and Arctic Ocean (Podobina 2000). Therefore, biostratigraphic correlations with

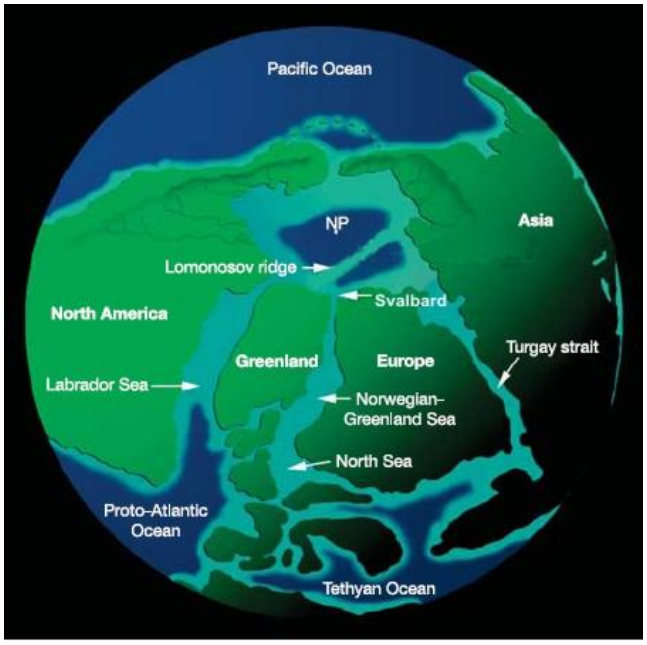

Figure 2-3: Palaeogeographic configuration of the Arctic Ocean in the late Palaeocene – early Eocene.

Modified from Sluijs et al. (2006).

assemblages from lower latitude have been found unreliable. In Svalbard's Palaeogene deposits only agglutinated benthic foraminifera are present, and Nagy (2005) has found that assemblages of the Todalen and Kolthoffberget Members are closely related to Palaeocene faunas described from the Beaufort-Mackenzie Basin in the Canadian Arctic by Mc Neil (1997), which supports a Palaeocene age of the Firkanten Formation.

Questions arose particularly on the exact position of the Palaeocene to Eocene boundary. Unpublished work by Harding et al. (2007) has now established this boundary on the basis of $\delta^{13}C_{org}$ excursion which is argued to represent the Palaeocene Eocene Thermal Maximum (PETM) and is located in the lowermost Gilsonryggen Member shales.

2.4 TECTONIC SETTING AND LOCAL TECTONIC REGIME

The currently accepted tectonic interpretation for the Palaeogene Central Basin has been developed by Steel et al. (1981) and Steel et al. (1985). The inferred shift of sediment influx from the east (Firkanten, Basilika and Grumantbyen formations) to influx from the west (Frysjaodden, Hollendardalen, Battfjellet and Aspelintoppen formations) has been interpreted as the onset of major western uplift which went hand in hand with a change from transtensional to transpressional regime along the sheared Western Spitsbergen margin (Steel et al. 1981).

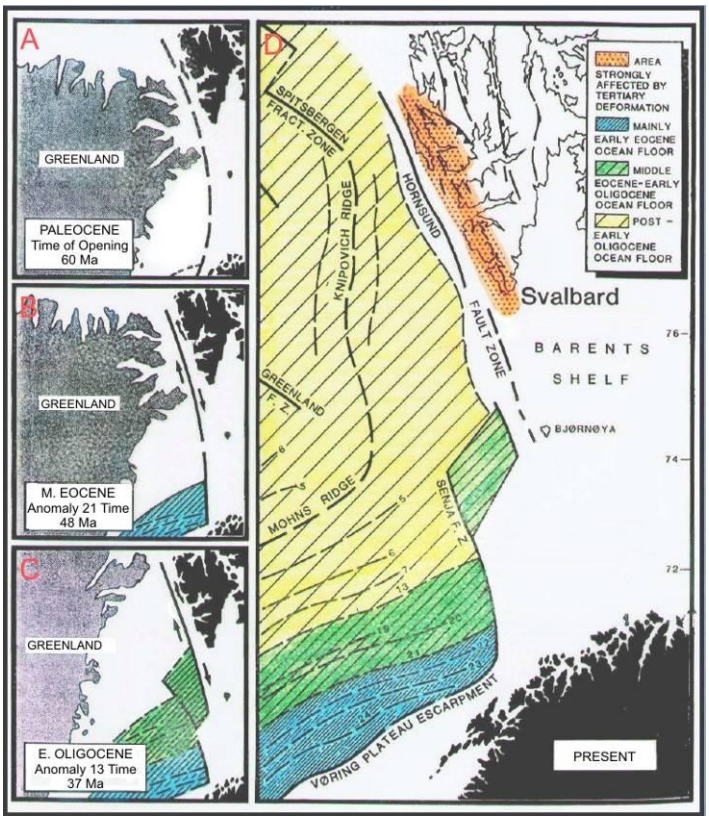

Figure 2-4 A-C: Stages of Tertiary displacement of Svalbard from Greenland during the opening of the Norwegian-Greenland Sea, and
D: present-day map of ocean floor generated by seafloor spreading.

Modified from Steel et al. (1985).

This interpretation also rests upon offshore evidence for a change in tectonic regime during the opening of the Norwegian-Greenland Sea and separation of Greenland from Eurasia. Beginning around 58Myrs before present, the first tectonic phase involved north-northwesterly rotation of Greenland along an inferred transform boundary (De Geer Line or De Geer–Hornsund Line; Figure 2-4A). Around 37Myrs ago the onset of a second tectonic phase is marked by the change of the pole of motion which resulted in west-northwesterly directed relative plate movement (Figure 2-4C). The associated plate boundary has been named Hornsund fault zone and is thought to be located at or near the continent-ocean boundary west of Spitsbergen (Steel et al. 1985).

The late Palaeocene to early Oligocene strike-slip regime and early Oligocene to Recent rift regime off western Svalbard have been accompanied by distinct sequences of sea-floor spreading progressively farther north of the Northern Norwegian coastline (Figure 2-4D). According to Steel et al. (1981; 1985) this shift in the tectonic regime of the Norwegian-Greenland Sea is reflected in the Palaeocene transtensional and Eocene transpressional phases of the Palaeogene Central Basin.

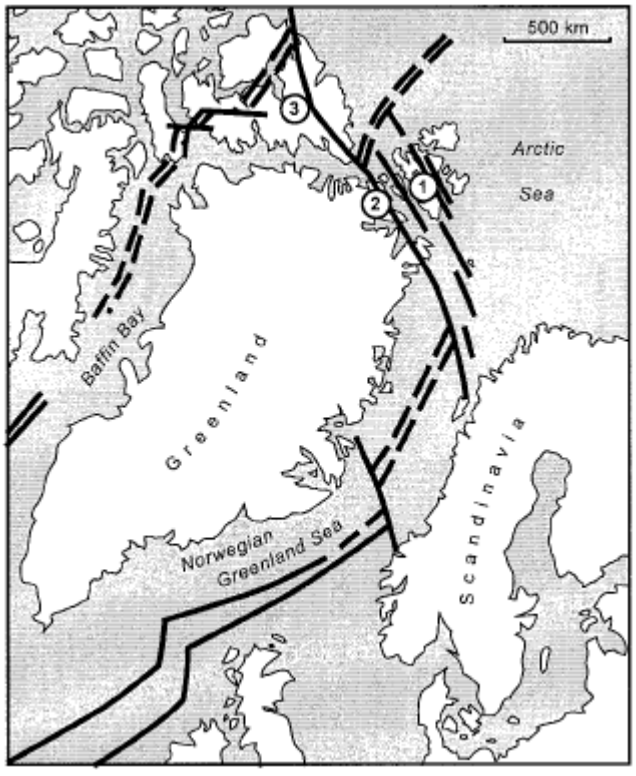

Figure 2-5: Palaeogeographic and palaeotectonic reconstruction in Late Cretaceous to earliest Palaeocene (Bruhn and Steel 2003):

"1. Spitsbergen. 2. Wandel Hav Strike-Slip Mobile Belt. 3. Ellesmere Island.
The De Geer Zone is the somewhat poorly constrained zone of strike-slip faults between Spitsbergen and Greenland"

Based on recent ocean-floor spreading models, tectonic evidence from the Western Spitsbergen Orogeny and sedimentary evidence from Palaeogene Central Basin successions, Bruhn and Steel (2003) present an alternative depositional model. According to the authors the change in sedimentary influx from east to west accounts for a shift from peripheral bulge

derived to thrust belt derived sediment supply occurring during the deposition of an eastward-migrating foreland basin. These two competing depositional models will be introduced in chapter 2.6.

Recent work on Norwegian-Greenland Sea and Arctic Sea plate tectonics yielded better time constraints and a more detailed palaeogeographic picture (see also Figure 2-5). The De Geer Zone, notably a complex transfer zone, is believed to have been active in Late Cretaceous and Palaeocene times while sea-floor spreading set in in the Oligocene (Bruhn and Steel 2003). The main plate-bounding fault migrated eastwards from the Wandel Hav Strike-Slip Mobile Belt in North Greenland towards Svalbard (Håkansson and Pedersen 2001).

Likewise recent tectonic evidence on the West Spitsbergen Orogeny confirm former findings, but render a more detailed picture and better time constraints on different tectonic phases (Bruhn and Steel 2003):

(1) onset of the initial thrust phase in the Late Cretaceous or early Palaeocene,
(2) element of coupled strike slip during earliest Palaeocene with east-west trending faults,
(3) main deformation phase (orogen-normal contraction with local orogen-parallel strike slip zones) in latest Palaeocene to Eocene age,
(4) late stage deformation of local orogen-parallel normal faults in latest Eocene to Oligocene, and
(5) onset of sea-floor spreading between Norway and Greenland in the Oligocene associated with ongoing regional uplift and erosion of Spitsbergen.

2.5 ENVIRONMENTAL AND SEQUENCE STRATIGRAPHIC INTERPRETATIONS OF THE VAN MIJENFJORDEN GROUP

The present distribution of sediment outcrop associated with the Palaeogene Central Basin of Spitsbergen renders an idea on the basin's size of approximately 200km length and 60km width, which can therefore be considered a sedimentary basin of smaller scale (Figure 2-6).

The present thickness of the Palaeocene to early Eocene clastic deposits of the Van Mijenfjorden Group varies from 1500m north to 2500m south of Van Mijenfjorden. The varying thickness presumably reflects the predominant sediment influx from north and northeast and the maximum downwarp of the basin to the south of Van Mijenfjorden (Steel et al. 1981). Vitrinite reflection analysis by Manum and Throndsen (1978) suggests that an

additional approximate thickness of 1700m of Eocene to Oligocene strata have been removed by erosion.

The Van Mijenfjorden Group rests on a regional unconformity which is developed across the northwest Barents Shelf. The corresponding hiatus encompasses the Late Cretaceous and increases northwards. Bruhn and Steel (2003) argue that regional uplift (thermal doming in northern Svalbard) during Late Cretaceous is in part responsible for the erosion. They stress the importance of the initial foreland basin peripheral-bulge formation in the creation of the unconformity. According to the authors the northerly source of sediment transport is only inferred for the lowermost Palaeocene basin-fill, which indicates that northern Spitsbergen may have been an elevated area in the Late Cretaceous, but not necessarily throughout the Palaeocene.

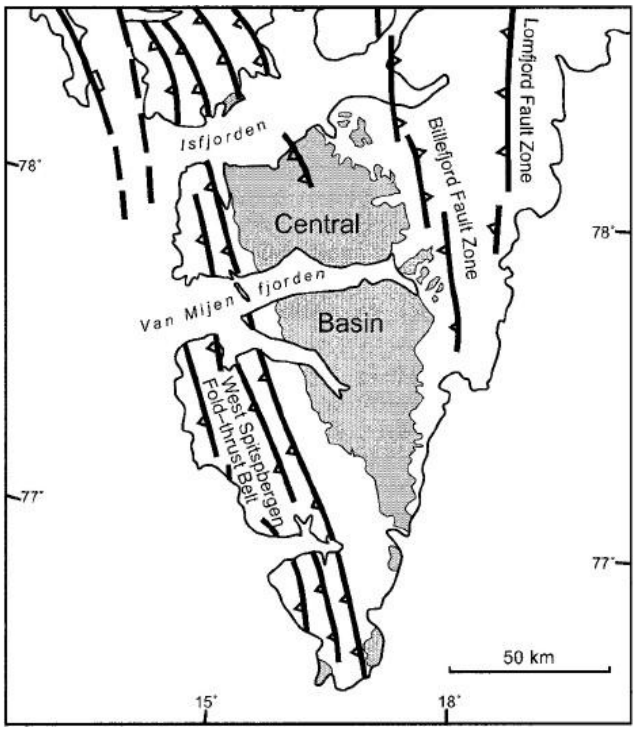

Figure 2-6: Map of south-western Spitsbergen, showing present day outcrop of the Palaeogene Central Basin in grey (Bruhn and Steel 2003).

Sedimentological and stratigraphic interpretations initially focused on the lowermost coal bearing Firkanten Formation, which is the most-studied part of the Svalbard Tertiary (e.g. Manum and Throndsen 1978b; 1978a; Nagy 2005). Lately sedimentological work has had a tendency to be centred on the uppermost formations: Frysjaodden to Aspelintoppen formations in Helland-Hansen (1990), Battfjellet in Mellere et al. (2002); Plink-Björklund and Steel (2004) and Aspelintoppen in Plink-Björklund (2005). To the present no detailed sedimentological interpretation has been published for the Hollendardalen Formation sand wedges.

The first interpretation of the entire Palaeogene Central Basin in transgressive-regressive terms was presented by Steel et al. (1981), based on correlated and measured sections both normal (in Adventdalen) as well as parallel to the West Spitsbergen Orogen (in the

easternmost part of the basin). The resulting stratigraphic model divided the Palaeogene succession in:

- Firkanten Formation and Basilika Formation: overall transgressive phase of basin infilling (consisting of up to 10 regressive cycles),
- Grumantbyen Formation and Hollendardalen Formation: regressive phase of basin infilling (notably derived from two different margins), and
- Gilsonryggen Formation [Gilsonryggen Member of the Frysjaodden Formation in Dallmann et al. (1999)], Battfjellet Formation, and Aspelintoppen Formation: second regressive phase of basin infilling following an initial non-accretionary transgression

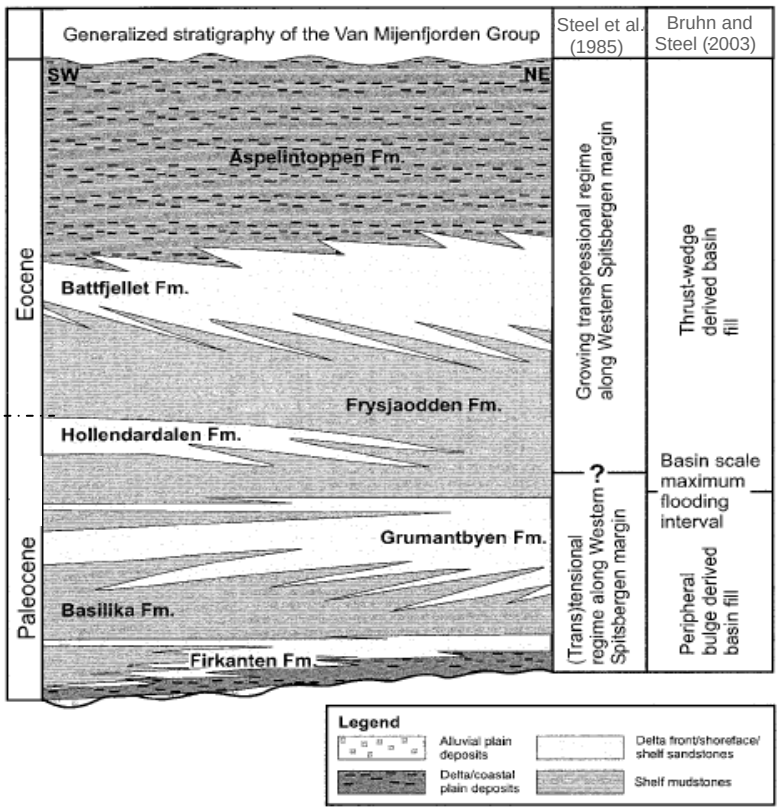

Figure 2-7: Palaeogene stratigraphy coupled with a comparison of the tectonic interpretation of Steel et al. (1985) and revised tectonic interpretations of Bruhn and Steel (2003). Modified from Bruhn and Steel (2003).

The more recent paper by Bruhn and Steel (2003) suggests an alternative depositional model for the Palaeogene Central Basin based on more recent plate tectonic constraints and in particular additional sedimentary field data from the Central Basin (see also chapter 2.6). Their sequence stratigraphic interpretation differs from the earlier interpretation in the suggested large and intermediate scale stratigraphic cycles for the Palaeocene deposits. They suggest a gradual albeit irregular transgression for this large-scale unit containing two intermediate-scale transgressive-regressive cycles. According to Bruhn and Steel (2003) the

up to 700m thick, east to northeast derived Palaeocene sedimentary succession consists of the following depositional environments (see also Figure 2-7):

- Firkanten Formation: coal-bearing delta plain and paralic to shoreface deposits
- Basilika Formation: shelf mudstone
- Grumantbyen Formation: highly bioturbated sandstones

The Firkanten Formation and the Basilika-Grumantbyen formations are coarsening-upwards units and represent the intermediate-scale sequences of 3 to 7Myrs, presumably developed due to episodic thrust loading. Bruhn and Steel's (2003) high-resolution analysis of the Palaeocene sequence also reveals small-scale stratigraphic sequences. Eight coarsening-upwards trends within the Firkanten Formation supposedly represent coastal progradations with average duration of less than 1Myr, while the six small-scale sequences within Grumantbyen Formation are thought to represent roughly 500,000 years each. The authors argue that cycles of such short duration in presumably ice-free periods are poorly understood, and that these short episodes of coastal build-out might be a feature of peripheral-bulge derived successions. The assumption of the Palaeocene as an ice-free period might however have to be revised, as is demonstrated in chapter 3.

Bruhn and Steel's (2003) sequence stratigraphic interpretation corresponds to the earlier interpretation of Steel et al. (1981) in suggesting a large-scale regressive unit for the Eocene succession. The west derived Eocene clastic deposits are more than 1400m thick and comprise the following depositional environments (Bruhn and Steel 2003; Figure 2-7):

- Frysjaodden Formation: deep-water marine shale with some deep-water sand-rich turbidite intervals
- Battfjellet Formation: series of clastic wedges of mostly shoreline to shelf facies
- Aspelintoppen Formation: coastal plain deposits

2.6 DEPOSITIONAL MODELS FOR THE PALAEOGENE CENTRAL BASIN

Steel et al. (1985) based their depositional model (Figure 2-8) on presumed tectonic forcings and on earlier environmental and sequence stratigraphic findings (as presented in Steel et al. 1981). The shift in sediment input from the east to the west between Grumantbyen and Frysjaodden formations is interpreted as the onset of a transpressional regime and the associated West Spitsbergen Orogeny.

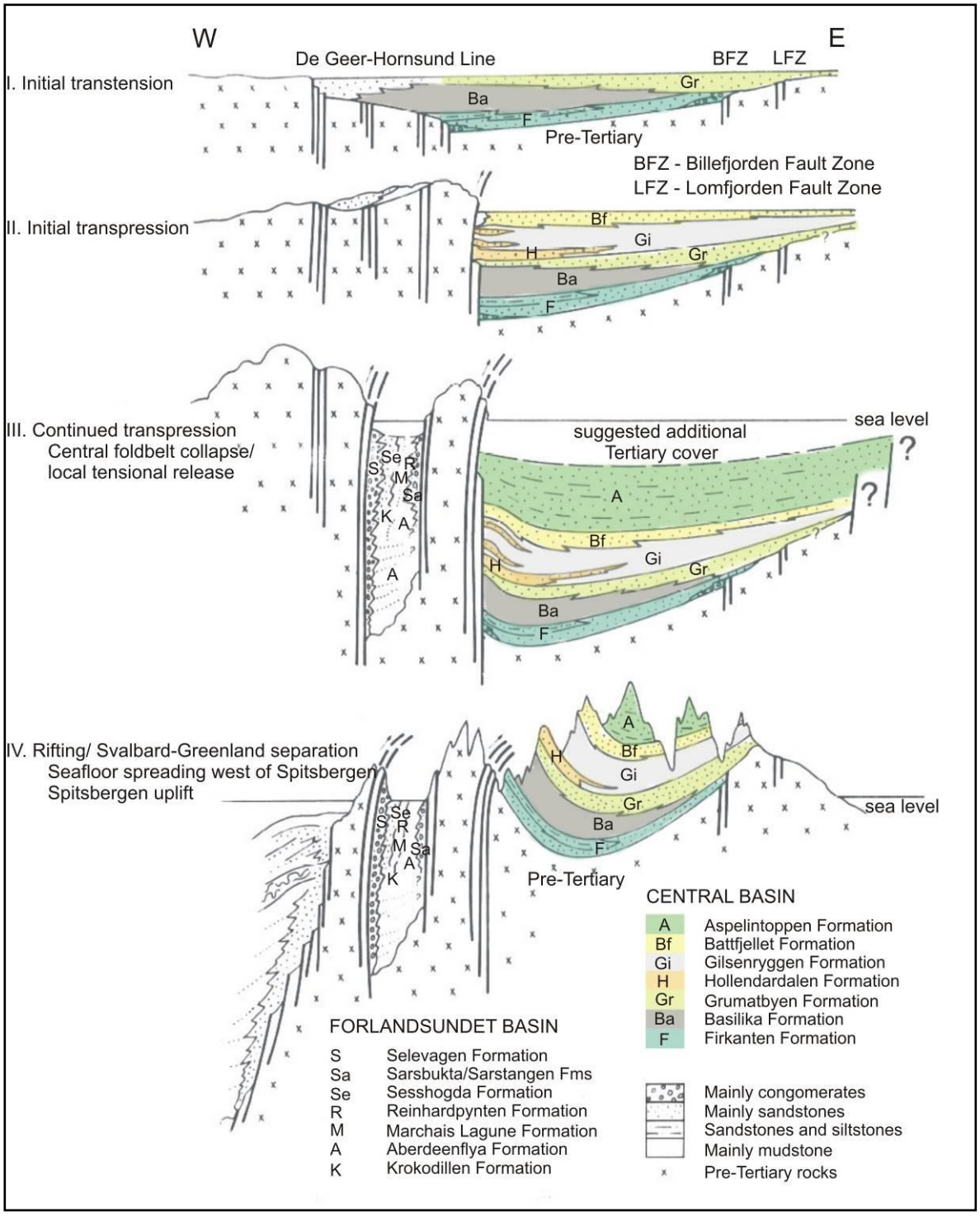

Figure 2-8: Depositional model for the Palaeogene Central Basin. Modified from Steel et al. (1985)

However Helland-Hansen (1990) and Bruhn and Steel (2003) argue that considering more recent data, there is no stratigraphic or structural evidence which might suggest a change in the tectonic setting from Palaeocene to Eocene basin-fill deposits. The drainage reversal from a west- to east-directed pattern can be explained through the eastward migration of the entire foreland basin and passage of the deepest point of the basin over the depositional

window which is preserved as outcrop today. The Palaeocene succession (with west-directed drainage) is interpreted as peripheral bulge derived and landward-stepping sequence. The shift from peripheral bulge derived to thrust belt derived influx is represented in Figure 2-9E.

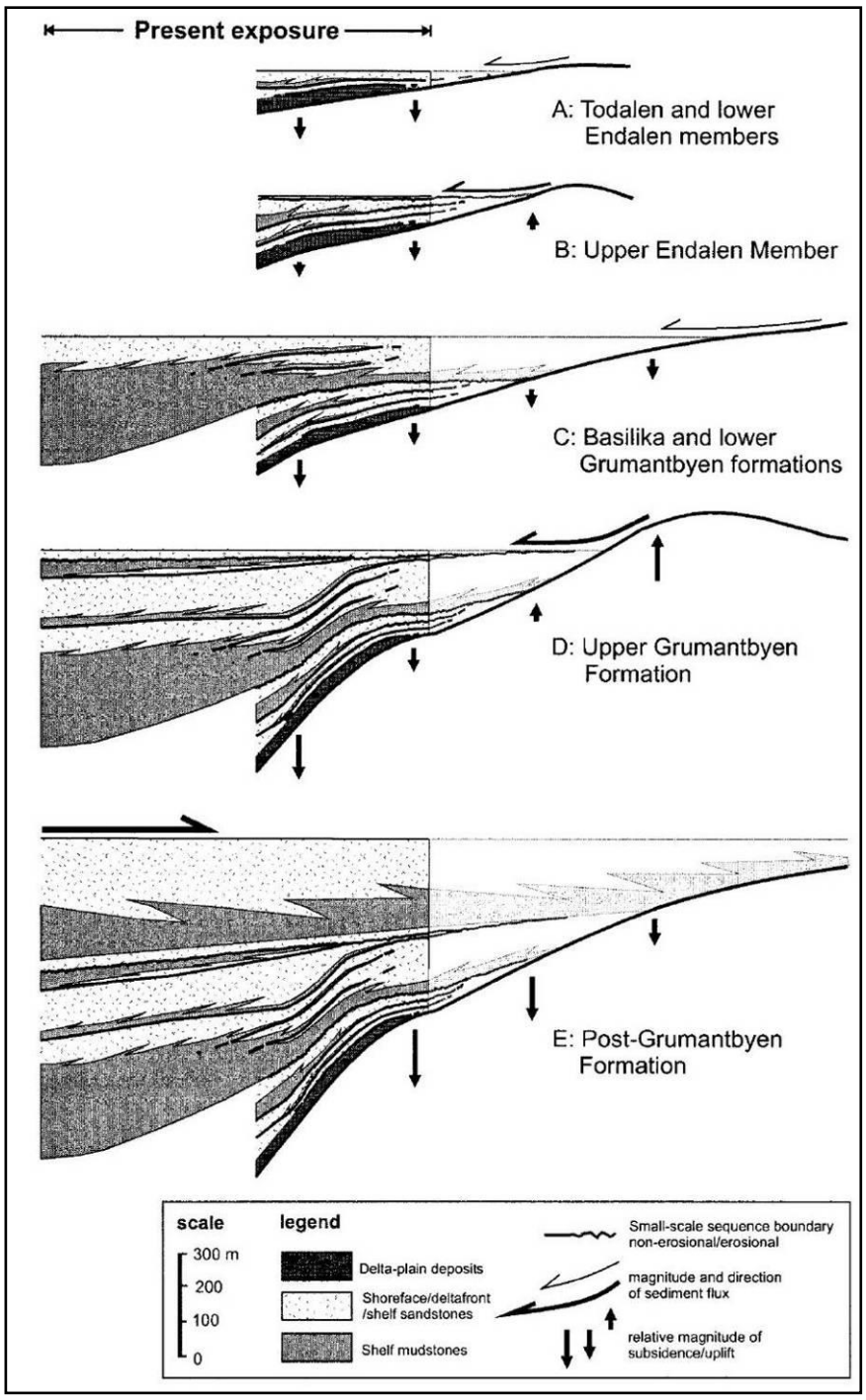

Figure 2-9: Depositional model for the Palaeogene Central Basin as suggested by Bruhn and Steel (2003)

3 CLIMATIC BACKGROUND

The major objective of the WUN group involved in the pACE initiative is to increase knowledge on climatic dynamics in the Palaeogene. The studied succession is of particular interest with respect to the understanding of the transition from a greenhouse to an icehouse state of the Earth. In this chapter the present state of research is presented by unravelling Palaeogene climate dynamics according to the geographic focus: a summary of the findings on global climate dynamics (chapter 3.1) will be followed by summaries of climate reconstructions in the Norwegian-Greenland Sea (chapter 3.2) and on Svalbard (chapter 3.3).

3.1 GLOBAL PALAEOGENE CLIMATE DYNAMICS

During the past twenty years evidence has increased to support that the Palaeogene represents a climatically highly dynamic period in Earth's history. Furthermore stable isotopes and other ocean temperature proxies unravel that this climatic history is highly complex and consists of periods of warming and cooling, taking place both gradually and suddenly (Shipboard Scientific Party 2004).

A 1Myr long global warming trend was initiated in the late Palaeocene and culminated in the early Eocene Climatic Optimum (EECO) which lasted 1 to 2Myrs. This stage comprises an extreme greenhouse interval known as Palaeocene/Eocene Thermal Maximum (PETM) at approximately 55.0Myrs ago (introduced as late Palaeocene Thermal Maximum [LPTM] by Zachos et al. 1993).

From early/middle Eocene to earliest Oligocene a 12Myrs-lasting cooling trend took place in several steps as indicated by various temperature-proxies. This stage involves the earliest Oligocene Glacial Maximum (EOGM) at approximately 33.4Myrs ago which represents the transition to permanent glacial conditions on Antarctica (Shipboard Scientific Party 2004). Therefore the transition from a greenhouse to an icehouse state of the Earth has not occurred gradually, but through a sequence of extreme transient climatic events.

Numerous hypothesises exist which aim at explaining the large-scale changes with obvious long-term significance in Palaeogene climate. To the present none of these are universally accepted, but the role of ocean gateways and circulation as well as greenhouse gas levels are thought to be key variables.

To many researchers the PETM is of particular interest because it represents one of the most prominent and abrupt climate anomalies in Earth history. Its negative carbon isotope

excursion (CIE) of 2‰-3‰ (Crouch et al. 2001) and inferred warming of sea surface temperature of as much as 5°C in the tropics and 8°C in the high latitudes (Zachos et al. 2006) demonstrate the scale of this climate anomaly. Detailed studies of the CIE suggest that $\delta^{13}C$ decreases within 20 kyrs, returning in roughly logarithmic pattern to near initial values throughout approximately 220 kyrs (Crouch et al. 2003). Therefore Crouch et al. (2003) argue that the magnitude, shape and global nature of the CIE indicate a massive injection of ^{13}C-depleted carbon into the ocean-atmosphere system. Zachos et al. (2007) quantify the rapidly released mass of ^{13}C-depleted carbon as being in the order of 2000Gt and greater. Pagani et al. (2006) further argue that the PETM may be the best ancient analogue for future anthropogenically caused increases in atmospheric CO_2 since isotopic and sedimentological data suggest that atmospheric CO_2 was the primary greenhouse gas responsible for the PETM.

Global warming as documented by the CIE induced further biological responses which include well-documented mass extinction of benthic foraminifera, turnovers in planctonic organisms, a global expansion of subtropical dinoflagellates (namely global acme of *Apectodinium*, 'PETM' peak in Figure 3-1) and the appearance of modern orders of mammals (Crouch et al. 2003; Pagani et al. 2006).

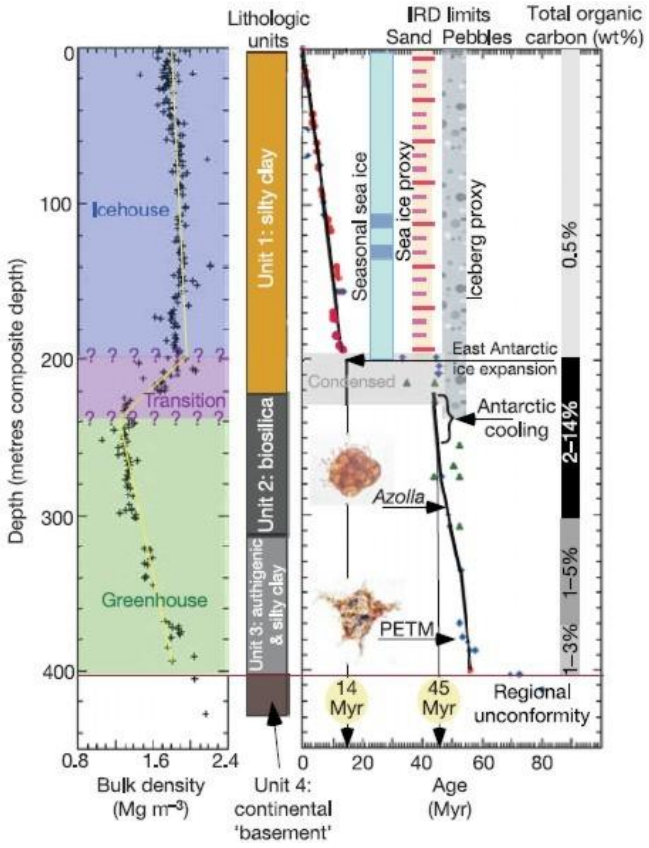

Figure 3-1: Schematic "Synthesis of the ACEX coring results [...] Age based on: palaeomagnetic stratigraphy shown as red circles; biostratigraphic data (dinocysts, blue diamonds; silicoflagellates, green triangles; and a few calcareous microfossils, squares which only occur in the upper 25m) [...] Two micrographs are shown in their stratigraphic position; the upper is *Azolla* and the lower is *Apectodinium*." (Moran et al. 2006)

Modified from Moran et al. 2006

When differentiating between ‘greenhouse’ and ‘icehouse world’ it needs to be stressed that polar ice caps may very well have been present in the greenhouse state of the Earth as well. In this context Miller et al. (2005) present evidence for global sea level changes in the Late Cretaceous to Early Eocene (99-49Myrs), which were as large (>25m) and rapid (<1Myr) that glacioeustasy is the only known mechanism that could account for their occurrence. Miller et al. (2005) demonstrate that despite general greenhouse conditions and warm high latitude surface waters ‘cold snaps’ existed and coincided with Milankovitch cycles. Ice sheets reached maximum volumes of $8\text{-}12 \cdot 10^6$ km^3 which correspond to medium size ice caps on Antarctica which did not reach the Antarctic coast (Miller et al. 2005).

3.2 PALAEOGENE CLIMATE DYNAMICS IN THE ARCTIC OCEAN AND NORWEGIAN-GREENLAND SEA

Sluijs et al. (2006), Brinkhuis et al. (2006), and Moran et al. (2006) present a Cenozoic palaeoceanographic record constructed from 400m of sediment core from the Lomonosov ridge recovered in the context of the ACEX expedition 302. Up to these publications the history of the Arctic Ocean was largely unknown from direct evidence. The Arctic Ocean is however of great significance for global climate, particularly due to extend of sea ice and involved changes in albedo as well as questions of formation of cold, dense bottom waters and their importance for global thermohaline circulation.

According to Moran et al. (2006) the greenhouse Arctic can be characterized as warm, ice-free, brackish and biologically productive environment. The typical warm water dinoflagellate genus *Apectodinium* dominates the sedimentary record during earliest Eocene (corresponding to the PETM; see also Figure 3-1). TEX_{86} analysis yielded peak PETM sea surface temperatures of above 23°C at these extremely high latitudes in the Arctic Ocean with background values of ~18°C immediately before and after the event (Sluijs et al. 2006).

At approximately 49Myrs before present the Lomonosov ridge record reveals first evidence of seasonal sea ice cover: proxies indicate fresh surface water conditions and TEX_{86} values are in the range of ~10°C. This interval marks the transition into an ‘icehouse’ Arctic. First occurrence of ice rafted debris (IRD) is recorded during middle Eocene (~45Myrs before present). A long episode of slow to non-deposition and erosion (~44 to 16Myrs before present), is followed by an interval dominated by IRD in form of dropstones and occurrence of sands extending to the Present where glacial and interglacial cycles are clearly resolvable (Moran et al. 2006).

Based on proxy data and IRD in the Nordic seas the existence of Northern Hemisphere ice sheets has been demonstrated back to middle Miocene (~15Myrs ago). New evidence hints to possible existence of ice sheets on Greenland about 20 Myrs earlier than previously documented (Figure 3-2). Beside evidence from Moran et al. (2006) presented above, Eldrett et al. (2007) demonstrate that ice rafting to the Norwegian-Greenland Sea was active during late Eocene and early Oligocene (38 to 30Myrs ago) on the basis of data from the Ocean Drilling Program site 913. The IRD is believed to originate in East Greenland and been rafted by glacial ice rather than sea ice, but whether this took place through smaller, isolated glaciers or under substantial ice-sheets remains unresolved.

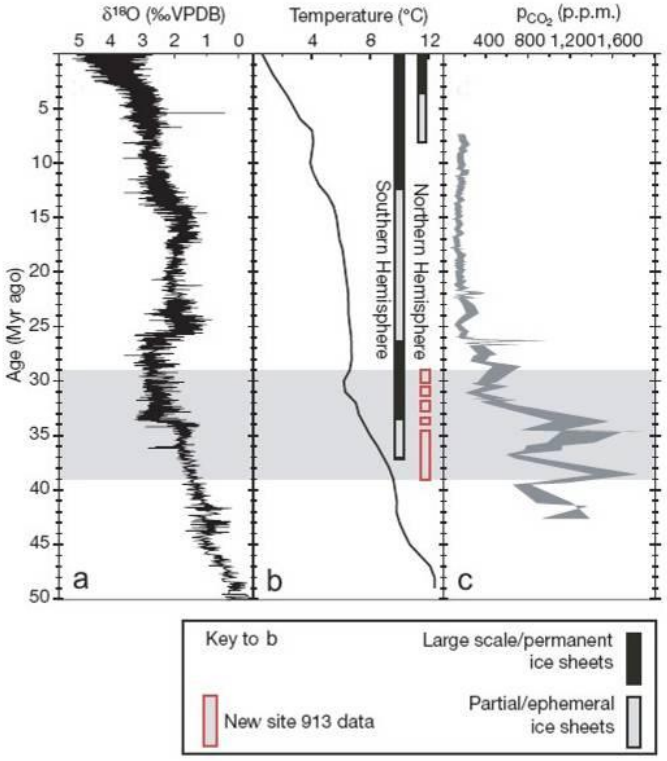

Figure 3-2: Climate Reconstruction for the past 50Myrs based on Ocean Drilling Project Leg 151, Site 913;
a: Mg/ Ca based bottom water temperatures
b: benthic $\delta^{18}O$ curve presented with generally accepted Southern and Northern Hemisphere Cenozoic glaciation
c: CO_2 partial pressure curve
Modified from Eldrett et al. (2007).

3.3 CLIMATE PROXIES IN THE PALAEOGENE OF SVALBARD

Up to the present, research with clear climatological focus on Svalbard's Tertiary is rare. In the face of further exploration of the PETM interval as well as the more general Palaeogene climate transition from greenhouse to icehouse world, possibilities on Svalbard are promising. However the application of palynomorphs and foraminifera for climate reconstruction may be limited due to seemingly low productivity and poor preservation of dynocysts and the virtually agglutinated nature of foraminiferal assemblages. Nagy (2005) summarizes the environmental conditions of the Palaeogene Central Basin of Svalbard as

being restricted with low salinities, low carbonate content, probably reduced oxygen values and generally unstable conditions. The palaeogeographic configuration of the Arctic Ocean and its marginal seas that resulted in a quasi-isolated Arctic Gulf is reflected biostratigraphically in the Boreal Realm.

Early contributions to the Palaeogene climate of Svalbard include analysis of erratic clasts occurring in Basilika to Hollendardalen Formation by Dalland (1976) and analysis of plant horizons in Firkanten and Aspelintoppen Formation by Schweitzer (1980).

Dalland (1976) differentiates in his study between clasts that are randomly scattered and those that occur in horizons with and without indications of erosional surfaces (Figure 3-3). On the basis of his observations he concludes that only shore ice is likely as a rafting agent of the clasts. With respect to climate he argues that conditions may well have been more continental than today with hot summers and cold winters which may primarily have been triggered by lack of solar radiation due to Svalbard's palaeolatitude of ~71° north during late Palaeocene. Low salinity of the Arctic Gulf in general and the Palaeogene Central Basin of Svalbard in particular may have facilitated the formation of seasonal sea ice. Dalland (1976) further draws on Early Tertiary evidence for ice caps on Antarctica to sustain the idea that in a greenhouse world climatic gradients between the equatorial and the polar regions may have been steep. He also refers to the Arctic Ocean as being a landlocked basin and argues that the opening may have resulted in relatively warmer Svalbard climates during Oligocene and Miocene despite the global cooling trend.

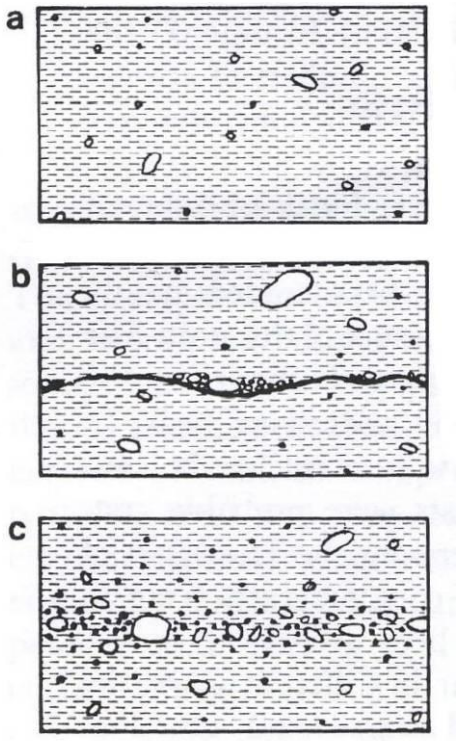

Figure 3-3: Differentiation between classes of erratic clasts in Dalland's study (1976):

a: randomly scattered erratic clasts

b: erratic clasts occurring in horizon with erosional surface and

c: erratic clasts occurring in horizon without erosional surface

In his contribution Schweitzer (1980) bases climatic reconstruction on floral assemblages. Deposition of the Palaeogene Central Basin of Svalbard has been terrestrial in the lowermost and uppermost part of the succession (Firkanten and Aspelintoppen formations) representing

Danian and Eocene times, respectively. Schweitzer (1980) summarizes that in the studied time periods a warm to temperate climate prevailed with estimated mean annual temperatures of 15 to 18°C and mentions the Chinese town of Nanchang as a modern analogue. The occurrence of the conifer genus *Glyptostrobus* even excludes the possibility of monthly isotherms lower than 0°C. In addition distinct development of growth rings in conifer woods indicate great seasonality of precipitation.

This seemingly contradictory evidence is accentuated in an unpublished paper of Harding et al. (2007) who report the occurrence of dropstones even within the interval of the PETM as indicated by a negative carbon isotope excursion of samples from Svalbard outcrop. At the same time their results point to the existence of a marked seasonal cycle with perennial sea ice induced by the darkness of the polar winter even during the most extreme greenhouse period. As has been argued by Sluijs et al. (2006) earlier estimates of arctic sea surface temperature during PETM based on TEX_{86} which were as high as 23°C may record summer temperatures in polar regions rather than average temperatures. In addition temperatures in the landlocked Palaeogene Central Basin of Svalbard may have been substantially lower, but an annual temperature gradient of more than 15°C remains difficult to imagine. This enigma only stresses the fact that further studies with climatic focus on Svalbard in particular and the Arctic in general are eligible.

4 METHODS AND MATERIAL

Several methods were used in order to reconstruct the depositional environments of Grumantbyen to upper Frysjaodden formations. The employed methods and materials from both sedimentology and micropalaeontology are described in the following chapters 4.1 through 4.9.

4.1 LOCATION OF THE STUDIED SECTION

A rough sedimentological log has already been conducted in 1997 for the purpose of positioning clay- and siltstone samples that had been collected for micropalaeontological analysis of the Palaeogene succession. Logging and sampling was conducted by Jenö Nagy at two sections Nordenskiöldfjellet 1 (N1) and Nordenskiöldfjellet 2 (N2) corresponding to two adjacent gullies, the topmost GPS positions of which yield a distance of 648m (see Figure 4-1 for their position). During field work in August 2007, sedimentary structures have been added to the existing log. According to Jenö Nagy who was present at both field work periods the section has been significantly altered by erosion and weathering during those ten years.

Figure 4-1: Topmost positions of each measured section (TOP N1, TOP N2 and TOP N3), mapped with the GPS software OziExplorer

In August 2007 a new section locality further to the south-southeast (349m from N1 and 994m from N2) has been chosen for detailed logging since its sandstone units are well exposed and preserved. The base of the measured section is situated at 228m to the east of the top and the section therefore stretches considerably along a moderate slope.

4.2 SEDIMENTOLOGICAL FIELD LOGGING

The field log has been recorded on logging sheets with millimetric column for observations of grain size and sedimentary structure. A copy of the logging sheet is included in Appendix 1. During the logging the following features were registered: bed and lamina thickness, structure, lithology, and grain size, sorting, colour, as well as intensity and orientation of fractures. Palaeoflow direction was measured if sedimentary structures allowed for it.

4.3 FACIES DESCRIPTION AND FACIES ASSOCIATIONS

Sedimentary facies were studied and identified during field logging on the basis of textures, structures, geometries, palaeo current indicators and lateral facies transition where possible. In section N3 studied in detail during field work in 2007 twelve facies have been distinguished and are presented in chapter 5.2, Table 5-1. Consecutive facies have been grouped into associations which represent specific depositional environments.

4.4 SAMPLING

From a total of 42 samples (29 at N1 and 13 at N2) collected in 1997 by Jenö Nagy, 22 were selected for a representative coverage of the upper Grumantbyen Formation to Gilsonryggen Member. Due to the purpose of conducting micropalaeontological analyses on those samples, they cover exclusively claystone and siltstone intervals of the studied succession.

Additional sandstone samples in sections N1 and N2 have been taken in August 2007, and will be analysed for mineralogical composition by Florin Burca in the context of his master thesis. In section N3, which was first-time logged in August 2007, a total of 30 samples have been taken throughout the entire thickness with the intention to achieve the most representative coverage of different lithologies, structures and textures. Due to time constraints, these samples are not included in this master thesis, but will be used by Florin Burca whose master thesis will be submitted at the end of spring semester 2008.

For the sedimentological logs and panels simplified sample IDs are being used. Short IDs for 1997 samples have the prefix ‘n’ for north, short IDs for 2007 samples the prefix ‘s’ for south (see Table 4-1 for renaming of 1997 samples and Appendix 2 for renaming of samples from both 1997 and 2007).

Table 4-1: Renaming of 1997 samples

short IDs	original IDs of 1997 samples
n1	N-1-2-97
n2	N-1-4-97
n3	N-1-5-97
n4	N-1-6-97
n5	N-1-7-97
n6	N-1-9-97
n7	N-1-11-97
n8	N-1-13-97
n9	N-1-15-97
n10	N-1-17-97
n11	N-1-19-97
n12	N-1-21-97
n13	N-1-24-97
n14	N-1-26-97
n15	N-2-2-97
n16	N-1-28-97
n17	N-2-3-97
n18	N-2-6-97
n19	N-2-8-97
n20	N-2-10-97
n21	N-2-11-97
n22	N-2-12-97

4.5 GEOCHEMICAL ANALYSES

In order to assist environmental interpretations of the studied section geochemical analyses of boron, total organic carbon, and calcium carbonate content have been conducted.

4.5.1 BORON

5g of pulverized material from each of the 22 samples has been sent to the private laboratory Actlabs in Ontario, Canada, in April 2007. According to their method description, the samples were encapsulated in a polyethylene vial and placed in a thermalized beam of neutrons produced from a nuclear reactor. Samples were then measured for prompt gamma ray at 478 KeV using a high purity GE detector. Calibration of the system is ensured by comparison to certified reference materials.

The significance of boron as an indicator of palaeosalinity is controversial (Curtis 1975; Dewis et al. 1975; Harder 1975a; 1975b). However, different authors agree on the primal dependency of boron content on the lithology since this trace element is held in the clay fraction of sediments. The clay mineralogy also plays an important role as illite (mica) contains more boron than other minerals; which implies that the source rock is of importance as well. Some authors claim that water temperature and salinity have a significant influence on the boron content in clays (Harder 1975a), whereas others rate salinity as a minor factor in determining boron content in clays (Dewis et al. 1975). In case of reworked mudstone the application of boron as a reliable palaeosalinity proxy is further limited.

4.5.2 TOTAL ORGANIC CARBON AND CALCIUM CARBONATE

Carbon analysis of the selected 22 samples has been conducted by Mufak Said Naoroz, at the University of Oslo. For this purpose he used 0.35g pulverized material from each sample and treated them with the CR-412 Carbon Analyser which is a non-dispersive infrared instrument for the determination of carbon content in a variety of materials.

In a first step samples are combusted at 1350°C, such that carbon-bearing compounds release the carbon which oxidizes to CO_2. On the basis of this sample gas the instrument determines the content of total carbon (TC) in the sample. In a second step 0.4g of pulverised sample material is treated with diluted hydrogen chloride (1:9), washed, and dried in order to remove carbonates from the sample. CR-412 measurements of the thus treated samples yield the content of total organic carbon (TOC).

Total inorganic carbon (TIC) content can be determined on the basis of measured TC and TOC content:

$$\mathrm{TIC} = \mathrm{TC} - \mathrm{TOC} \tag{1}$$

Calcium carbonate ($CaCO_3$) content is calculated based on the assumption that total inorganic carbon consists exclusively of $CaCO_3$ and that the following equation applies:

$$\mathrm{CaCO_3}(\%) = \mathrm{TIC} * \frac{\mathrm{M_W(CaCO_3)}}{\mathrm{M_W(C)}} = \mathrm{TIC} * 8.333 \tag{2}$$

where $M_W(CaCO_3)$ and $M_W(C)$ are molecular weights of calcium carbonate and carbon, respectively.

The accuracy of the CR-412 is ±1% of the measured value, since calcium carbonate content is not measured directly the standard error propagates to ±11.8%. In this study, the inaccuracy of measured TC and TOC that are drawn upon to calculate calcium carbonate content, accounts for the occurrence of negative values which are obviously an artefact of insufficient accuracy.

4.6 PREPARATION OF FORAMINIFERAL SAMPLES

Roughly 100g of each of the 22 sedimentary rock samples has been processed with the purpose of disintegrating them without damaging any of the fossil content. The disintegration procedure includes crushing of the samples to sizes of max 0.5cm^2, submerging the rock fragments in tenside and mixing with approximately the same amount of methanol. After 3 to 5days under the extractor hood and occasional stirring, the samples

have been washed and sieved through sieves of mesh widths of 63, 90, 125, and 500µm. Upon drying and weighing, it was decided that all of the samples needed a second treatment of setting in tenside solution, washing and sieving. Sieving has been accompanied by gentle rubbing of the sediments with a rubber block in the sieves from the 500 µm mesh downwards. Nevertheless two of nine selected samples (see subsequent chapter 4.7) needed even a third treatment.

4.7 PICKING AND COUNTING ROUTINES

The 90 to 125 µm and 125 to 500 µm fractions of all 22 samples were viewed in a first step. Upon this screening, four of the samples were suspected to be barren of foraminifera three had apparently very low abundance and for another two high residue content and seemingly very low abundance was established.

Nine samples were chosen for detailed analysis with the objective to get a good coverage of the entire succession and limit the work to a manageable extent. An additional criterion of sample selection was to include key intervals like the shales preceding and following a debris flow event present in upper Marstranderbreen Member.

The 90 to 125 µm and 125 to 500 µm fractions of the selected nine samples were mixed and split to manageable amounts. These were then picked entirely to avoid bias due to sorting of grains upon pouring of sediment on the petri dish. More than 200 individuals were picked from each sample. The 63 to 90 µm fraction was found unsuitable for picking, since the size of the foraminifera and foraminifera fragments did not allow reliable taxonomic identification. The identification of species was an iterative process and included consultation of studies on Boreal foraminiferal assemblages (e.g. Schröder-Adams and McNeil 1994; McNeil 1996a; 1996b; 1997; Nagy et al. 2000).

4.8 MICROPALAEONTOLOGICAL INDICES AND PRESENTATION TECHNIQUES

Once the identifications and counting of species had been completed, basic micropalaeontological calculations have been carried out with Excel. In addition the software Past for palaeontological statistics has been employed to validate results obtained for the calculation of micropalaeontological indices (for a general introduction to Past see Hammer et al. 2001).

4.8.1 ABUNDANCE

The abundance is the number of specimens occurring in a population, which is normally given as individuals per gram dry sediment for fossil assemblages. For this purpose the number of specimens in the picked fraction was extended to the total number of specimens expected in the sample and divided by the original dry weight of the sample. Abundance is determined by biological productivity of the depositional area, but is influenced by variations in sedimentation rates and possibly by diagenetic processes (Nagy 2007).

4.8.2 DOMINANCE

Species dominance in an assemblage is defined as the percentage value of the most common species in a population. When calculating the percentage for each species, foraminifera labelled as *Textulariina genus indet* were excluded from the total number of specimens in the denominator. Generally, restricted environments are reflected by high dominance of one or a few species, whereas stable environments display a more balanced distribution of species percentages (Nagy 2007).

4.8.3 DIVERSITY

One basic measure of diversity in an assemblage is the number of species in the sample.

The alpha diversity index, first described by Fisher et al. (1943), allows the comparison of samples of different size and can be determined using following equation:

$$\alpha = \frac{N\,(1-x)}{x} \tag{3}$$

where x is a constant of a value <1 and N is the size of the sample (number of specimens). Therefore the alpha index postulates a logarithmic relationship between number of specimens and number of species. Alpha values can be read out of a base graph which facilitates its application (Figure 4-2).

The Shannon-Weaver diversity index employed by Buzas and Gibson (1969) is based on the information function. It takes both the number of species and their relative frequency into account and is calculated as follows:

$$\mathrm{H(S)} = -\sum_{i=1}^{S} p_i \ln p_i \tag{4}$$

where S is the number of species and p_i is the fraction of the *i*th species. When all species in an assemblage have equal relative abundance a maximal value for H(S) is achieved.

Diversity indices generally decrease when going from normal marine to unstable or extreme environments (Nagy 2007).

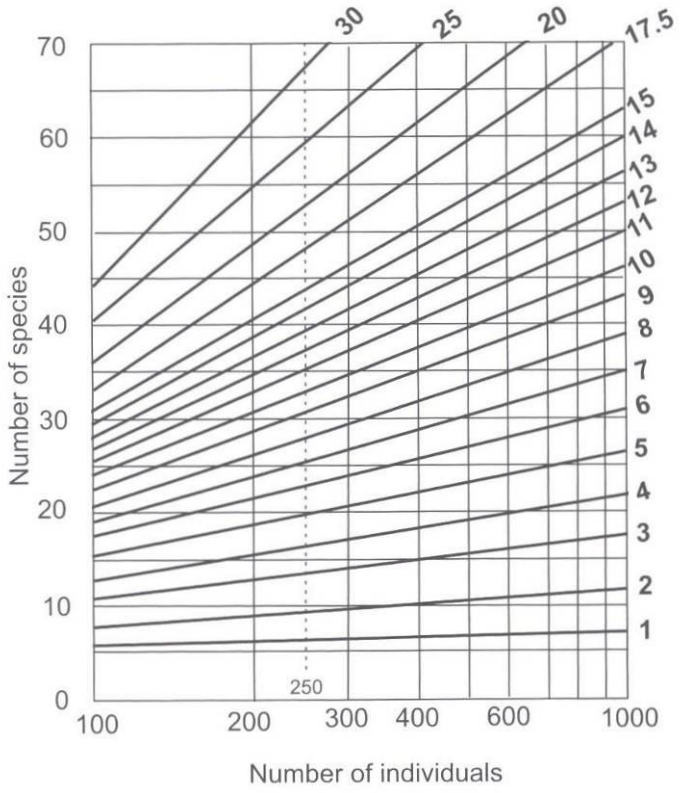

Figure 4-2: Alpha diversity base graph which is used for determination and illustration of the relation between the number of individuals and number of species in an assemblage (Murray 2006).

4.8.4 SIMILARITY

For the purpose of a pair wise comparison of assemblages (samples), Sanders (1960) defined a similarity index. The similarity or affinity between two assemblages a and b with the total number of n species is calculated using following formula:

$$A = \sum_{i=1}^{n} Min(f_{ia}, f_{ib}) \quad (5)$$

Thus for each species common to two assemblages, the lower percentage occurrence is taken and summed over all species. Theoretically the maximal value will be 100%, but in practice two samples with similarity above 80% are treated as identical (Murray 1973).

4.8.5 MORPHOGROUP ANALYSIS

Since the 1970s morphological units of foraminifera defined on the basis of wall composition and structure have been employed to recent and fossil faunas (Wright and Murray 1972; Murray 1973; Nagy et al. 1990). Since the adaptation of foraminifera to the environmental characteristics of their surroundings is reflected in their morphologies, it is possible to conclude from morphologies to depositional environments in reverse.

More sophisticated foraminiferal morphogroups were developed in the late 1970s and 1980s drawing on test morphologies and feeding habits (Chamney 1976; Severin 1983; Jones and Charnock 1985). Nagy (1992) has further elaborated the morphogroup concept and the resulting scheme is presented in Figure 4-3.

MORPHO-GROUP AND SUBGROUP		MORPHOTYPE	CHAMBERS	SUPPOSED FEEDING HABIT	SIMULATED LIFE POSITION (Deployment of pseudopodia →)	
1	1-a	Tubular	Unilocular	Primary suspension-feeder	Epifaunal elevated	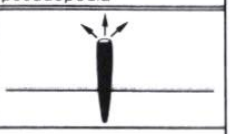
2	2-a	Globular	Unilocular	Passive deposit-feeder	Surficial	
	2-b	Planoconvex-trochospiral, Planoconvex-streptospiral	Multilocular	Active herbivore, detritivore, omnivore	Surficial	
3	3-a	Rounded-planispiral	Multilocular	Active detritivore, bacterivore, herbivore	Infaunal to surficial	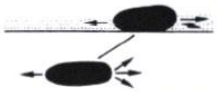
	3-b	Subcylindrical, Tapered	Multilocular	Detritivore, bacterial scavenger	Infaunal	
4	4-a	Flattened-planispiral, Irregular	Bilocular	Active to passive herbivore, detritivore	Epifaunal to phytal	
		Flattened-trochospiral	Multiloc.			
	4-b	Irregular-attached	Unilocular	Passive herbivore	Epifaunal to phytal	

Figure 4-3: Morphological units comprising morphogroups, subgroups and morphotypes, defined by their inferred feeding habits and life positions (Nagy 1992).

Nagy (1992) emphasized that application of morphological categories is principally a data reduction, having several advantages:

(1) It reduces the effect of taxonomical divergences caused by biological evolution and therefore allows reliable comparison of assemblages of different ages.
(2) Using morphogroups means reducing the number of variables, which simplifies analysis and comparison.
(3) Taxonomical determinations on species level are not required for morphogroup analysis and a lot of time can hereby be saved.

Range charts in this study are based both on species level as well as on morphogroups. Therefore the time-saving effect does not apply, but simplification of the analysis and facilitation of comparisons play an important role.

4.8.6 PHOTOGRAPHY AND GRAPHICS

The quantitatively or qualitatively more important species of the assemblages were selected and the best preserved individuals were chosen to be presented on plate. Photographs of foraminifera were taken with the help of a digital camera mounted to a light microscope. An additional x1.5 magnification objective was mounted to the binocular and it was used in the ranges of x4 to x8 magnifications. Before shooting pictures, the size of the individual was determined using the microscope grid and noting the magnification. The resulting pictures have then been further processed in Corel Photo-Paint 12 and Corel Draw 12. Moreover, this software has been used for the handling of field photographs and the creation of other graphics in this thesis.

4.9 SHORELINE TRAJECTORIES AND SEQUENCE STRATIGRAPHY

The terms transgression and regression refer to a horizontal displacement of the shoreline. The reality however is more complex, since stable relative sea level is geologically rather exceptional. The direction of the shoreline trajectory – which is the path of the shoreline viewed along a cross-sectional depositional-dip section (Helland-Hansen and Martinsen 1996) – is a function of rate of relative sea level changes, sediment supply and basin physiography.

The concept of shoreline trajectories aims at reducing the complexity of possible shoreline displacements through introducing distinct classes on the basis of a shoreline trajectories circle (Figure 4-4). The resulting classes are accretionary transgression, non-accretionary transgression, normal regression, accretionary forced regression and non-accretionary forced regression. In the case of non-accretionary episodes, accomodation is larger than sedimentation and vice-versa in the case of accretionary episodes.

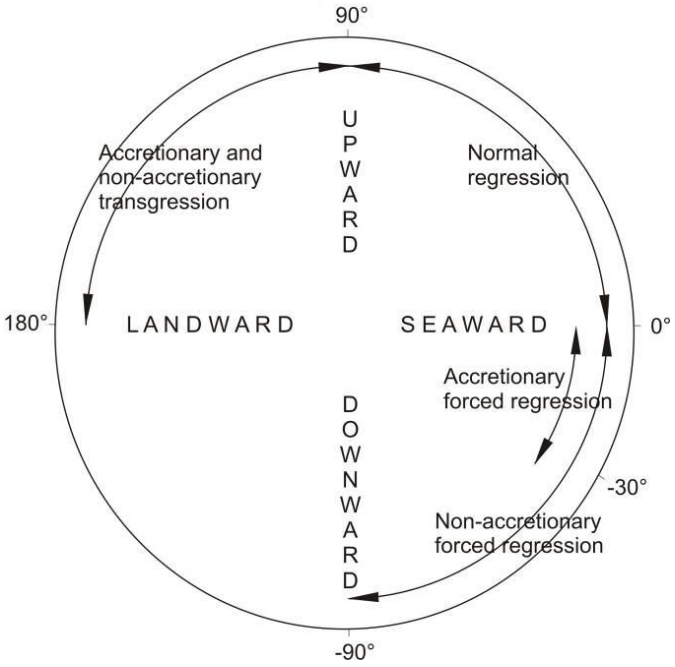

Figure 4-4: Shoreline trajectory circle indicating the ranges of shoreline displacement directions for the distinct classes (after Helland-Hansen and Martinsen 1996).

Walther's law (1893-1894; treated by Middleton 1973) states that over time sedimentary environments or facies that developed side-by-side to each other, will be stacked on top of each other due to transgression and regression. The vertical sequence of facies therefore mirrors the original lateral distribution of sedimentary environments. However during sedimentary evolution changes in relative sea level can cause hiatuses by the formation of erosional surfaces, either by subaerial erosion during relative sea level fall or ravinement surfaces during a fast relative sea level rise. Understanding these hiatuses and their bounding relations is fundamental in sequence stratigraphy.

In principle four surfaces are able to bind a depositional cycle: subaerial unconformity, ravinement -, maximum transgressive - or maximum regressive surface (Figure 4-5). Subaerial unconformity is the surface that builds out at lowest relative sea level which is continued basinwards as a correlative conformity. Due to hiatus caused by subsequent transgressions, this boundary is however seldom preserved along the entire systems tract. The lower bounding surface of transgressive systems tracts is possibly marked by a clear ravinement surface. In the absence of the subaerial unconformity this ravinement surface may be used to encompass a depositional cycle. Where no marine erosion happens during

sea level rise, the ravinement surface will merge with the underlying maximum regressive surface which overlies the lowstand wedge systems tract.

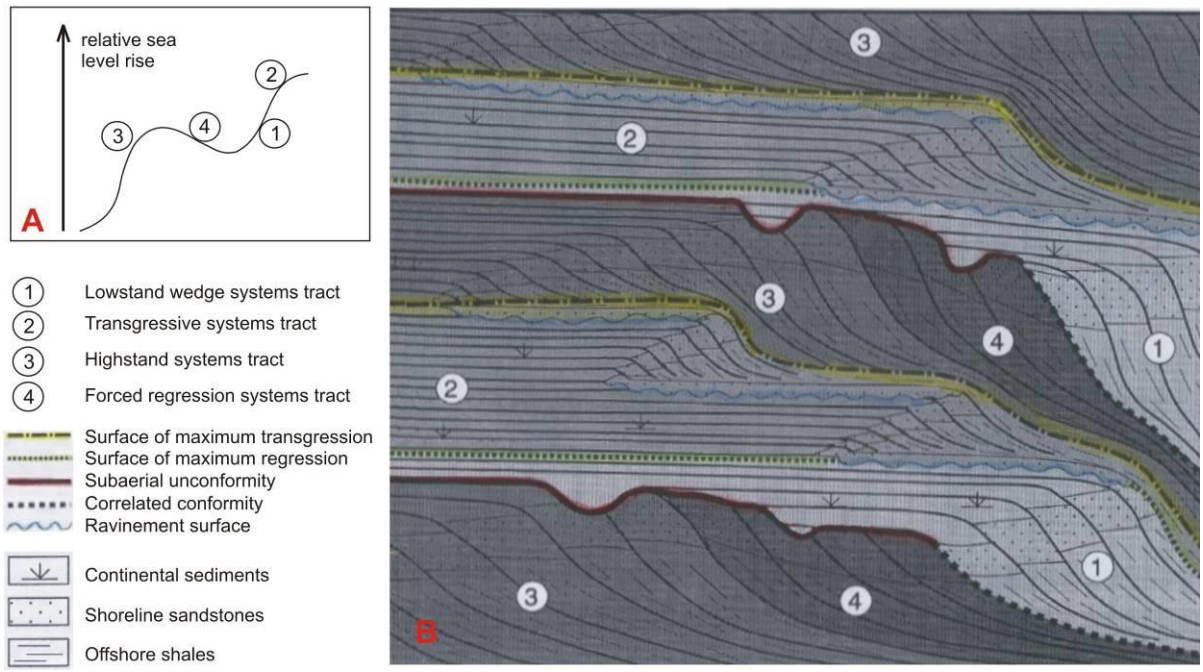

Figure 4-5 A: Relative sea level curve with the indications of corresponding systems tracts. **B:** Systems tracts and corresponding bounding surfaces. Modified from Helland-Hansen and Martinsen (1996).

In terms of preservation the maximum transgressive surface or maximum flooding surface as suggested by Galloway (1989), separating transgressive deposits below from regressive deposits above, is most applicable as boundary of a depositional cycle, particularly in basins dominated by marine deposition. Maximum transgressive or flooding surfaces are relatively easy to assess in the field, mainly by the first occurrence of marine shales. But in this study sequence stratigraphic interpretations are not only based on field logs and sedimentary parameters, but also on foraminiferal analysis. Following a multi-tool approach allows for a more exact positioning of maximum transgressive surfaces.

5 SEDIMENTARY AND GEOCHEMICAL STRATIGRAPHY

Detailed field logs have been carried out at section Nordenskiöldfjellet 3 (N3) in August 2007. At the same time the composite field logs from 1997 Nordenskiöldfjellet 1 and 2 (N1+2) were updated and supplemented with new sedimentological details (for their location see Figure 4-1). The sedimentological logs are introduced in chapter 5.1. An overview of the various facies recognised in section N3 is given in chapter 5.2 in form of a table which forms the basis of the presentation of facies associations in chapter 5.3. The characteristic facies of the resulting seven facies associations in section N3 are described in detail in chapters 5.3.1 to 5.3.7. The most important sedimentary features of sections N1+2 are described in chapter 5.4. Results from the geochemical analyses on boron, total organic carbon and calcium carbonate content which have been carried out on the 1997 samples from sections N1+2 are being presented in chapter 5.5.

5.1 SEDIMENTOLOGICAL LOGS

Presented below are two versions of the sedimentological logs. The first (Figure 5-1) is a mutual presentation of field logs from Nordenskiöldfjellet section N3 and sections N1+2. Differences in thicknesses between N3 and N1+2 of measured sections corresponding to the Marstranderbreen Member (~1.2m thicker in N3) and Hollendardalen Formation (~4m thinner in N3) are apparent. GPS coordinates from the top of each measured section yielded distances of roughly 350m between N3 and N1, and roughly 1000m between N3 and N2 (see Figure 4-1 for location on map). According to the generally accepted interpretation, Hollendardalen Formation corresponds to sand wedges derived from the Western Spitsbergen fold and thrust belt at an early point of the orogeny, consequently variations in thickness are very likely. At this point the logs are introduced, whereas detailed discussion and interpretation of the presented logs will follow in chapters 7.

The second version presented here (Figure 5-2) focuses on section N3 and includes suggested facies associations, and a zoom into Hollendardalen Formation. The numbering of facies as listed in the legend corresponds to those introduced in chapter 5.2 and treated in detail in chapter 5.3.

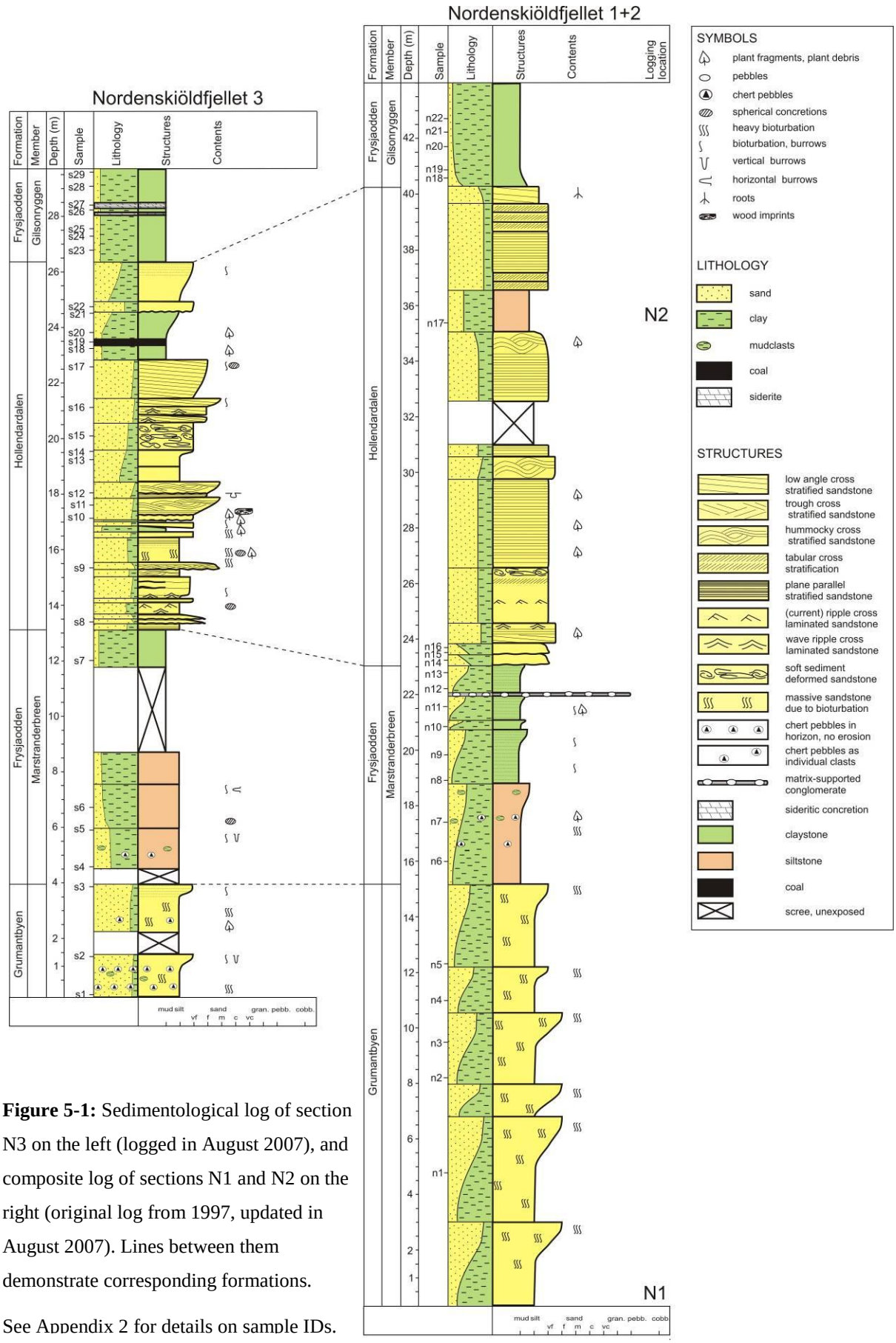

Figure 5-1: Sedimentological log of section N3 on the left (logged in August 2007), and composite log of sections N1 and N2 on the right (original log from 1997, updated in August 2007). Lines between them demonstrate corresponding formations.

See Appendix 2 for details on sample IDs.

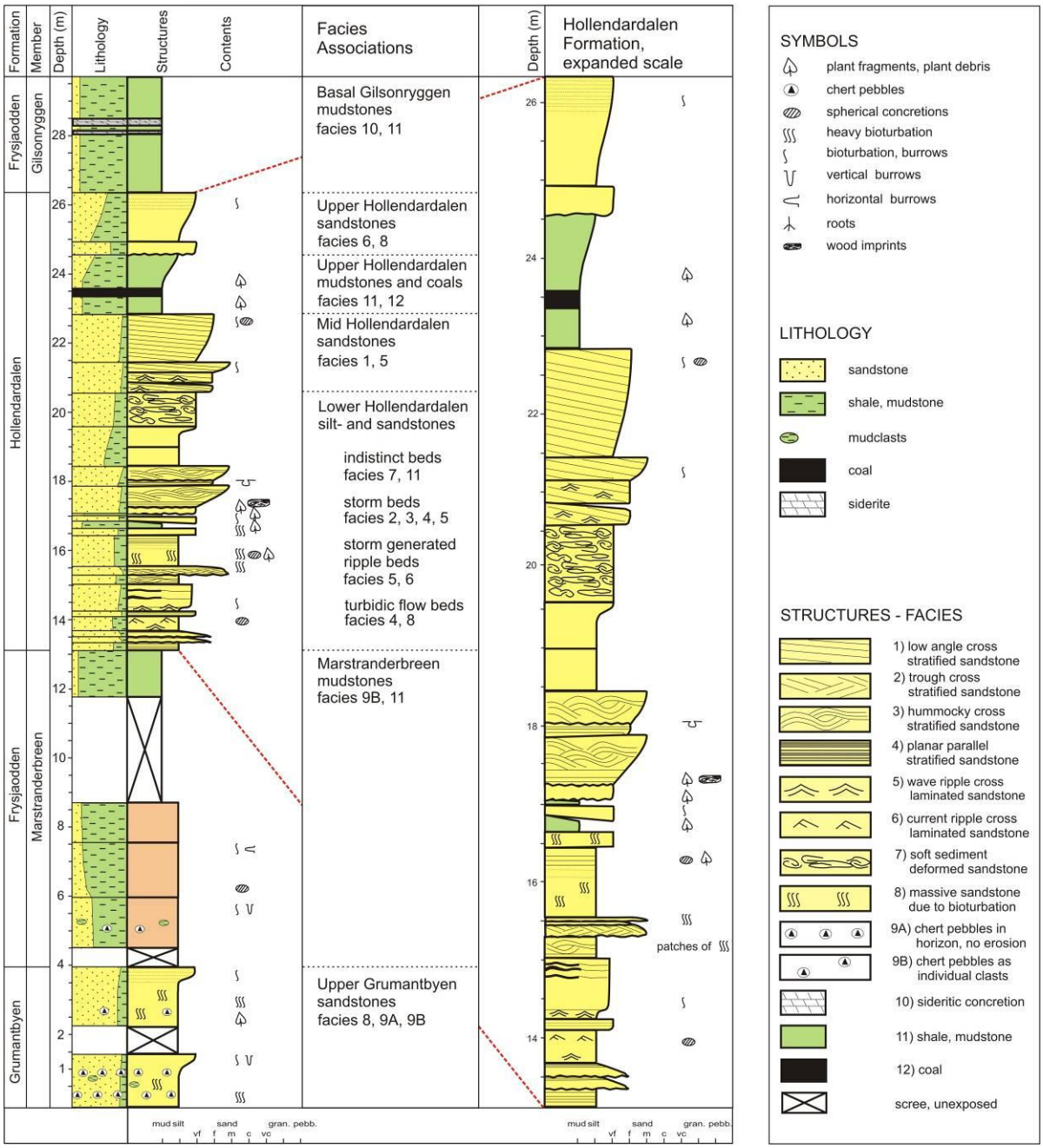

Figure 5-2: Detailed log from section N3 together with facies associations and Hollendardalen Formation in expanded scale.

5.2 FACIES DESCRIPTION OF NORDENSKIÖLDFJELLET 3

At Nordenskiöldfjellet section 3, twelve facies could be distinguished based on grain size, palaeo current measurements, physical and biological structure, bed (and lamina) thickness, and bounding relations. The facies are presented in Table 5-1, while photographs, referred to for illustration of facies, can be found in chapter 5.3.

Table 5-1 Sedimentary facies of section Nordenskiöldfjellet 3 from uppermost Grumantbyen sandstones to Gilsonryggen shale

FACIES		grain-size	palaeo-transp. towards	physical& biological structures	bed thickness	lower bounding relation	example
1.	**Low angle cross stratified sandstones**	very fine to medium sand	126°	bioturbation, spherical concretions, some ripple beds	28-140cm	conformable	Figure 5-15
2.	**Trough cross stratified sandstones**	very fine to medium sand	147°		14cm	erosional	Figure 5-9
3.	**Hummocky cross stratified sandstones (HCS)**	fine to medium sand	360°, 36°	groove casts, one storm bed rich in plant fragments, locally highly bioturbated	16-50cm	conformable, (from PPS to increasingly HCS)	Figure 5-10; Figure 5-11
4.	**Plane parallel stratified sandstones (PPS)**	silt to fine sand		poorly sorted or unsorted, sometimes organic rich	~3-16cm (indication of PPS in bed of 86cm)	erosional, amalgamation with under-lying bed	Figure 5-6
5.	**Wave ripple cross laminated sandstones**	silt to fine sand	40°; 180°	symmetrical ripples	~3-40cm	conformable	Figure 5-15
6.	**Current ripple cross laminated sandstones**	silt	76°	non-symmetrical ripples, concretions	~8cm	conformable	Figure 5-8
7.	**Soft sediment deformed sandstones**	very fine sand		large-scale bulging of sedimentary layers, convolute	100cm	conformable	Figure 5-14
8.	**Highly bioturbated sandstones**	silt to medium sand		mud clasts, chert pebbles, decreasing bioturbation towards top	3-125cm	conformable	

FACIES	grain size	palaeo-transp. towards	physical& biological structures	bed thickness	bounding relation	example
9. Chert pebbles occurring						
A. in horizon without erosional surface	medium to very coarse pebbles	320°, 360°, 352°	indication of imbrication, very rounded	~5-10cm	non-erosional	Figure 5-3
B. as individual clasts	fine to medium pebbles		very rounded	clasts: 2-5cm		Figure 5-4
10. Siderites	mud		bed forming concretions, some separate nodules	5-20cm	sharp boundary	Figure 5-18
11. Shales and mudstones	mud to silt		spherical concretions, mud clasts, burrows, sometimes rich in plant debris	1-900cm	sharp boundary	
12. Coal	mud		plant debris in mudstone below and above	20cm	sharp boundary	Figure 5-16; Figure 5-17

5.3 FACIES ASSOCIATIONS OF NORDENSKIÖLDFJELLET 3

The recognized facies can be grouped into seven facies associations. Each of these associations consists of a characteristic set of facies which are indicated by their number as listed in Table 5-1:

A. Upper Grumantbyen sandstones: facies 8, 9A, 9B
B. Marstranderbreen mudstones: facies 9B, 11
C. Lower Hollendardalen silt- and sandstones:
    - Turbidic flow beds: facies 4, 8
    - Storm generated ripple beds: facies 5, 6
    - Storm beds: facies 2, 3, 4, 5
    - Indistinct beds: facies 7, 11
D. Mid Hollendardalen sandstones: facies 1, 5, 7
E. Upper Hollendardalen mudstones and coal: facies 11, 12
F. Upper Hollendardalen sandstones: facies 6, 8
G. Basal Gilsonryggen mudstones: facies 10, 11

The facies present in each association will be described in detail in chapters 5.3.1 to 5.3.7, while corresponding depositional environments for each facies association are suggested and discussed in chapter 7.1.

5.3.1 UPPER GRUMANTBYEN SANDSTONES (0-4M IN LOG N3)

The lowermost facies association consists mostly of heavily bioturbated silty sandstone, which results in a massive character and almost complete lack of sedimentary structures. Detailed logging included the two uppermost coarsening-upwards episodes of the Grumantbyen Formation. Both intervals have an olive grey colour, are roughly 150cm thick and develop from very highly bioturbated siltstone into bioturbated very fine sandstone where burrows are visible.

Two distinct chert pebble horizons are present at 60cm and 105cm of the lower interval and round to elongate mud clasts of 2-8cm diameter occur towards the top of the interval. The pebbles are 2-5cm in diameter, very rounded, of black chert, and show indications of imbrication where palaeoflow measurements yielded north-westerly to northerly flow direction. The horizons could be traced laterally several meters of the exposed section and do not display any erosional base (Figure 5-3).

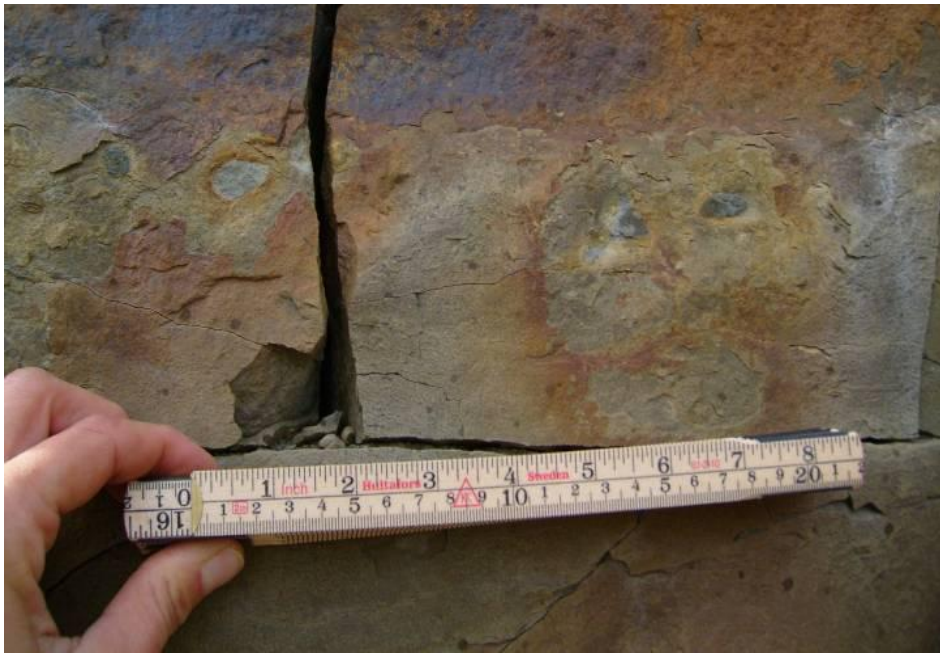

Figure 5-3: First chert pebble horizon without erosional base in lowermost coarsening-upwards interval (at 0.6m in log N3)

Pebbles in the upper interval are equally well rounded, but of smaller dimension (0.5-1.5cm), black or whitish grey in colour and occur as individual clasts (Figure 5-4).

Figure 5-4: Individual chert pebbles occurring in second coarsening- upwards interval (at 2.6m in log N3)

5.3.2 MARSTRANDERBREEN MUDSTONES (4-13.2M IN LOG N3)

The mudstone deposits of Marstranderbreen Member are not entirely exposed in the logged section. The interval from 8.8-11.8m of log N3 was covered by scree and the existence of mudstones only inferred from the preceding and subsequent interval.

Occasional mud clasts and individual pebbles of 1-2cm dimensions occur in the first 140cm interval of siltstone with grey to olive grey colour. Decreasing bioturbation from high to moderate towards the top of the interval, enables the identification of lamination and vertical burrows of 1mm in diameter and 1-2cm length.

The next 160cm interval of moderately bioturbated siltstone displays horizontal burrows of the same dimension. Spherical concretions or cemented nodules could be observed at the bottom of the interval (Figure 5-5).

Figure 5-5: Spherical concretions in siltstone (at 6.2m in log N3)

5.3.3 LOWER HOLLENDARDALEN SILT- AND SANDSTONES (13.2-20.7M IN LOG N3)

This rather complex interval is further grouped into four deposits identified on the basis of characteristic combinations of facies which occur throughout this facies association (numbering of facies according to Table 5-1):

- Turbidic flow beds: facies 4, 8
- Storm generated ripple beds: facies 5, 6
- Storm beds: facies 2, 3, 4, 5
- Indistinct beds: facies 7, 11

TURBIDIC FLOW BEDS

The transition from Marstranderbreen mudstones into Grumantbyen sandstones commences at 13.2m in log N3 with the deposition of a 20cm thick very fine sandstone interval with plane parallel lamination. Grains are very well sorted as expressed by coarse sand on the bedding planes. Next, two fining-upwards episodes were observed. Both are 15cm thick, have an undulating, poorly sorted lower part with erosional base, and develop into plane parallel lamination towards the top (Figure 5-6).

Figure 5-6: Two fining-upwards (FU) intervals from poorly sorted sandstone to plane parallel stratified (PPS) siltstone, interpreted as turbidity flow deposits (at 13.4m in log N3).

STORM GENERATED RIPPLE BEDS

The subsequent episode (at 13.7m in log N3) represented by 40cm ripple cross laminated siltstone indicates north-easterly palaeoflow direction. Being symmetric with a wave length of 10-15cm and amplitude of 1-3cm the ripples are most likely wave generated. Bioturbation is present in form of black spots and horizontal burrows (Figure 5-7). Plant fragments and

Figure 5-7: Bioturbation in ripple cross laminated siltstone bed (13.7m in log N3)

debris are abundant along bedding planes and a spherical concretion occurs in the middle of the interval.

Figure 5-8: Siltstone bed with non-symmetrical ripple, interpreted as current generated (at 14.25m in log N3).

At 14.1m in log N3, a 15cm wedge of very fine laminated sand is followed by 8cm of ripple cross laminated siltstone with easterly palaeoflow direction (Figure 5-8). The ripple of 5 to 6cm wavelength is non-symmetrical and possibly current generated. The migrating ripple has resulted in the deposition of tangential foresets. The siltstone is well sorted and distinct colour alternations are visible as illustrated in Figure 5-8.

The subsequent 70cm interval (at 14.4m in log N3) consists of alternating very fine sandstone and mud drapes. The bounding surfaces of the mud drapes are undulating with 60cm wavelength and clay thickness varies from ~4cm in troughs to ~1cm at crests.

STORM BEDS/ STORM GENERATED RIPPLE BEDS

A 27cm thick siltstone interval interpreted as small storm bed starts with plane parallel stratification at the base and goes over into well sorted, very low to low angle hummocky cross stratification with wavelengths of 10 to 40cm and amplitudes of 1 to 2cm. Locally, there are zones of massive character due to high degree of bioturbation.

Within the next 25cm three fining-upwards episodes are present which all have erosional bases and mud drapes with plant fragments and debris on bedding planes and can be interpreted as periods of marked fluctuations in wave intensities. The first and thickest

episode displays trough cross stratification with palaeoflow direction to the south-east whereas no sedimentary structures are visible in the upper two due to heavy bioturbation (Figure 5-9).

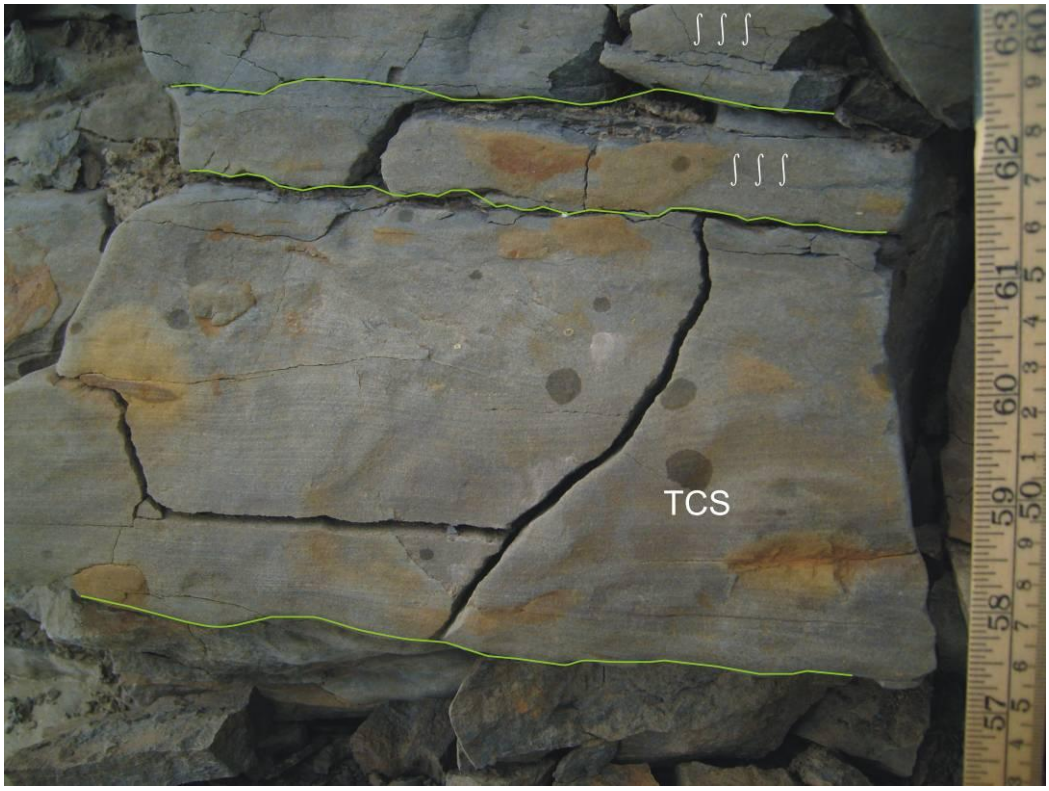

Figure 5-9: Three beds with erosional bases (indicated in green), the lowermost with low angle trough cross stratification (TCS), the upper two no structure due to heavy bioturbation (∫∫∫), at 15.4m in log N3.

TURBIDIC FLOW BEDS

Next interval of 86cm thickness consists of heavily fractured and bioturbated siltstone with some cemented nodules. Bioturbation decreases towards the top and burrows as well as parallel lamination become visible. Plant debris content is high and fossil plant fragments are present on bedding planes. No grading could be observed, but clay and silt sized grains were poorly sorted.

INDISTINCT BEDS

In the following (at 16.5m in log N3), 59cm two intervals of mudstone rich in plant debris which are pinching out to the west, are interbedded with very fine, highly bioturbated sandstone intervals.

STORM BEDS

Subsequently (at 17m in log N3), two prominent coarsening-upwards episodes of 80cm and 71cm thickness are deposited, which are interpreted as storm beds (Figure 5-10; Figure 5-11). The lower one commences with an interval of 3D ripple deposition of 6cm wavelength with organic rich mud lamina. Following an erosional surface the coarsening from very fine to medium sand commences. This level is poorly sorted and high in organic matter, but its content of fossil plant leaves, wood imprints, and plant debris (Figure 5-12) on bedding planes is decreasing upwards. At the same time hummocky cross stratification of ~50cm wavelength becomes more and more pronounced.

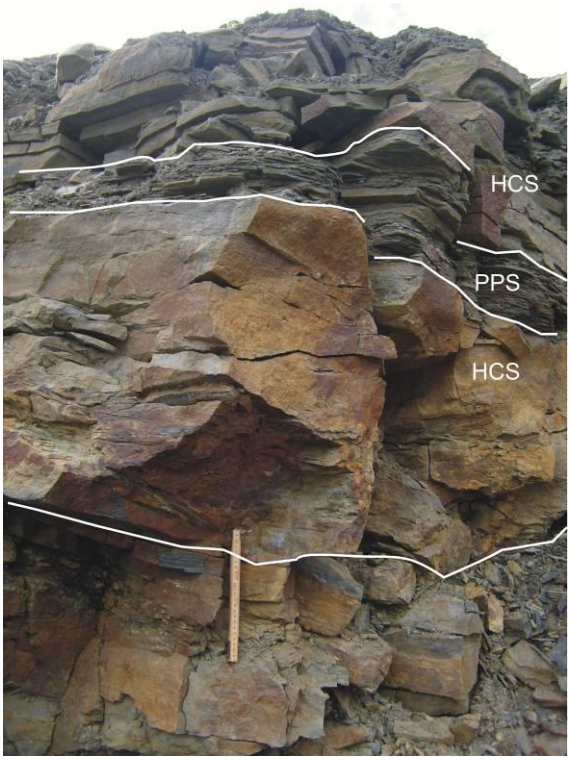

Figure 5-10: Coarsening-upwards interval rich in plant fragments with hummocky cross stratification (HCS) followed by second coarsening-upwards interval with plane parallel stratification (PPS) at the base to HCS (at 17-18.5m in log N3).

Figure 5-11: Hummocky cross stratification in less organic rich coarsening-upwards interval at 18m in log N3.

At 18m in log N3, deposition of plane parallel laminated fine sandstone precedes the upper coarsening-upwards episode for which an erosional base including groove casts with palaeoflow orientation of roughly north-south could be observed (Figure 5-13). At the base of this episode grains are unsorted and mica-rich, and very fine lamination (1mm) was

observed, which possibly corresponds to plane parallel stratification. Upwards the sedimentary structures develop into hummocky cross stratification of the same dimensions as in the lower coarsening-upwards episode, but it is not as rich in plant fragments.

Figure 5-12: Plant fragments and wood imprint (arrow) at the base of the lower coarsening-upwards interval (at 17.1m in log N3).

Figure 5-13: North-south trending groove cast (arrow) at the base of upper coarsening-upwards interval (at 17.95m in log N3).

INDISTINCT BEDS

Subsequently (at 18.5m in log N3), 115cm of heavily fractured siltstones are deposited which show parallel lamination with some thin mud lamina and fossil imprints at mm-scale. At the top a gradual transition into very fine sandstone could be observed.

Next (at 19.7m in log N3), a 100cm thick interval of very fine sandstone with soft sediment deformation is deposited. The convolute lamination occurs not only locally, but over the entire bed thickness suggesting very fast and uniform deposition where pore water expulsion after deposition was abrupt and discontinuous (Figure 5-14).

Figure 5-14: Siltstone with soft sediment deformation (at 19.65m in log N3).

5.3.4 MID HOLLENDARDALEN SANDSTONES (20.7-22.9M IN LOG N3)

At 20.7m in log N3, a 58cm thick interval of low angle cross stratified fine sandstone with occasional ripple cross lamination follows after the soft sediment deformation. The low angle cross stratification yielded a dip towards south-east. The sand is well sorted and homogeneous. Ripples are symmetrical, with wave lengths of ~30cm and amplitudes of ~1cm, and yield a southerly palaeoflow direction (Figure 5-15).

Figure 5-15: Fine sandstone with low angle cross stratification with occasional wave ripple beds (at 20.9m in log N3).

The overlying bed of low angle cross stratified sandstone coarsens upwards from fine to medium sand, displays finer lamina and some bioturbation. The next and uppermost foreshore interval of 140cm thick low angle cross stratification is coarsening from very fine to fine sand, is moderately sorted and shows some spherical cementation and bioturbation.

5.3.5 UPPER HOLLENDARDALEN MUDSTONES AND COAL (22.9-24.6M IN LOG N3)

Mud is deposited immediately following low angle cross stratified sandstone at 22.9m in log N3. A sharp base could be identified, albeit direct contact is difficult to observe. 50cm of mudstone rich in plant debris alternating with sideritic horizons precede a coal seam of 20cm thickness which is then followed by 100cm of siltstone where plant debris rich mud is alternating with sideritic intervals in thinner laminas, organic content is decreasing, and grain sizes are increasing upwards (Figure 5-16; Figure 5-17).

Figure 5-16: Mudstones with coal seam at 22.9m in log N3

Figure 5-17: Coal seam in the upper part of the picture resting on mud rich in plant debris and sideritic horizons

5.3.6 Upper Hollendardalen sandstones (24.6-26.4m in Log N3)

An interval of 180cm thick, very fine sandstone is deposited above the coastal marsh strata (at 24.6m in log N3). Its base is undulating and the first 40cm show some non-symmetric ripple lamination, while only faint lamination could be observed in the uppermost 140cm due to bioturbation. The sandstones are very dirty and do not bear any indications of terrestrial deposition.

5.3.7 Basal Gilsonryggen mudstones (26.4m to top in Log N3)

The transition into mudstones is sharp and shales are relatively fine grained and of dark colour.

Three horizons of bed forming siderite are found in the basal Gilsonryggen shales: two thin layers at 170cm and 175cm and a 20cm thick bed at 195cm over the base (Figure 5-18).

Figure 5-18: Thickest bed forming sideritic concretion

5.4 SUMMARIZED FACIES DESCRIPTION OF NORDENSKIÖLDFJELLET 1+2

During field work in 2007 sections 1+2 were measured to confirm and elaborate the 1997 log (positions of sections 1 and 2 in Figure 4-1). The 2007 log at location N1 started with the uppermost Grumantbyen coarsening-upwards unit where no sedimentary structures are present due to heavy bioturbation (at 10.5m in log N1+2 in Figure 5-1). Also in the subsequent interval of Marstranderbreen Member shales, coarsening upwards tendencies from clay- to siltstone could be observed. In the lower part of the Marstranderbreen chert pebbles as well as mud nodules occur as occasional clasts. The sediment is rich in plant debris, but sedimentary structures are absent due to heavy bioturbation. As the degree of bioturbation decreases towards the middle of Marstranderbreen plane parallel lamination is visible, and organic fragments are found on bedding planes. In upper Marstranderbreen (at 22m in log N1+2; Figure 5-1) a 5 to 10.5cm thick conglomerate bed was observed. It is matrix supported, poorly sorted and grain sizes range from less than 1mm to 3cm. Grain shapes include angular fragments to well rounded clasts. Many of the pebbles and cobbles seem to be rather well rounded. The matrix supported, poorly sorted nature of the conglomerate deposit in association with a very sharp – possibly erosional – lower boundary suggests this deposit to originate from a mass flow (Figure 5-19).

Figure 5-19: Matrix supported, poorly sorted mass flow deposits with sharp erosional base (at 22m in log N1+2)

At 1m above the mass flow deposit (23m in log N1+2), Hollendardalen sandstones commence. In the lowest unit (~1.50m) several thin fining upwards intervals with erosional bases – suggesting turbidity flows – are followed by a package of low angle to parallel bedded very fine to fine sandstones with occasional indications of current ripples (Figure 5-20).

Figure 5-20: Parallel bedded, occasionally ripple cross laminated sandstone (at 24.5m in log N1+2)

Measurements in a thin subsequent wave ripple interval yielded north-westerly palaeo-transportation directions. In a 2m interval of very fine sandstone, ripples are present in the lower half, developing into tabular cross stratification and soft sediment deformation at the top.

This is followed at 26.5 in log N1+2, by 3.80m of parallel bedded very fine sandstone. After 0.80m of hummocky cross stratified very fine to fine sandstone, deposits change back to parallel bedded very fine sandstone (0.40m). Subsequent at 31m in log N1+2, 1.60m of covered scree is possibly indicating a mudstone interval, succeeded by a 1.80m interval of parallel bedded fine sandstone developing into 0.80m of hummocky cross stratified very fine sandstone.

From level 35m in log N1+2, the composite log is measured at Nordenskiöldfjellet 2, which is located 650m north of Nordenskiöldfjellet 1, but general trends of thicknesses are comparable in the two locations. After the hummocky cross stratified interval correlated with the top of section 1, 1.50m of mudstone are present in section N2. This low energy interval is followed by 0.60m of tabular cross bedded fine sandstones which indicate a change in palaeoflow from north-west in the first half to north-east in the upper half. Subsequently, at 37.2m in log N1+2, 1.50m of parallel bedded, and 1.00m of tabular cross bedded fine sandstones were deposited. The latter displays changing palaeoflow directions from east at the base to west at the top. The top of Hollendardalen at this location (N2) is marked by a 60cm interval of low angle cross stratified very fine sandstone with palaeoflow directions to south and south-west where the uppermost deposits show distinct rootlets (Figure 5-21).

Figure 5-21: Rootlets at the top of Hollendardalen Formation at Nordenskiöldfjellet 2

5.5 GEOCHEMICAL ANALYSIS

The geochemical parameters boron, total organic carbon (TOC), and calcium carbonate ($CaCO_3$) are important proxies for the environmental interpretation of the studied succession. Analyses have been carried out on samples from sections N1 and N2 collected in 1997 and are presented in Figure 5-22 (see Appendices 3 and 4 for results in table form). Due to foraminifera being originally the main objective of the project, sampling has been concentrated on claystones and siltstones.

5.5.1 BORON

Boron content in marine sediment may serve as an indicator for palaeosalinity albeit the complex nature of this relationship. The boron content in parts per million (ppm) varies significantly throughout the section. Peak values are reached at 2m into Gilsonryggen shales (158ppm) and immediately above a mass flow conglomerate in Marstranderbreen shales (144ppm). Values in Grumantbyen Formation and lowest Marstranderbreen Member are low (between 58 and 100ppm). The siltstone interval in Hollendardalen Formation represented by sample n17 yielded boron content of 122ppm, which is comparatively high.

5.5.2 TOTAL ORGANIC CARBON AND CALCIUM CARBONATE

Total organic carbon (TOC) content mirrors the boron content curve in upper Grumantbyen Formation and Marstranderbreen Member. In the thin siltstone interval in Hollendardalen Formation TOC content is however rather low despite elevated boron content. Likewise in the Gilsonryggen TOC content is rather low in the interval of highest boron concentration. Highest – overall peak – TOC values of 2.40% and 2.38% occur at the base of Gilsonryggen shales where boron content and thus supposedly salinity is low.

Due to the indirect measurement of calcium carbonate and the propagation of measuring inaccuracies, negative values occur. The content of calcium carbonate is below the detection boundaries in these cases, but equally positive values of the same magnitude have to be taken with caution which is why all values in the range of 0.0 to ±0.4% are represented as arrows in Figure 5-22. With 1.5% the absolute peak value is attained at 60cm above the base of Gilsonryggen shales which coincides with peak values of TOC.

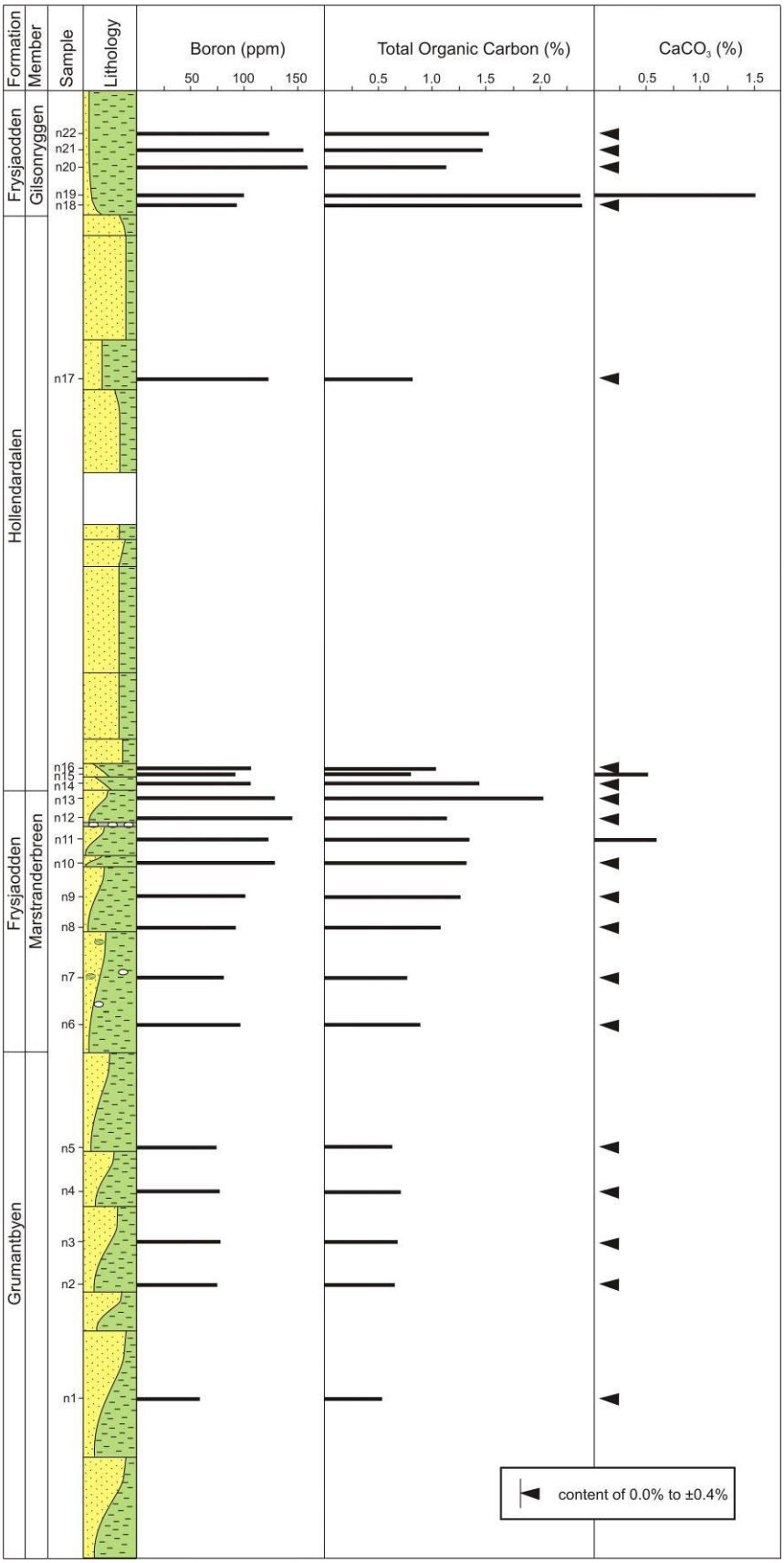

Figure 5-22: Distribution of boron, total organic carbon (TOC), and calcium carbonate ($CaCO_3$). Analyses based on samples of section N1 and N2, sampled in 1997.

6 FORAMINIFERAL STRATIGRAPHY

Out of 22 processed samples from Grumantbyen, over Hollendardalen to upper Frysjaodden formations nine were chosen for detailed analysis. After first screening, samples from Grumantbyen showed to be either barren of foraminifera or of very low abundance. Therefore environmental reconstruction based on foraminiferal analysis focuses on lower to upper Frysjaodden (see Figure 6-1 for the distribution of selected samples over the studied succession).

1,920 benthic foraminifera have been picked in total from this interval. These were exclusively agglutinated foraminifera which is consistent with expectations based on known assemblages from the carbon starved Arctic Basin. Out of a total of 30 species which occur throughout the studied interval, 16 species have been identified with full nomenclature. In addition five species were decided to bear affinity to particular species (aff.), three were found to belong to specific genera without being represented by existing species (numbered sp.), and in six cases only the affiliation to a specific genera was possible (sp.).

6.1 FORAMINIFERAL INDICES AND RANGE CHART

Following picking, sorting, counting and identification of species, most analytical work has been conducted with the help of an Excel spreadsheet. In Appendices 5 and 6 corresponding range charts are given in table form and Figure 6-2 displays the results graphically in a range chart diagram. Figure 6-1 summarizes the most important micropalaeontological parameters which characterize the samples (see Appendix 7 for table form).

All assemblages display a generally low abundance as reflected by the total number of specimens per gram dry sediment which range from 3.1 to 16.3g throughout the nine samples. 16.3g in sample n10 is an exceptionally high abundance in the context of this study which may be due to high productivity, coupled with lower sedimentations rates.

The average dominance is 33.0% and it ranges from 21.5 to 42.8% which signify both rather low values and a rather small range of dominance. Nevertheless, samples can be differentiated on the basis of differing values of dominance where higher values suggest rather restricted environments and lowest dominance is expected in marine conditions. Upon this criterion samples n6, n19 and n21 reflect the most marine conditions, whereas samples n12 and n14 represent highly restricted environments.

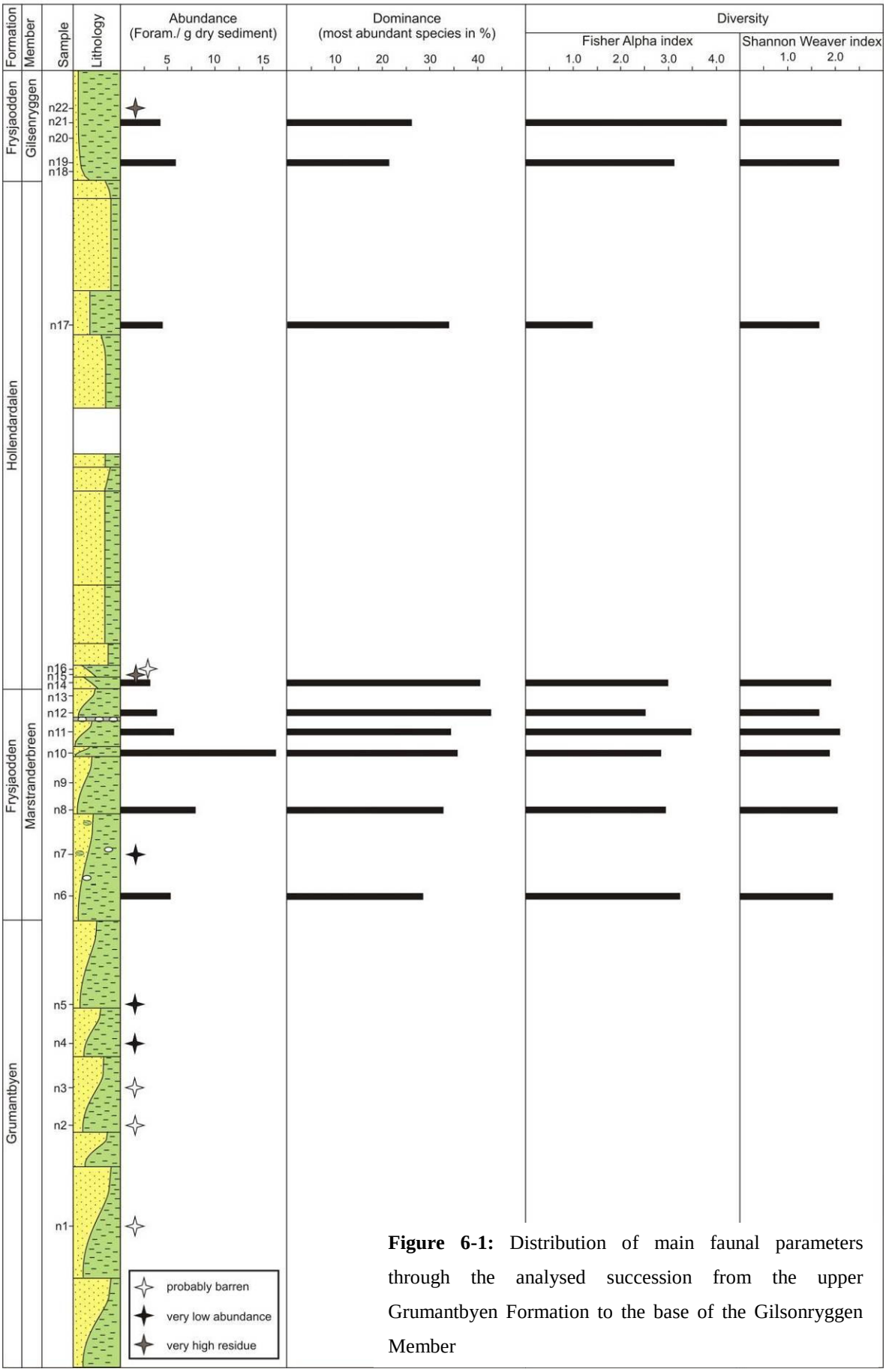

Figure 6-1: Distribution of main faunal parameters through the analysed succession from the upper Grumantbyen Formation to the base of the Gilsonryggen Member

The Shannon Weaver index is sensitive towards relative frequencies of species in a sample, rather than giving equal weight to all occurring species as is the case for the Fisher Alpha index. However, in the studied succession the two diversity indices show essentially the same trend, even though differences between samples are not as pronounced on the basis of the Shannon Weaver index. Alpha values range from 1.4 to 4.2 with a mean of 3.0 and Shannon Weaver values range from 1.7 to 2.1 with a mean of 1.9. The only clear exception where values of the two diversity indices differ substantially is sample n21. An extremely high alpha value of 4.2 occurs together with a moderately high Shannon Weaver index of 2.1 which demonstrates that many different species were present while the majority of them had very low frequencies.

The lower the diversity value, the more restricted is the given environment, while normal marine environments have a tendency to display highest diversity values. With regard to the Fisher Alpha index sample n17 really stands out by attaining a minimum diversity value of 1.4 as compared to a range of 2.5 to 4.2 for all other samples. As for the Shannon Weaver index the minimum value of 1.7 is likewise reached in sample n17, but differences with respect to other samples are not as pronounced. Nevertheless evidence is unambiguous that the siltstone interval represented by sample n17 was deposited under extremely restricted conditions.

In the Marstranderbreen Member represented by samples n6 to n14 no clear trend can be deduced, since alpha values fluctuate between 2.5 to 3.5 and Shannon Weaver values range between 1.7 and 2.1. Diversities are relatively high and suggest marine conditions, although values are clearly below those typical for modern normal marine shelf conditions. As will be argued in chapter 7.2, different criteria have to be applied in the Boreal realm. Towards the top of Marstranderbreen the alpha diversity does not reveal any change into less marine conditions.

The diversity values in the lower Gilsonryggen Member as expressed by samples n19 and n21 however, clearly are in the upper range for both alpha and Shannon Weaver indices. This reflects increased normal marine influence.

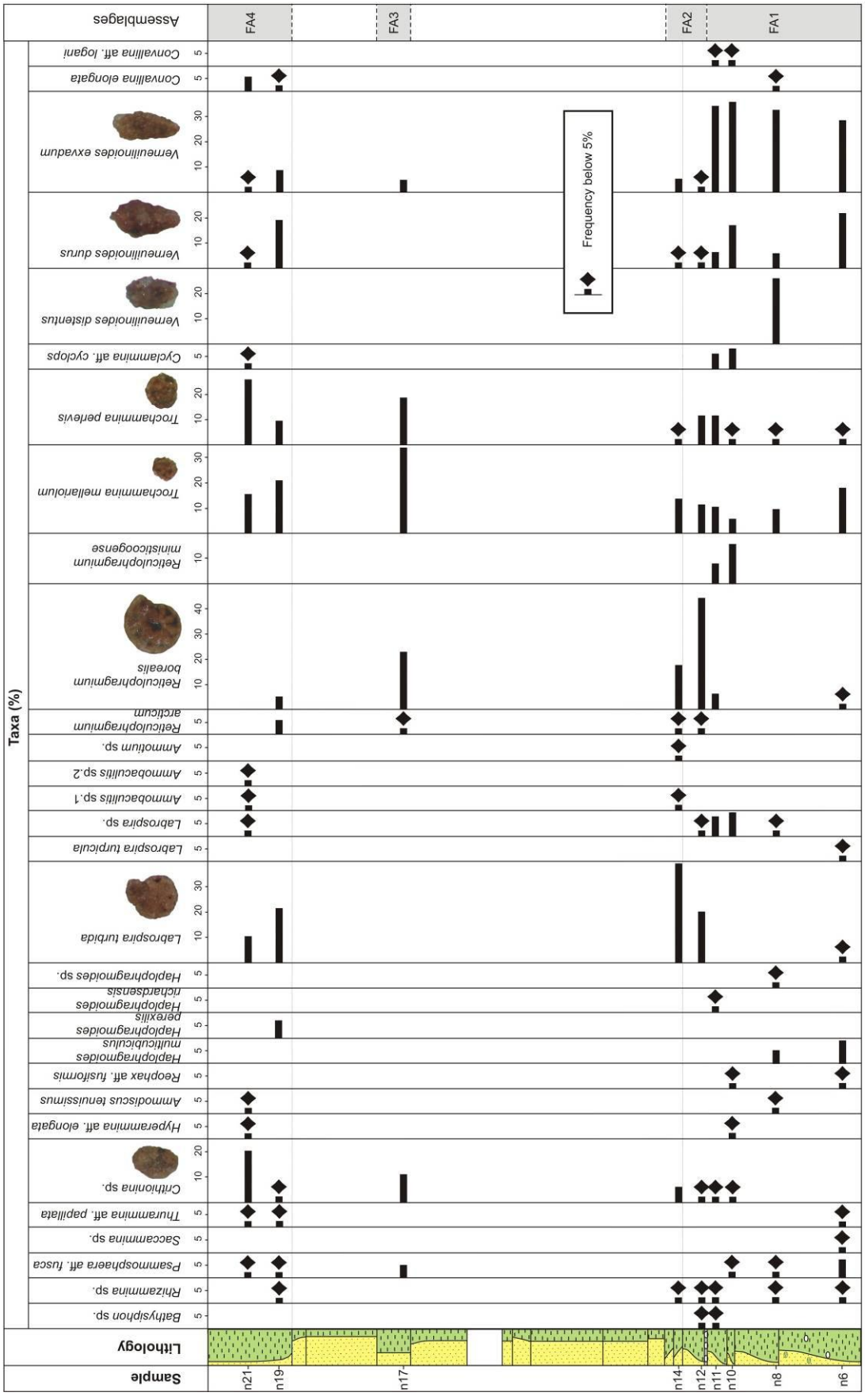

Figure 6-2: Range chart illustrating percentage distribution of species throughout the analysed section. Positions of samples are indicated by reference to the lithological column to the left, foraminiferal assemblages defined in this study are indicated in the right column.

6.2 FORAMINIFERAL ASSEMBLAGES

Based on the calculation of similarity indices and additional considerations of dominance, diversities, and species composition, the assemblages have been divided into four groups:

FA1. *Verneuilinoides exvadum – Verneuilinoides durus* assemblage:
n6 (N-1-09-97), n8 (N-1-13-97), n10 (N-1-17-97), n11 (N-1-19-97)
FA2. *Reticulophragmium borealis – Labrospira turbida* assemblage:
n12 (N-1-21-97), n14 (N-1-26-97)
FA3. *Trochammina mellariolum – Reticulophragmium borealis* assemblage:
n17 (N-2-03-97)
FA4. *Trochammina perlevis– Labrospira turbida* assemblage:
n19 (N-2-08-97), n21 (N-2-11-97)

Similarity index values are generally rather low, with a mean value of 40.3% for 36 possible sample combinations (see Appendix 8 for the chart displaying all similarity index results). The denotation of assemblages on the basis of marker species already indicates that some clusters show higher degrees of affinities amongst each other than others.

6.2.1 FA1: *VERNEUILINOIDES EXVADUM – VERNEUILINOIDES DURUS* ASSEMBLAGE

FA1 is the foraminiferal assemblage encompassing most samples. This cluster suggests itself relatively strongly as documented by the range of similarities of 48.0% to 65.8% as compared to the range of 16.1% to 40.7% for all possible combinations with assemblages outside of FA1. This observation excludes sample n19 which bears strongest similarity to sample n6 in FA1 (54.8%). Since this is however accompanied by below average similarity indices of n19 with respect to other samples in FA1, it is not included in FA1.

The high similarity between samples n6, n8, n10 and n11 is mostly due to the occurrence of *Verneuilinoides exvadum* which is the dominant species in all of these samples (with 28.6-35.8%). Locally common species include *Verneuilinoides durus, Trochammina mellariolum,* and *Verneuilinoides distentus*.

6.2.2 FA2: *RETICULOPHRAGMIUM BOREALIS – LABROSPIRA TURBIDA* ASSEMBLAGE

FA2 is formed by samples n12 and n14 which were grouped together based on a similarity index of 66%. Similarity with samples from FA1 is low as demonstrated by a range of 19.3 to 39.6%, while FA2 has much more in common with FA3 and FA4 as indicated by similarity values between 42.5 and 57.8%. Nevertheless, the differentiation is justifiable owing to typical species compositions. FA2 is clearly dominated by *Reticulophragmium borealis* in the case of sample n12 (42.8%) and *Labrospira turbida* in sample n14 (40.4%).

The co-dominant species is *Labrospira turbida* for sample n12 (20.9%), and *Reticulophragmium borealis* for sample n14 (18%).

6.2.3 FA3: *TROCHAMMINA MELLARIOLUM – RETICULOPHRAGMIUM BOREALIS* ASSEMBLAGE

FA3 consist of only one sample, which is closely related to FA2. However, grouping them all together would result in less pronounced marker species. They primarily coincide in the occurrence of *Reticulophragmium borealis* and *Reticulophragmium arcticum*. The diversity in FA3 is markedly smaller, which is an important additional argument for this classification.

The dominant species in FA3 is *Trochammina mellariolum* (34.0%), followed by *Reticulophragmium borealis* (23.1%) and *Trochammina perlevis* (18.9%). All of these species tolerate extreme conditions, notably low salinity and hypoxic situations.

6.2.4 FA4: *LABROSPIRA TURBIDA – TROCHAMMINA PERLEVIS* ASSEMBLAGE

Samples n19 and n21 are included in FA4 with a similarity value of 51%. This is the highest similarity value sample n21 attains with any other sample, whereas sample n19 has better matches with FA2 (57.4% and 57.8%) and sample n6 (54.8%). The correspondence between samples n19 and n6 is best explained by the importance of *Verneuilinoides durus* and *Verneuilinoides exvadum* which may be interpreted as reflecting increased marine influence.

The recognition of FA4 is primarily based on species composition and dominance of *Trochammina*. In sample n19 where balanced dominances may be interpreted as another marine indicator, most dominant species are *Labrospira turbida* (21.5%), *Trochammina mellariolum* (20.5%), and *Verneuilinoides durus* (18.5%). In sample n21, dominance shifts slightly to *Trochammina perlevis* (26.2%), *Crithionina* sp. (20.8%), *Trochammina mellariolum* (16.4%) and *Labrospira turbida* (10.4%). The dominance of *Trochammina* and *Crithionina* over *Labrospira* suggest a more restricted environment than in sample n19.

6.3 MORPHOGROUPS

Morphogroup analysis has proven to be useful in order to reduce inevitable complexity when dealing with foraminiferal assemblages on species level. The scheme proposed by Nagy (1992) is based on morphological features like the test shape and arrangement of chambers. At the same time supposed life positions and feeding habits are given for the resulting groups (four) and subgroups (seven in total).

The species present in this study have been assigned to four groups and six subgroups, based on their observed morphologies and inferred feeding habits (Table 6-1).

Table 6-1: Division of species identified in the studied interval into morphogroups.

Morphogroups	Species occurring in Frysjaodden and Hollendardalen formations
1a:	*Bathysiphon* sp. *Rhizammina* sp. *Hyperammina* aff. *elongata*
2a:	*Psammosphaera* aff. *fusca* *Saccammina* sp. *Thurammina* aff. *papillata* *Crithionina* sp.
2b:	*Trochammina mellariolum* *Trochammina perlevis*
3a:	*Haplophragmoides multicubiculus* *Haplophragmoides perexilis* *Haplophragmoides richardsensis* *Haplophragmoides* sp. *Labrospira turbida* *Labrospira turpicula* *Labrospira* sp. *Reticulophragmium arcticum* *Reticulophragmium borealis* *Reticulophragmium ministicoogense* *Cyclammina* aff. *cyclops*
3b:	*Reophax* aff. *fusiformis* *Ammobaculitis* sp.1 *Ammobaculitis* sp.2 *Ammotium* sp. *Verneuilinoides distentus* *Verneuilinoides durus* *Verneuilinoides exvadum* *Convallina elongata* *Convallina* aff. *logani*
4a:	*Ammodiscus tenuissimus*

On the basis of these groups percentages have been calculated (Appendix 9, see Figure 6-3 for corresponding range chart). The Foraminifera Assemblages suggested on the species' level are visually confirmed by the range chart. Calculations of similarity values for the morphogroups yielded generally high values, but support the suggested classification (see Appendix 10 for similarity index chart based on morphogroups).

FA1 (samples n6, n8, n10, and n11) is particularly characterized by the importance of morpho-subgroup 3b, which comprises serial species characteristically living submerged in sediment. In FA2 (samples n12 and n14) morpho-subgroup 3a is dominating. Species belonging to this subgroup are believed to have a surficial to infaunal mode of life, and have a rounded-planispiral morphology. FA3 (sample n17) differs from all other samples in being highly dominated by morpho-subgroup 2b. This subgroup comprises species with planoconvex-trochospiral and planoconvex-streptospiral morphology which presumably live at the sediment surface. In FA4 (samples n19 and n21) the most characteristic feature is a relatively even morpho-subgroup distribution, where 2b, 3a, and 3b all play an important role.

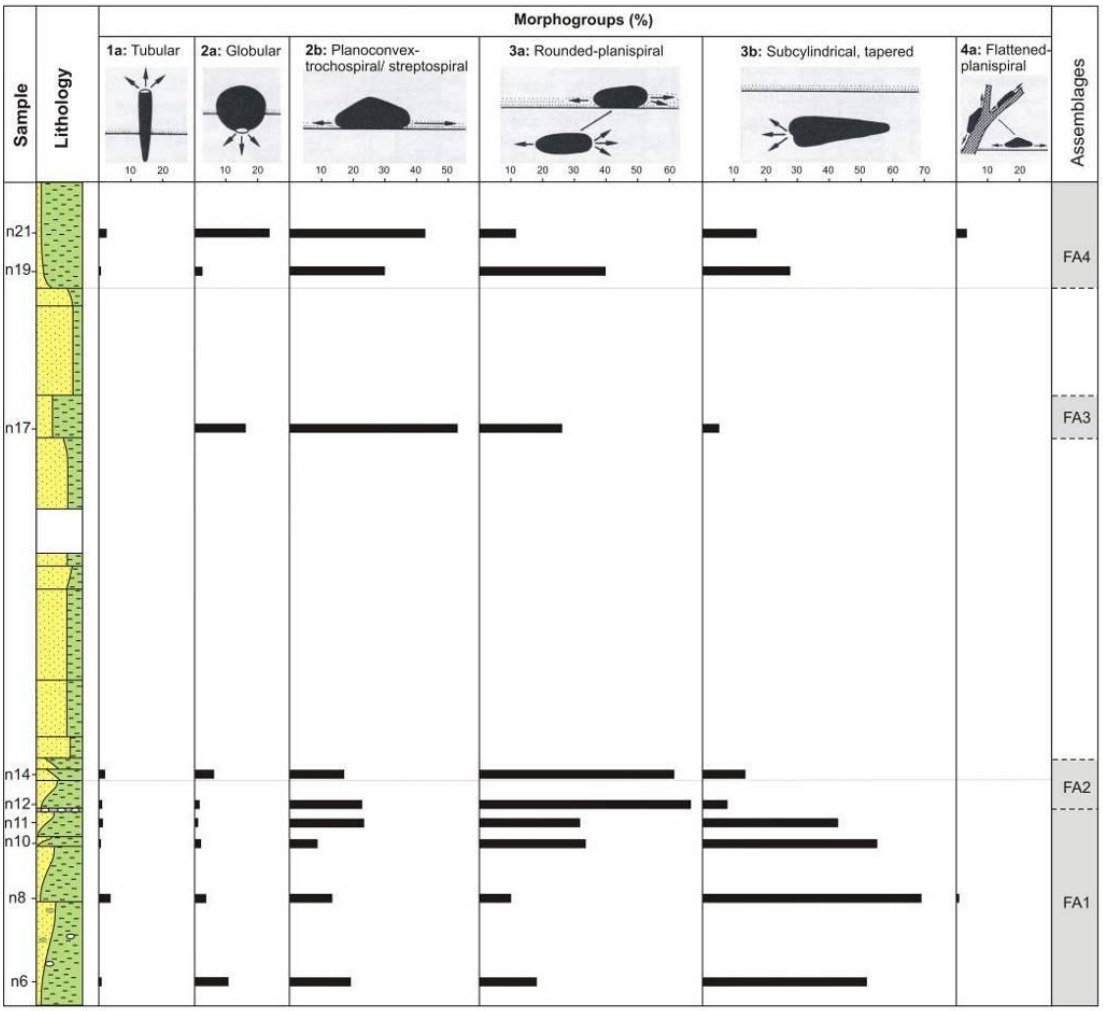

Figure 6-3: Range chart illustrating distribution of morphogroups throughout the studied section together with indication of foraminiferal assemblages.

7 DEPOSITIONAL ENVIRONMENTS

The discussion of depositional environments of the analysed succession from upper Grumantbyen to upper Frysjaodden formations includes lithofacies interpretation (chapter 7.1), biofacies interpretation (chapter 7.2), the presentation of a depositional model (chapter 7.3), as well as the shoreline evolution and sequence stratigraphy (chapter 7.4).

7.1 LITHOFACIES OF NORDENSKIÖLDFJELLET 3

Facies associations have been presented with respect to their characteristic facies in chapter 5.3. Here the results are discussed with regard to possible depositional environments. Table 7-1 summarizes suggested environments of deposition for the seven facies associations which are arranged according to their position in the succession.

Table 7-1: Summary of suggested depositional environments at Nordenskiöldfjellet 3

Facies association	Included facies:	Suggested depositional environment:
Basal Gilsonryggen mudstones	10: sideritic concretion 11: mudstone	Shelf
Upper Hollendardalen sandstones	6: current ripple cross laminated sandstone 8: massive sandstones due to bioturbation	Transgressive sands
Upper Hollendardalen mudstones and coal	11: mudstone 12: coal	Coastal marsh
Mid Hollendardalen sandstones	1: low angle cross stratified sandstone 5: wave ripple cross laminated sandstone	Foreshore
Lower Hollendardalen silt- and sandstones		Offshore transition to shoreface
Turbidic flow beds	4: planar parallel stratified sandstone 8: massive sandstones due to bioturbation	
Storm generated ripple beds	5: wave ripple cross laminated sandstone 6: current ripple cross laminated sandstone	
Storm beds	2: trough cross stratified sandstone 3: hummocky cross stratified sandstone 4: planar parallel stratified sandstone 5: wave ripple cross laminated sandstone	
Indistinct beds	7: soft sediment deformation 11: mudstone	
Marstranderbreen mudstones	9B: Chert pebbles as individual clasts 11: mudstone	Shelf
Upper Grumantbyen sandstones	8: massive sandstones due to bioturbation 9A: Chert pebbles in horizon, no erosional base 9B: Chert pebbles as individual clasts	Offshore bars (?)

UPPER GRUMANTBYEN SANDSTONES (0-4M IN LOG N3)

The environmental interpretation of Upper Grumantbyen sandstones as offshore bars is tentative because sedimentary structures are almost completely absent due to heavy bioturbation. Dallmann et al. (1999) also stress the problematic origin of the Grumantbyen sandstones. They argue in favour of an entirely submarine, shelfal origin due to its glauconitic, bioturbated, and massive character as well as absence of subaerial facies.

MARSTRANDERBREEN MUDSTONES (4-13.2M IN LOG N3)

On the basis of observed mudstone and shale beds in Marstranderbreen Member, this facies association is referred to as shelf environment. Occasional mud clasts and individual pebbles occurring in the lower Marstranderbreen Member of N3, are most likely shore ice rafted (see Dalland 1976 or chapter 3.3 of this thesis for a more detailed discussion).

LOWER HOLLENDARDALEN SILT- AND SANDSTONES (13.2-20.7M IN LOG N3)

The lower silt- and sandstones of the Hollendardalen Formation are a complex succession of turbidity flow beds, storm generated ripple beds, storm beds, and indistinct beds.

Turbidity flow deposits occur predominantly in the first half of this interval (13.2-16.5m in log N3). The turbidity beds observed here are of 3cm to 20cm thickness, while the interpretation of an 86cm thick bed as of turbiditic origin is tentative due to intense bioturbation. Turbidity currents are sustained by fluid turbulence and may travel for hundreds of kilometres downslopes, so that turbidic flow deposits are common features in modern shelf to deeper seas (Reading 1996). The facies observed here are typical for deposits of the upper flow regime of turbidity currents and correspond to intervals A and B or interval B in the classical model presented by Bouma (1962). Two mechanisms are most likely to be responsible for the initiation of the corresponding turbidity currents. The low salinity situation of the Palaeogene Central Basin is documented by its overall restricted foraminiferal assemblages (Nagy 2005). Together with expected sediment laden influent in connection with an active orogeny, hyperpycnal flow is a first very likely initiation mechanism. Plink-Björklund and Steel (2004) report evidence for extensive turbidic flow deposits on continental slope and basin floor of the Eocene Central Basin (Battfjellet Formation). A second likely initiation mechanism during active orogeny is seismically triggered subaerial slides within the drainage area.

Short intervals of both wave as well as current generated ripple cross stratified siltstones also occur in the first half of Lower Hollendardalen silt- and sandstones (13.2-16.5m in log N3).

Due to the lithology (silt) and the position in the succession, they are interpreted as storm generated beds. Based on the existence of these storm generated ripple beds together with turbidic flow deposits of upper flow regime, the first half referred to here is interpreted as offshore transition. The alternations of mudstones deposited in fair weather periods with sandstones deposited during storms typical for offshore transitions are not present. The environment has been highly agitated and possible low energy deposits have not been preserved.

Due to the regressive development during deposition of Hollendardalen sandstone wedges, and the interpretation of the next facies association as foreshore, a shoreface interval would be expected. Evidence for this is however not present in the succession. It is possible that the interval of two considerable storm beds consists of reworked shoreface facies (16.5-18.5m in log N3). The very high content in plant debris and fragments, particularly for the lower storm bed, suggests important terrigenous input and an occurrence of the storms in a near shore environment. Further evidence for a shallow environment comes from the storm bed facies which correspond to the model for shallow-marine, fine-grained storm beds as presented in Cheel and Leckie (1993). Ideally, such storm deposits have an erosional base with sole marks and a marked increase in grain size with respect to underlying fair weather deposits and are fining upwards. Horizontal lamination in the lowermost part is followed by a thicker interval of hummocky cross stratification and symmetrical ripples on top. The only deviation to the model is that the two storm deposits reported here are coarsening upwards rather than fining upwards.

The subsequent indistinct beds (18.5-20.7m in log N3), consisting of siltstone and soft sediment deformed very fine sandstone, are interpreted as a local rise and subsequent lowering in sea level due to the shifting of channel or levee progradation. Such a parasequence may have been triggered by storm induced shifts of bigger sand bodies. The subsequent deposition of very fine sandstone with soft sediment deformation suggests that the development into shallower environments occurred relatively fast.

MID HOLLENDARDALEN SANDSTONES (20.7-22.9M IN LOG N3)

The subsequent facies association of Mid Hollendardalen sandstones consists of low angle cross stratified sandstone and occasional wave ripple lamination. These facies are known to be typical indicators of foreshore environments (Reading 1996).

UPPER HOLLENDARDALEN MUDSTONES AND COALS (22.9-24.6M IN LOG N3)

A thin coal seam together with organic rich mudstones alternating with sideritic horizons, suggest an entirely terrestrial origin of this facies association. Some cracks below the coal seam bared resemblance to rootlets, but due to the highly fractured nature of the mudstones, this observation is not assured. Particularly the 20cm preceding and succeeding the coal seam are extremely rich in plant fragments and organic matter. The coals can only be traced laterally for approximately ten meters. Whether this is due to small spatial extend of the deposits or due to non-preservation is difficult to decide because the interval is only exposed in one location. Based on the lithology these facies suggest a low energy environment of terrestrial origin, possibly in form of marshes and lagoons.

UPPER HOLLENDARDALEN SANDSTONES (24.6-26.4M IN LOG N3)

Due to an observed undulating, possibly erosional base, and very dirty nature of these sandstones this facies association is interpreted as transgressive sands. Since they are thought to have been deposited during a rise in relative sea level, they mark the sequence boundary and the erosional base is interpreted as transgressive surface.

BASAL GILSONRYGGEN MUDSTONES (26.4M TO TOP OF LOG N3)

This facies association is decided to be of marine origin due to generally accepted knowledge on the sequence stratigraphic development. Furthermore, the Gilsonryggen shales are of important thickness, so that an offshore origin is the only plausible explanation. In this study only the base of Gilsonryggen mudstones is included. Three bed forming horizons of sideritic concretions at 1.7m above the transgressive sands indicate an interval of maximum flooding (28.1m in log N3). Analysis of foraminiferal assemblages presented in the following chapter 7.2 renders a more exact picture of the depositional environment of basal Gilsonryggen mudstones.

7.2 BIOFACIES OF NORDENSKIÖLDFJELLET 1+2

The geochemical results for upper Grumantbyen to upper Frysjaodden formations presented in chapter 5.5 support the idea of the carbonate starved nature of the Arctic Ocean. On the basis of the calcium carbonate content which is extremely low throughout the succession (averaging to 0.19%), it is difficult or not possible to distinguish local effects of deltaic influence from regional features of the Arctic Ocean. The total organic carbon (TOC)

content in the studied succession is also low (averaging to 1.19%), which is in accordance with the entirely agglutinated nature of the foraminiferal assemblages found in this study.

The variations in species abundance, dominance, and diversity throughout lower to upper Frysjaodden Formation have been presented in chapter 6.1. In order to interpret these micropalaeontological indices more universally, comparisons with other Boreal foraminiferal assemblages deposited in the Arctic Gulf is necessary. The guideline of alpha diversities higher than 5 signifying normal marine assemblages on usual shelves (Murray 1973), does not apply here due to generally restricted conditions of the Boreal Realm.

Nagy et al. (2000) have studied Late Palaeocene to Early Eocene foraminiferal successions from exploratory wells in the Tromsø and Hammerfest basins, and from two onshore sections in the Central Basin of Spitsbergen. They arrived at a palaeobathymetric model based on the distribution of foraminiferal groups and diversities (Figure 7-1).

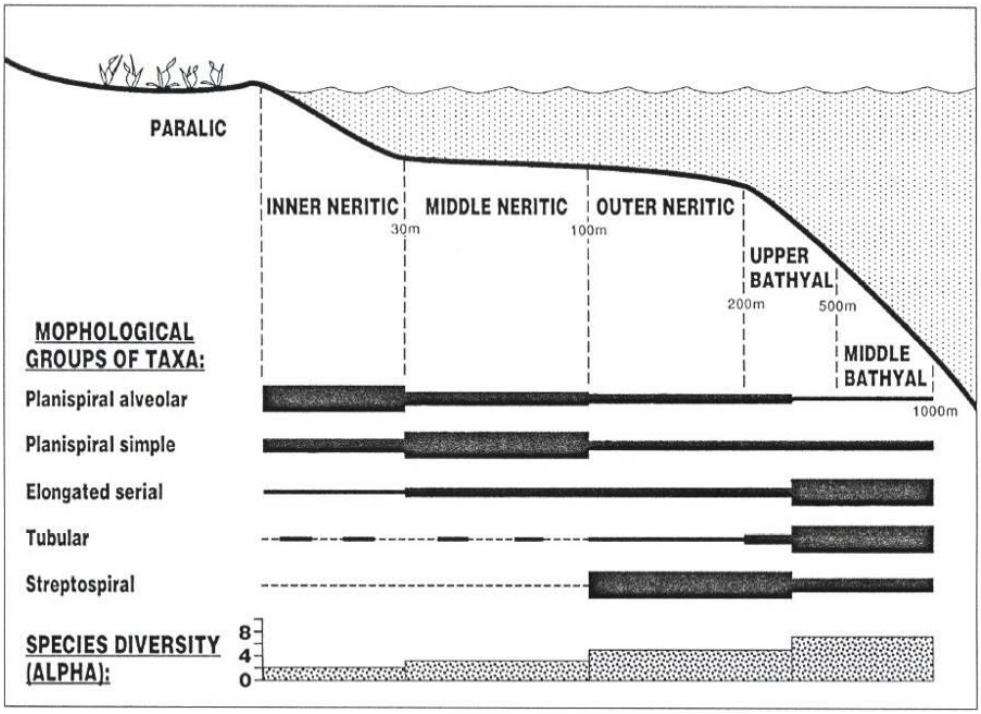

Figure 7-1: Generalized overview of the palaeobathymetric distribution of foraminiferal groups and diversities in the Palaeogene of the southern Barents Sea and Svalbard." (Nagy et al. 2000)

Alpha values which are to be expected in the Boreal Realm are below 2.0 for inner neritic settings, range from 2.0 to 3.5 for middle neritic settings, and from 3.5 to 5.0 for outer neritic settings. Alpha diversities determined in this study range from 1.39 to 4.21. This suggests an entirely neritic and paralic nature of the studied foraminiferal assemblages.

FORAMINIFERAL ASSEMBLAGE 1 (FA1)

Nagy (2005) found an average alpha diversity of 2.7 (ranging from 2.0 to 3.5) for Kolthoffberget Member prodelta facies of the Firkanten Formation. FA1 determined on the basis of the study at hand, has an average alpha diversity of 3.11 and the corresponding biofacies are therefore interpreted to originate from a distal prodelta setting.

The relative distribution of morphogroups in FA1-samples (Figure 6-3) supports the interpretation as distal prodelta: Morpho-subgroup 3b (subcylindrical, tapered morphotypes) dominates, morpho-subgroups 3a (rounded-planispiral) and 2b (planoconvex-trochospiral) have important occurrences, while morpho-subgroups 1a (tubular) and 2a (globular) play a minor role. In his study of the North Sea Jurassic Nagy (1992) interpreted the Drake Formation in three different wells to represent prodelta biofacies. This formation shows similar relative frequencies of morphological units, but the frequency of morpho-subgroup 2b is higher, while that of morpho-subgroup 3a is much lower as compared to FA1. Morpho-subgroup 3a can be interpreted as a slightly deeper living fauna than morpho-subgroup 2b (Nagy 1992), suggesting relatively deep water prodelta conditions.

FORAMINIFERAL ASSEMBLAGE 2 (FA2)

With an average alpha diversity of 2.74, FA2 determined in this study is clearly in the range of prodelta facies as defined by Nagy (2005), but more proximal than FA1. *Verneuilinoides exvadum*, *Verneuilinoides durus* and *Trochammina mellariolum* are characteristic for FA1 and these are amongst the common species or genera in Nagy et al.'s (2000) prodelta-shelf biofacies. *Reticulophragmium borealis* and *Labrospira turbida* are dominant in FA2, which finds its analogue in the dominance of *Reticulophragmium arcticum* and *Labrospira turbida* in Nagy et al.'s (2000) delta front-prodelta biofacies.

FORAMINIFERAL ASSEMBLAGE 3 (FA3)

FA3 has an extremely low alpha diversity of 1.39 which lies in the range 0.6 to 1.5 as established for the lagoonal facies of Todalen Member (Firkanten Formation) by Nagy (2005). This assemblage is dominated by *Trochammina mellariolum*, followed by *Reticulophragmium borealis* and *Trochammina perlevis*. In the Todalen Member lagoonal biofacies the dominant species is *Trochammina* sp.1. The genus *Trochammina* is known to be common in modern hyposaline environments, where it is often dominant, but also has a broad general distribution, albeit mostly in small frequencies (Murray 1973). FA3 appears to have developed in a protected, probably back barrier, lagoonal setting. Freshwater input is

derived from deltas which developed along the north-south trending coastline of the Palaeogene Central Basin.

In FA3 morpho-subgroup 2b dominates clearly. The bathymetric distribution of agglutinated morphogroups (Figure 7-2) demonstrates that this morphogroup is expected to be important in lagoonal and marsh settings which supports the interpretation as back barrier lagoon as suggested on the basis of alpha values and species dominance.

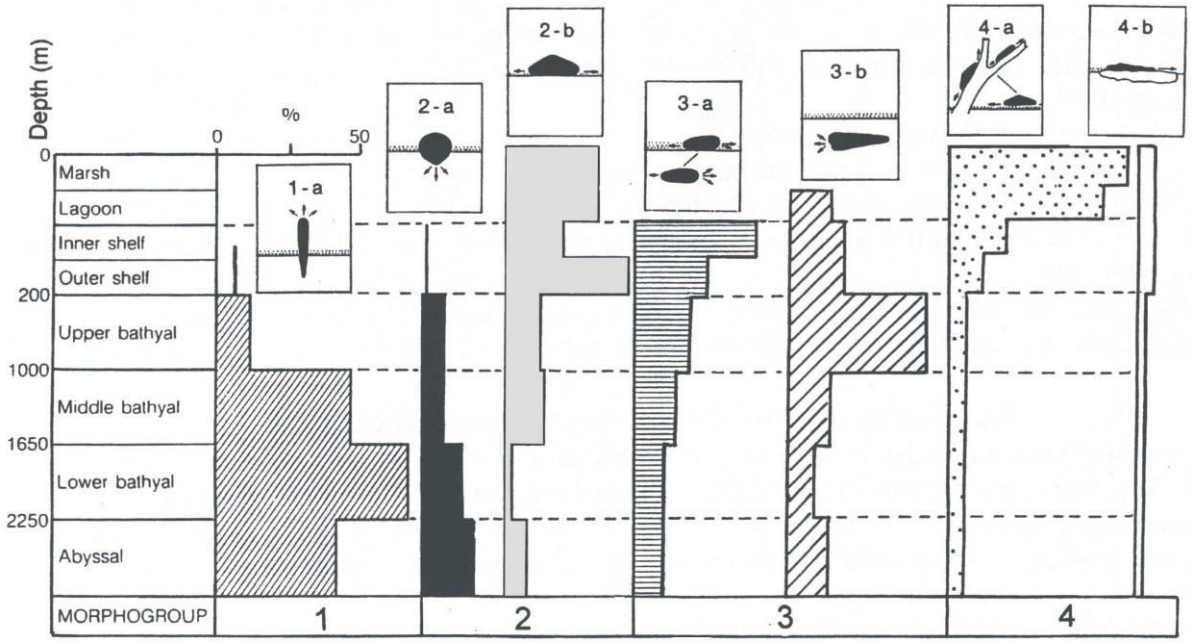

Figure 7-2: Bathymetric distribution of agglutinated morphogroups. Modified from Murray (1991) and Jones and Charnock (1985) by Nagy (2007) according to his morphogroups (Nagy 1992).

FORAMINIFERAL ASSEMBLAGE 4 (FA4)

FA4, determined on the basis of this study, has an average alpha diversity of 2.58 and falls therefore in the prodelta range (2.0-3.5) defined by Nagy (2005). This demonstrates that a transgression introduced the Gilsonryggen shales over Hollendardalen sandstones. In FA4 *Labrospira turbida* is dominant and the genus *Trochammina* is important which finds its analogue in the prodelta-shelf biofacies of Nagy et al. (2000), characterized by the dominance of *Labrospira* aff. *turbida* and importance of *Reticulophragmium arcticum* and *Trochammina mellariolum*. Similarly, Schröder-Adams and McNeil (1994) differentiate between five biofacies in the Oligocene through Middle Miocene of the Beaufort-Mackenzie Basin on the basis of dominant species and assemblage composition. Their biofacies 1 of

inferred delta front environment includes *Labrospira turbida* as dominant species, while species of the genera *Haplophragmoides, Reticulophragmium, Insculptarenula*, *Cyclammina*, and *Trochammina* show significantly increased abundances. The importance of these genera and *Labrospira turbida* demonstrates a general similarity of their biofacies 1 (delta front) with FA4, and – albeit less pronounced – also with FA2. Relative frequencies of morphogroups in FA4 (Figure 6-3) show a distribution which corresponds closely to the prodelta assemblages reported from the North Sea Jurassic by Nagy (1992).

Besides the alpha diversities mentioned earlier, evidence for the entirely paralic and neritic nature of the studied assemblages also comes from the relative frequencies of morphogroups. Based on the generalized bathymetric distribution model modified from Murray (1991) by Nagy (2007) (Figure 7-2), it can be concluded that none of the foraminiferal assemblages recognized in the Marstranderbreen to basal Gilsonryggen members have been deposited in deeper waters than marine shelf. This interpretation is possible based on the observation that neither morpho-subgroup 1a, nor 2a occur in noteworthy frequencies in any of the studied assemblages, but are expected to attain important occurrences once bypassing the shelf-edge. Morpho-subgroup 1a, supposedly upright standing, suspension feeding species, are dominant in modern deep ocean and dislike strong currents and turbidity as typical for paralic and neritic settings. Morpho-subgroup 2a are assumed to be surficial passive deposit feeders and are expected in bathyal to abyssal depths (Nagy 1992; Nagy 2007).

7.3 DEPOSITIONAL MODEL

GRUMANTBYEN FORMATION

Grumantbyen sandstones are supposedly derived from the eastern and north-eastern margin of the Palaeogene Central Basin (Bruhn and Steel 2003). Due to high degree of bioturbation other sedimentary structures are rare. Exceptions are chert pebbles occurring as individual clasts as well as in two distinct horizons without erosional base. The phenomenon of dropstones in Grumantbyen to Hollendardalen formations has been studied in detail by Dalland (1976) who concludes that shore ice is the most likely transporting agent. Therefore, the Palaeocene seems to represent a period of accentuated seasonal temperature gradients. Perennial shore ice formation may well have been restricted to exceptionally cold winters, explaining the occurrence of individual clasts. Colder winter conditions must have prevailed for extended time periods of decades and centuries, accounting for pebble horizons without

erosional surface. Moreover these conditions of possibly episodic marked seasonal cycles cover a considerable time span, approximately 9.7 Myrs.

MARSTRANDERBREEN MEMBER

According to Bruhn and Steel (2003) basin scale maximum flooding occurs in lower Frysjaodden Formation. This time interval coincides with the initiation of the west Spitsbergen Orogeny which resulted in a deepening of the foreland basin. The Marstranderbreen Member shales, derived from the western margin, were deposited in this environment of newly created accommodation space due to tectonic forcings. In section N1 a conglomerate deposit, of suggested mass flow origin, is present about one meter below the base of the Hollendardalen Formation. The presence of the conglomerate in N1 marks its distal location with respect to a river channel of a delta or estuarine system (Figure 7-3A).

No mass flow deposits could be located in N3 where Marstranderbreen Member is however poorly exposed. Moreover Marstranderbreen is 7.8m thick in N1, but attains a thickness of 9m in N3. Erosion took place prior to the deposition of the unsorted mass flow deposits of mud to cobble fraction as demonstrated by the erosional surface at the base of the conglomerate. One possible explanation for the greater thickness of Marstranderbreen Member in N3 than in N1 is that no substantial mass flow took place at this location.

HOLLENDARDALEN FORMATION

According to the general depositional setting Hollendardalen Formation sandstones prograded into Marstranderbreen Member shales during a regressional stage as paralic sand wedges, derived from the West Spitsbergen Orogen. The two sedimentary logs (N1+2, N3) from the three locations along the inferred ancient shoreline on a north-northwest to south-southeast axis unravel an even more detailed depositional history.

A first striking difference between Hollendardalen sandstones in sections N1+2 and N3 is that thicknesses of Hollendardalen Formation in locations N1 and N2 correspond roughly and encompass approximately 17m, whereas the corresponding regressive part of Hollendardalen in section N3 only accounts for 11.5m. One explanation for this observation may be better preservation potential in N1+2. The existence of a mass flow deposit in Marstranderbreen shales together with a prodelta palaeodepth as determined on the basis of foraminiferal assemblages, suggests its distal location with respect to a clastic source area.

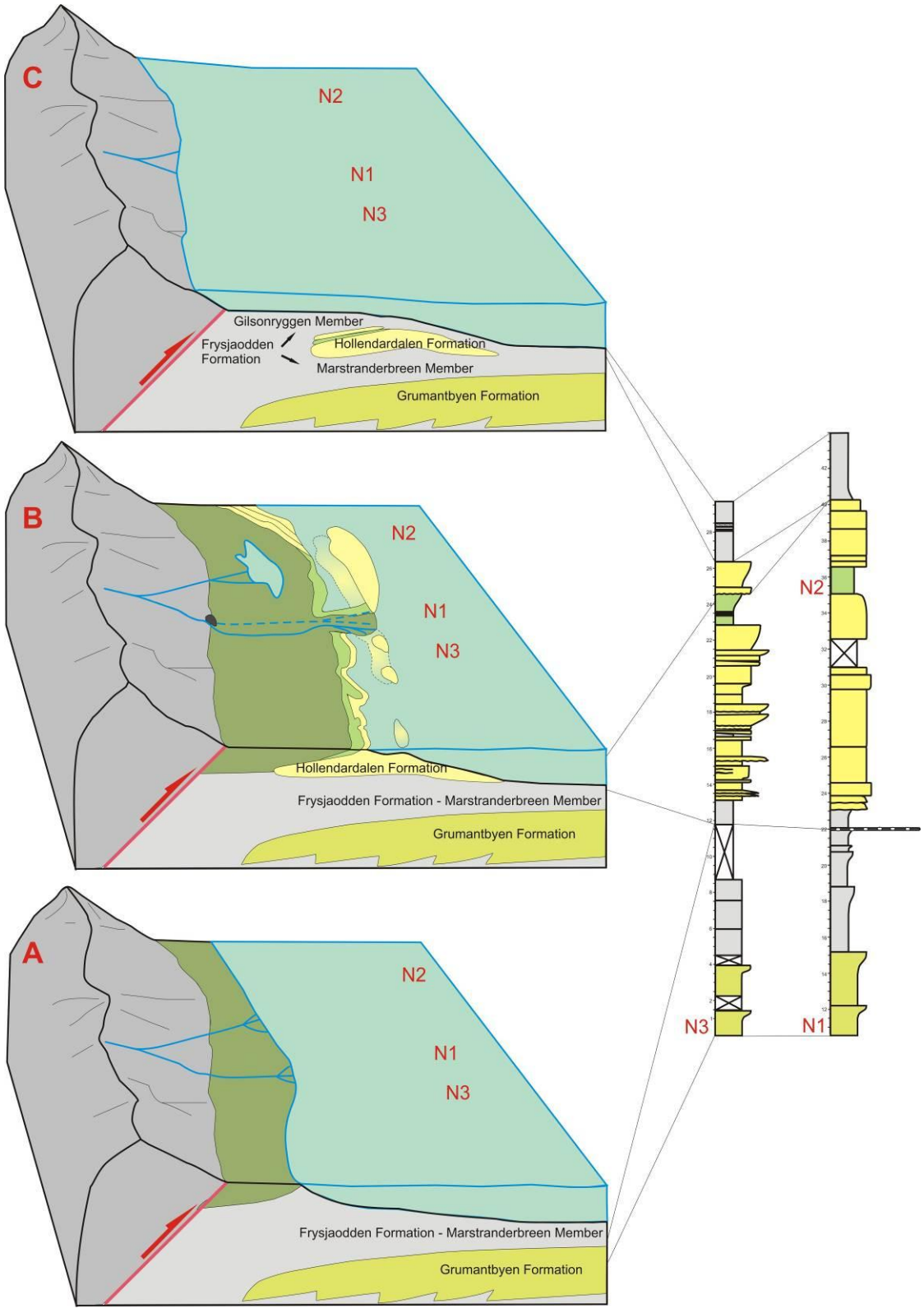

Figure 7-3: Suggested depositional model for upper Grumantbyen Formation to basal Gilsonryggen Member.

A: Configuration before the mass flow occurs in upper Marstranderbreen Member

B: Channel shifting due to mass flow event in upper Marstranderbreen Member. Configuration during deposition of Hollendardalen Formation (possible further channel shifting)

C: Transgressive development resulting in deposition of Gilsonryggen Member

Due to the regressive situation during the deposition of Hollendardalen Formation the feeding channel is interpreted as a delta rather than estuarine system, even though accumulation space and preservation potential might be higher in the case of an estuary.

The predominant facies in N1+2 are parallel bedded sandstones with occasional ripple lamination. Two intervals of hummocky cross stratified sandstones suggest storm events. Further up in the succession tabular cross stratification becomes a more dominant feature, indicating influence of currents and finally low angle cross bedded sandstones with rootlets mark the maximal regressive stage of an upper foreshore environment (see Reading 1996 for basic sedimentological interpretations). The absence of large scale cross stratified sandstones at supposed proximity to a deltaic river mouth may be explained by the shifting of the feeding channel. Due to consideration of palaeoflow directions in N1+2 and N3, it is suggested that the feeding channel shifted southwards. In N1 the 12m thick sandstone interval below the lagoonal facies (basal Hollendardalen Formation) shows evidence of north-westerly palaeoflow directions. Based on wave- and current-generated ripples in lower Hollendardalen of N3 easterly palaeoflow directions prevail. It is possible that the channel was blocked by larger boulders and debris further upstream in the course of the seemingly considerable mass flow event which occurred in upper Marstranderbreen Member. In this case accumulation space was created in form of the abandoned channel (Figure 7-3B).

In the offshore transition of section N3, inferred from the existence of turbidite-flow deposits, no extensive fair weather deposits (mudstones) are present. The stacking of storm wave generated beds, turbidites and tempestites which are extremely rich in plant fragments of suggested terrestrial origin, suggest the proximity of location N3 to a feeding channel.

It is however possible that the feeding channel shifted further during the deposition of Hollendardalen formation. The siltstone interval preceding foreshore deposits in N3 (at 18.5-19.7m) and a possible clay or siltstone interval in N1 (at 31-32.5m) form relatively abrupt changes into deeper environments, which are interpreted as a local phenomenon. The interval following the siltstone in section N3 is soft sediment deformed, very fine grained sandstone, suggesting very fast deposition, most likely occurring during the readjustment (lowering) of the relative sea level.

In N3 the coal interval is interpreted as most terrestrial influenced environment of Hollendardalen sandstones, while in N2 the maximum regressive surface is marked by the occurrence of rootlets at the top of low angle cross stratified upper foreshore deposits.

GILSONRYGGEN MEMBER

In N3 1.8m of transgressive very dirty Hollendardalen sandstones are present before the Gilsonryggen shales commence. At 1.7m into the shales three distinct bed forming sideritic concretions are found possibly marking a maximum flooding stage. In N2 the peak in total organic carbon and calcium carbonate at the base of the Gilsonryggen Formation (of minor magnitude due to generally very low values), suggest the existence of a condensed section and marks the transgressive surface or first major flooding following the maximal regressive stage at this location (illustration of transgressive stage of deposition in Figure 7-3C).

7.4 SHORELINE EVOLUTION AND SEQUENCE STRATIGRAPHY

On the basis of both sedimentary as well as foraminiferal analysis, depositional environments can be determined. Section N3 was the focus of our sedimentological analyses and was logged in detail in August 2007, while the foraminiferal interpretations are exclusively based on analyses of 1997 samples of N1+2. Figure 7-4 combines these sections and the environmental interpretations derived from litho- and biofacies, illustrating the evolution of the ancient shoreline in a sequence stratigraphic and depositional perspective. Some implications with respect to regressive and transgressive developments have been discussed already, but this chapter aims at treating sequence stratigraphy more systematically.

GRUMANTBYEN FORMATION

The upper two coarsening upwards units of the supposedly six small-scale Grumantbyen sequences (Bruhn and Steel 2003) are covered by the detailed log N3. Whether these sequences reflect changes in accommodation space due to the initial foreland basin formation or are glacially induced sea level changes remains to be resolved.

Another question that needs further investigation is the location of the maximum regressive surface which does not correspond to the boundary between Grumantbyen Formation and Marstranderbreen Member. The two coarsening upwards units are retrogradational parasequences of a transgressive systems tract. The maximum regressive surface is believed to be located shortly below the base of log N3. Samples from these intervals proved either barren of foraminifera or were extremely difficult to disintegrate. Therefore, further field logging is suggested to resolve this issue on the exact position of the sequence boundary.

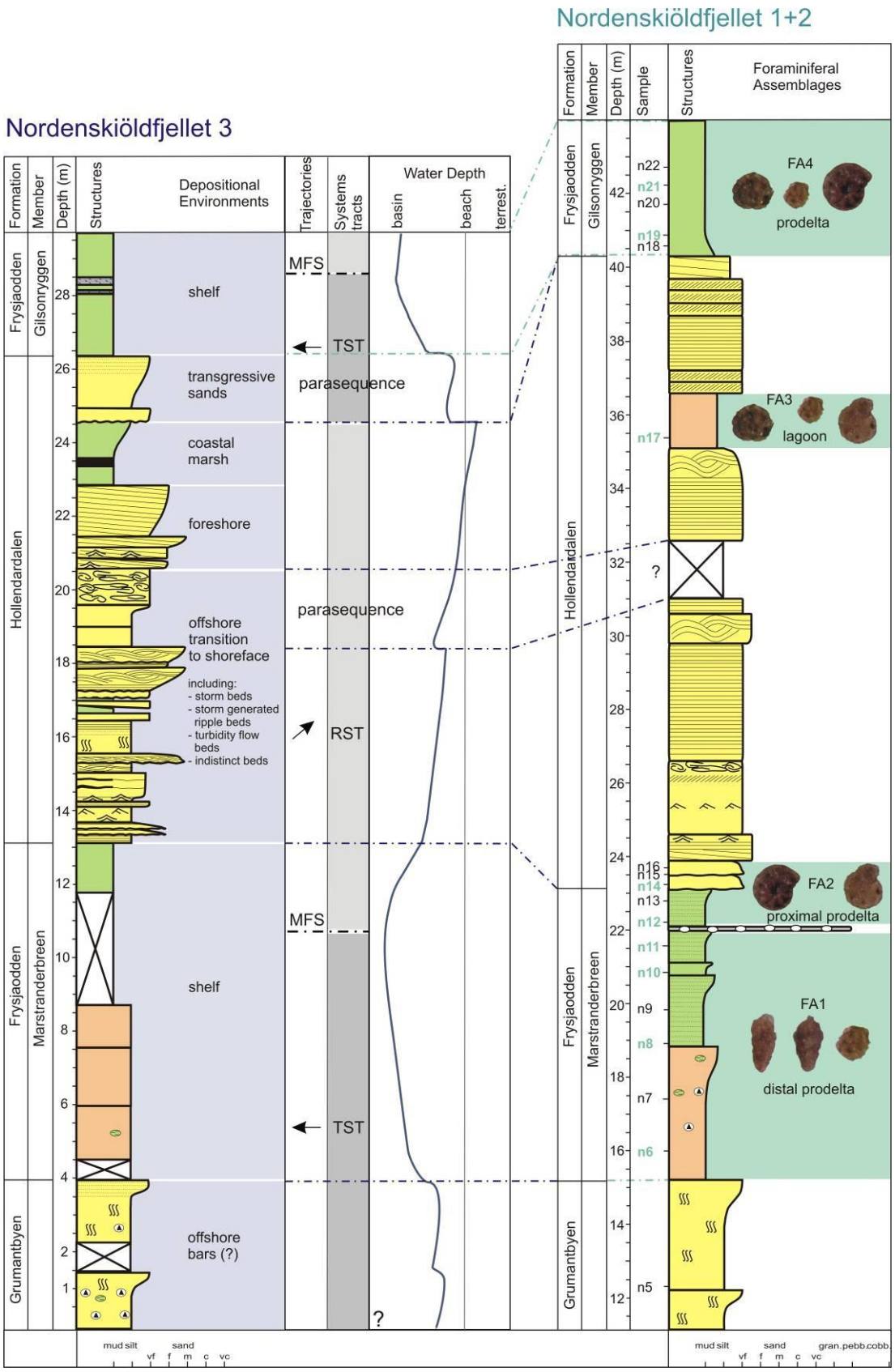

Figure 7-4: Shoreline evolution and sequence stratigraphic interpretation combined with summary of sedimentary and foraminiferal results. See previous logs for legend (Figure 5-1; Figure 5-2).

MARSTRANDERBREEN MEMBER

At the onset of the deposition of the Marstranderbreen Member the rise in relative sea level continues. The maximum flooding interval is determined on the basis of foraminiferal abundance and diversity, geochemical parameters as well as the lithology in Marstranderbreen mudstones. Foraminiferal abundance of 16.3g per gram dry sediment, reached in sample n10, is exceptionally high in the context of this study and amongst Marstranderbreen Member assemblages, species diversity is highest in sample n11 (Figure 6-1). Moreover boron and total organic carbon concentrations suggest a gradual deepening throughout upper Grumantbyen Formation and Marstranderbreen Member until the conglomerate deposit (Figure 5-22). Based on these proxies the 1.3m thick interval immediately below the conglomerate bed in N1 reflects the most open marine conditions.

Besides the general transgressive trend of lower Marstranderbreen Member, small-scale sequences could be inferred based on the lithology. Those cycles are represented by coarsening upwards siltstone and claystone intervals of 1m to 3.5m thickness. In section N3 where the exposure is younger, the coarsening upwards intervals do not suggest themselves from a distance as they do in section N1. Grain size variations determined through field measurements were not pronounced enough to include these small-scale cycles in the sequence stratigraphy.

HOLLENDARDALEN FORMATION

Hollendardalen Formation sandstones commence with turbidites resting directly on upper Marstranderbreen shales without clear erosional bases both in sections N3 and N1. These sands mark the advancing shoreline which was prograding from the west. Following two storm beds an interval consisting of siltstones to very fine, soft sediment deformed sandstones (at 18.5-20.5m in log N3) is deposited. These indistinct beds of deeper depositional environment are provisionary correlated to a possible mudstone interval in N1 and interpreted as parasequence. Following the parasequence, the shoreline progrades until the maximum regressive deposits are reached in both sections (coal interval in N3 and rootlet horizon in N2). In section N3 direct contact between the top of the coal bearing interval and a subsequent sandstone interval could be observed. The sandstone is rather poorly sorted and has an undulating, possibly erosional base, interpreted as the transgressive surface. The sand interval forms a coarsening upwards unit which is interpreted to represent

a parasequence. It may have been formed by the build out and break down of barrier islands causing fluctuations of local sea level in the course of general relative sea level rise.

GILSONRYGGEN MEMBER

In N3 the maximum flooding interval is determined on the basis of the occurrence of three bed forming sideritic concretions, deposited at level 28-28.5m. In N2 the transgressive surface coincides with the dark-grey shales deposited above the rootlet horizon. At N2 about 20cm above the base of Gilsonryggen Member, total organic carbon and calcium carbonate concentrations reach peak values, hinting to the existence of a condensed section. The maximum flooding interval in N2 can not be clearly determined on the basis of the two foraminiferal assemblages studied here (samples n19 and n21). According to the Shannon Weaver index these two samples show no significant difference in diversity. Species composition in sample n19 reflects a slightly deeper living fauna due to lower dominance and the joint importance of *Verneuilinoides durus*, *Labrospira turbida* and *Trochammina mellariolum*. For better determination of the maximum flooding interval in N2 a higher sample resolution would be needed.

8 CONCLUSIONS

The reconstruction of depositional environments of upper Grumantbyen Formation to basal Gilsonryggen Member is based on combined evidence from sedimentary field logging, geochemical analysis and study of foraminiferal assemblages. The studied sections are located on a south-northern axis (N3, N1, N2), along the ancient shoreline at distances of 350m between N3 and N1, and of 1000m between N3 and N2. The following conclusions can be drawn:

1. In upper Grumantbyen Formation two coarsening upwards units of highly bioturbated, glauconitic sandstones are interpreted as retrogradational deposits of shelf origin, possibly offshore bars. Chert pebble horizons without erosional base and individual chert pebble clasts observed in Grumantbyen Formation and Marstranderbreen Member suggest ice rafting as transport agent. This indicates the existence of marked seasonal cycles with low winter temperatures at palaeolatitude of 71° during a generally warm late Palaeocene greenhouse climate.

2. A conglomerate present in upper Marstranderbreen Member in section N1 is interpreted as mass flow deposit and indicates the proximity to a feeding channel. No evidence of mass flow impact could be found in section N3 in the correlative interval. Maximum flooding occurs in the 1.3m interval below the conglomerate as determined on the basis of foraminiferal species diversity, abundance, geochemical parameters and lithology. Retrogradational parasequences are indicated by coarsening upwards motives in the lower to middle Marstranderbreen mudstones.

3. The Hollendardalen sandstones in section N3 are interpreted as offshore transition to shoreface, and foreshore deposits. Hyperpycnal flows or subaerial slides triggered several turbidity flows. Two storm bed deposits rich in plant fragments imply the proximity to highly vegetated terrestrial environments. The maximal regressive environment is a coal seam interval, which rests on the foreshore deposits, and is interpreted as coastal marsh. The subsequent transgressive systems tract starts with a short interval of transgressive sands deposited with erosional base on the coastal marsh deposits.

4. The Hollendardalen sandstones in section N1+2 show different facies as compared to N3. The depositional model suggested here assumes that the feeding channel shifted to the south. The accumulation space at N1 in form of an abandoned channel has

subsequently been filled with predominantly parallel bedded sandstones which accounts for the greater thickness of Hollendardalen in N1+2 than in N3. A siltstone interval in N2 is interpreted as a lagoonal deposit on the basis of its foraminiferal content. The overlying sandstones with root horizons towards the top mark the maximum regressive stage in N2.

5. In N1, at 1.7m into the Gilsonryggen mudstones, the maximum flooding interval is indicated by the existence of bed forming sideritic concretions. In section N2 the root horizon sandstones are directly followed by Gilsonryggen mudstones and maximum values of total organic carbon and calcium carbonate suggest a condensed section coinciding with the transgressive surface. In N2 the maximum flooding is suspected to occur shortly above the base of Gilsenryggen mudstones as suggested by the foraminiferal fauna.

9 TAXONOMY

Taxonomic determinations follow the classification of Loeblich and Tappan (1988). The listing order reflects the taxonomic scheme. First describer and year are given for each taxonomic unit. If the nomenclature has changed, authors are given in parentheses.

For those species that were relevant in the study quantitatively or qualitatively, digital photographs have been taken under the light microscope. The cross-reference to plate and figure is given after the taxonomic citations on species' level.

For foraminifera with full nomenclature and those with affinity to a species (aff.), the reference is given based on which they have been identified. These citations also include the specification of plate and figure numbers and these sources are included in the reference list.

Order FORAMINIFERIDA Eichwald, 1830
Suborder TEXTULARIINA Delage and Hérouard, 1896
Superfamily ASTRORHIZACEA Brady, 1881
Family BATHYSIPHONIDAE Avnimelech, 1952
Genus *Bathysiphon* Sars, 1872
***Bathysiphon* sp.**
Plate 1, Figure 1

Family RHABDAMMINIDAE Brady, 1884
Subfamily RHABDAMMININAE Brady, 1884
Genus *Rhizammina* Brady, 1879
***Rhizammina* sp.**

Family PSAMMOSPHAERIDAE Haeckel, 1894
Subfamily PSAMMOSPHAERINAE Haeckel, 1894
Genus *Psammosphaera* Schulze, 1875
Psammosphaera* aff. *fusca Schulze, 1875
Plate 1, Figure 3
aff. *Psammosphaera fusca* Schulze – Schröder-Adams and McNeil 1994, Plate 2, figures 7-9

Family SACCAMMINIDAE Brady, 1884
Subfamily SACCAMMININAE Brady, 1884
Genus *Saccammina* Carpenter, 1869
***Saccammina* sp.**

Subfamily THURAMMININAE Miklukho-Maklay, 1963
Genus *Thurammina* Brady, 1879
Thurammina* aff. *papillata Brady, 1879
Plate 1, Figure 4
aff. *Thurammina papillata* Brady – Nagy et al. 2000, Plate 2, figures 11, 12

Family HEMISPHAERAMMINIDAE Loeblich and Tappan, 1961
Subfamily CRITHIONININAE Hofker, 1972
Genus *Crithionina* Goës, 1894
***Crithionina* sp.**
Plate 1, Figure 5

Superfamily HIPPOCREPINACEA
Family HIPPOCREPINIDAE
Subfamily HYPERAMMININAE
Genus *Hyperammina* Brady, 1878
Hyperammina* aff. *elongata Brady, 1878
Plate 1, Figure 2
aff. *Hyperammina elongata* Brady 1878, Plate 20, Figure 2

Superfamily AMMODISCACEA Reuss, 1862
Family AMMODISCIDAE Reuss, 1862
Subfamily AMMODISCINAE Reuss, 1862
Genus *Ammodiscus* Reuss, 1862
Ammodiscus tenuissimus Grzybowski, 1898
Plate 1, Figure 11
Ammodiscus tenuissimus Grzybowski, Schröder-Adams and McNeil 1994,
Plate 3, figures 4a,b

Superfamily HORMOSINACEA Haeckel, 1894
Family HORMOSINIDAE Haeckel, 1894
Subfamily REOPHACINAE Cushman, 1910
Genus *Reophax* de Montfort, 1808
Reophax* aff. *fusiformis (Williamson, 1858)
aff. *Proteonina fusiformis* Williamson 1858, Plate 1, Figure 1

Superfamily LITUOLACEA de Blainville, 1827
Family HAPLOPHRAGMOIDIDAE Maync, 1952
Genus *Haplophragmoides* Cushman, 1910
Haplophragmoides richardsensis McNeil, 1997
Haplophragmoides richardsensis McNeil 1997, Plate 3, figures 3a,b; 4a,b

Haplophragmoides multicubiculus McNeil, 1997
Plate 1, Figure 14
Haplophragmoides multicubiculus McNeil 1997, Plate 2, figures 2a,b; 3a-c; 4a,b

Haplophragmoides perexilis McNeil, 1997
Haplophragmoides perexilis McNeil 1997, Plate 2, figures 5a-c; 6a-c; 7a-c

***Haplophragmoides* sp.**

Genus *Labrospira* Höglund, 1947
Labrospira turpicula McNeil, 1997
Plate 1, Figure 7
Labrospira turpicula McNeil 1997, Plate 3, figures 8a-c; 9; Plate 4, figures 1a,b; 2a,b

Labrospira turbida Schröder-Adams and McNeil, 1994
Plate 1, Figure 6
Labrospira turbida Schröder-Adams and McNeil – Nagy et al. 2000, Plate 1, figures 11-13

***Labrospira* sp.**
Plate 1, Figure 8

Family LITUOLIDAE de Blainville, 1827
Subfamily AMMOMARGINULININAE Podobina, 1978
Genus *Ammobaculitis* Cushman, 1910
***Ammobaculitis* sp.1**
Plate 1, Figure 9

***Ammobaculitis* sp.2**
Plate 1, Figure 10

Genus *Ammotium* Loeblich and Tappan, 1953
***Ammotium* sp.**

Superfamily LOFTUSIACEA Brady, 1884
Family CYCLAMMINIDAE Marie, 1941
Subfamily ALVEOLOPHRAGMIINAE Saidova, 1981
Genus *Reticulophragmium* Maync, 1955
Reticulophragmium arcticum (Petracca, 1972)
Plate 1, Figure 16
Cyclammina arctica Petracca 1972, Plate 1, figures 1-4
Reticulophragmium arcticum Petracca – Nagy et al. 2000, Plate 1, figures 14-17;
Plate 2, figures 20,21

Reticulophragmium borealis (Petracca, 1972)
Plate 1, Figure 15
Cyclammina borealis Petracca 1972, Plate 1, figures 5,6

Reticulophragmium ministicoogense McNeil, 1997
Plate 1, Figure 17
Reticulophragmium ministicoogense McNeil 1997, Plate 6, figures 1a,b; 2a-c; 3a,b; 4; 5a,b

Superfamily TROCHAMMINACEA Schwager, 1877
Family TROCHAMMINIDAE Schwager, 1877
Subfamily TROCHAMMININAE Schwager, 1877
Genus *Trochammina* Parker and Jones, 1859
Trochammina rutherfordi mellariolum Eicher, 1965
Plate 1, Figure 12
Trochammina rutherfordi mellariolum Eicher – Nagy et al. 2000, Plate 2, Figure 23

Trochammina perlevis McNeil, 1997
Plate 1, Figure 13
Trochammina perlevis McNeil 1997, Plate 8, figures 6a-d; 7a-c; Plate 9, figures 1a-c; 2a-c

Superfamily LOFTUSIACEA Brady, 1884
Family CYCLAMMINIDAE Marie, 1941
Subfamily CYCLAMMININAE Marie, 1941
Genus *Cyclammina* Brady, 1879
Cyclammina* aff. *cyclops McNeil, 1988
Plate 1, Figure 18
aff. *Cyclammina cyclops* McNeil – Schröder-Adams and McNeil 1994, Plate 8, figures 8a-c

remarks: *Cyclammina cyclops* is first reported in Late Eocene by McNeil (1997). The species reported here has a slightly different morphology; less chambers and less open umbilicus; but clearly has more chambers and a more open umbilicus than *Reticulophragmium borealis* and *arcticum*.

Superfamily VERNEUILINACEA Cushman, 1911
Family VERNEUILINIDAE Cushman, 1911
Subfamily VERNEUILINOIDINAE Suleymanov, 1973
Genus *Verneuilinoides* Loeblich and Tappan, 1949
Verneuilinoides distentus McNeil, 1997
Verneuilinoides distentus McNeil 1997, Plate 10, figures 2a,b; 3a,b; 4a,b

Verneuilinoides durus McNeil, 1997
Plate 1, Figure 20
Verneuilinoides durus McNeil 1997, Plate 10, figures 5a-c; 6a-c; 7a-c; 8a-c

Verneuilinoides exvadum McNeil, 1997
Plate 1, Figure 19
Verneuilinoides exvadum McNeil 1997, Plate 11, figures 1a-c; 2a-c; 3a-c; 4a-c

Subfamily ATAXOPHRAGMIACEA Schwager, 1877
Family ATAXOPHRAGMIIDAE Schwager, 1877
Subfamily ATAXOPHRAGMIINAE Schwager, 1877
Genus *Convallina*, McNeil, 1997
Convallina elongata McNeil, 1997
Plate 1, Figure 21
Convallina elongata McNeil 1997, Plate 12, figures 5a-c; 6a-c; Plate 13, figures 1a,b; 2a-c

Convallina* aff. *logani McNeil, 1997
Plate 1, Figure 22
aff. *Convallina logani* McNeil 1997, Plate 13, figures 3a-c; 4a-d; 5a-c

REFERENCES

Bouma, A.H. 1962. *Sedimentology of some Flysch deposits: a graphic approach to facies interpretation*, Amsterdam: Elsevier. 168 pp.

Brady, H.B. 1878. On the reticularian and radiolarian Rhizopoda (Foraminifera and Polycystina) of the North Polar Expedition of 1875-76. *Annals and Magazine of Natural History* 1 (5), 425-550.

Brinkhuis, H., Schouten, S., Collinson, M.E., Sluijs, A., Sinninghe Damsté, J.S., Dickens, G.R., Huber, M., Cronin, T.M., Onodera, J., Takahashi, K., Bujak, J.P., Stein, R., van der Burgh, J., Eldrett, J.S., Harding, I.C., Lotter, A.F., Sangiorgi, F., van Konijnenburg-van Cittert, H., de Leeuw, J.W., Matthiessen, J., Backman, J., Moran, K. and the Expedition 302 Scientists. 2006. Episodic fresh surface waters in the Eocene Arctic Ocean. *Nature* 441 (1), 606-609.

Bruhn, R. and Steel, R. 2003. High-resolution sequence stratigraphy of a clastic foredeep succession (Paleocene, Spitsbergen): An example of peripheral-bulge-controlled depositional architecture. *Journal of Sedimentary Research* 73 (5), 745-755.

Buzas, M.A. and Gibson, T.G. 1969. Species diversity; benthic Foraminifera in Western North Atlantic. *Science, American Association for the Advancement of Science* 163 (72-75).

Cheel, R.J. and Leckie, D.A. 1993. Hummocky cross-stratification. *Sedimentology review* 1, 103-122.

Crouch, E.M., Dickens, G.R., Brinkhuis, H., Aubry, M.P., Hollis, C.J., Rogers, K.M. and Visscher, H. 2003. The Apectodinium acme and terrestrial discharge during the Paleocene-Eocene thermal maximum: new palynological, geochemical and calcareous nannoplankton observations at Tawanui, New Zealand. *Palaeogeography Palaeoclimatology Palaeoecology* 194 (4), 387-403.

Crouch, E.M., Heilmann-Clausen, C., Brinkhuis, H., Morgans, H.E.G., Rogers, K.M., Egger, H. and Schmitz, B. 2001. Global dinoflagellate event associated with the late Paleocene thermal maximum. *Geology* 29 (4), 315-318.

Curtis, C.D. 1975. *Studies on the use of boron as a paleoenvironmental indicator*. *In* Walker, C.T. (ed). Geochemistry of Boron. Benchmark Papers in Geology. 23. Stroudsburg: Dowden, Hutchinson& Ross Inc.

Dalland, A. 1976. Erratic clasts in the Lower Tertiary deposits of Svalbards - evidence of transport by winter ice. *Årbok - Norsk Polarinstitutt* 1976, 151.165.

Dallmann, W.K., Midbøe, P.S., Nøttvedt, A. and Steel, R.J. 1999. *Tertiary lithostratigraphy*. *In* Dallmann, W.K. (ed). Lithostratigraphic Lexicon of Svalbard, 215-263.

Dewis, F.J., Levinson, A.A. and Bayliss, P. 1975. *Hydrogeochemistry of the Surface Waters of the Mackenzie River Drainage Basin, Canada: IV. Boron-Salinity-Clay Mineralogy Relationship in Modern Deltas*. *In* Walker, C.T. (ed). Geochemistry of

Boron. Benchmark Papers in Geology. 23. Stroudsburg: Dowden, Hutchinson& Ross Inc.

Eldrett, J.S., Harding, I.C., Wilson, P.A., Butler, E. and Roberts, A.P. 2007. Continental ice in Greenland during the Eocene and Oligocene. *Nature* 446 (7132), 176-179.

Fisher, R.A., Corbet, A.S. and Williams, C.B. 1943. The relationship between the number of species and the number of individuals in a random sample of an animal population. *Journal of Animal Ecology* 12, 42-58.

Galloway, W.E. 1989. Genetic stratigraphic sequences in basin analysis I: Architecture and genesis of flooding-surface bounded depositional units. *AAPG Bulletin* 73, 125-142.

Håkansson, E. and Pedersen, S.A.S. 2001. The Wandel Hav Strike-Slip Mobile Belt - A Mesozoic plate boundary in North Greenland. *Bulletin of the Geological Society of Denmark* 48, 149-158.

Hammer, Ø., Harper, D.A.T. and Ryan, P.D. 2001. Past: Paleontological Statistics Software Package for Education and Data Analysis. *Palaeontological Electronica* 4 (1), 9pp.

Harder, H. 1975a. *Boron Content of Sediments as a Tool in Facies Analysis*. *In* Walker, C.T. (ed). Geochemistry of Boron. Benchmark Papers in Geology. 23. Stroudsburg: Dowden, Hutchinson& Ross Inc.

Harder, H. 1975b. *Contribution to the Geochemistry of Boron: II. Boron in Sediments*. *In* Walker, C.T. (ed). Geochemistry of Boron. Benchmark Papers in Geology. 23. Stroudsburg: Dowden, Hutchinson& Ross Inc.

Harding, I.C., Marshall, J.E.A., Pälike, H., Wilson, P.A., Roberts, A.P., Jarvis, E., Thorne, R., Morris, E., Moremon, R., Pearce, R. and Akbari, S. 2007. *Sea ice during the Palaeocene/Eocene thermal maximum in the high Arctic*: School of Ocean and Earth Science, University of Southampton.

Helland-Hansen, W. 1990. Sedimentation in Paleogene Foreland Basin, Spitsbergen. *The American Association of Petroleum Geologists Bulletin* 74 (3), 273-295.

Helland-Hansen, W. and Martinsen, O.J. 1996. Shoreline trajectories and sequences: description of variable depositional-dip scenarios. *Journal of Sedimentary Research* 66, 670-688.

Jones, R.W. and Charnock, M.A. 1985. 'Morphogroups' of agglutinated Foraminifera. Their life positions and feeding habits and potential applicability in (paleo)ecological studies. *Revue de Paléobiologie* 4, 311-320.

Livšic, J.J. 1967. *Tertiary deposits in the western part of the Archipelago of Svalbard*. *In* Sokolov, V.N. (ed). Materialy po stratigrafii Špicbergena. Leningrad: NIIGA, 185-204.

Livšic, J.J. 1974. Paleogene deposits and the platform structure of Svalbard. *Norsk Polarinstitutt Skrifter* 159, 1-50.

Loeblich, A.R. and Tappan, H. 1988. *Foraminiferal genera and their classification*. New York. Van Nostrand Reinhold Company. 970 pp.

Major, H. and Nagy, J. 1964. *Adventdalen. Geologisk kart*. Norsk Polarinstitutt.

Major, H. and Nagy, J. 1972. Geology of the Adventdalen map area. *Norsk Polarinstitutt Skrifter* 138, 1-58.

Manum, S.B. and Throndsen, T. 1978. Rank of coal and dispersed organic matter and its geological bearing in the Spitsbergen Tertiary. *Norsk Polarinstitutt Årbok 1977*, 159-177.

Manum, S.B. and Throndsen, T. 1986. Age of Tertiary formations. *Polar Research* 4 (1), 103-131.

McNeil, D.H. 1996a. *Distribution of Albian to Maastrichtian benthic foraminifers in the Beaufort-Mackenzie Basin*. *In* Dixon, J. (ed). Geological Atlas of the Beaufort-Mackenzie Area: Geological Survey of Canada, Miscellaneous Report, 59, fig.69.

McNeil, D.H. 1996b. *Distribution of Cenozoic agglutinated benthic foraminifers in the Beaufort-Mackenzie Basin*. *In* Dixon, J. (ed). Geological Atlas of the Beaufort-Mackenzie Area: Geological Survey of Canada, Miscellaneous Report, 59, fig.70.

McNeil, D.H. 1997. *New Foraminifera from the Upper Cretaceous and Cenozoic of the Beaufort-Mackenzie Basin of Arctic Canada*. Edited by Culver, S.J. Special Publication No. 35, London: Cushman Foundation for Foraminiferal Research.

Mellere, D., Plink-Bjorklund, P. and Steel, R. 2002. Anatomy of shelf deltas at the edge of a prograding Eocene shelf margin, Spitsbergen. *Sedimentology* 49 (6), 1181-1206.

Middleton, G.V. 1973. Johannes Walther's Law of the Correlation of Facies. *Geological Society of America Bulletin* 84 (3), 979-987.

Miller, K.G., Wright, J.D. and Browning, J.V. 2005. Visions of ice sheets in a greenhouse world. *Marine Geology* 217 (3-4), 215-231.

Moran, K., Backman, J., Brinkhuis, H., Clemens, S.C., Cronin, T., Dickens, G.R., Eynaud, F., Gattacceca, J., Jakobsson, M., Jordan, R.W., Kaminski, M., King, J., Koc, N., Krylov, A., Martinez, N., Matthiessen, J., McInroy, D., Moore, T.C., Onodera, J., O'Regan, M., Palike, H., Rea, B., Rio, D., Sakamoto, T., Smith, D.C., Stein, R., St John, K., Suto, I., Suzuki, N., Takahashi, K., Watanabe, M., Yamamoto, M., Farrell, J., Frank, M., Kubik, P., Jokat, W. and Kristoffersen, Y. 2006. The Cenozoic palaeoenvironment of the Arctic Ocean. *Nature* 441 (7093), 601-605.

Murray, J.W. 1973. *Distribution and Ecology of Living Benthic Foraminiferids*, London: Heinemann Educational Books.

Murray, J.W. 1991. *Ecology and Palaeoecology of Benthic Foraminifera*, Essex: Longman Scientific& Technical.

Murray, J.W. 2006. *Ecology and Applications of Benthic Foraminifera*, Cambridge: Cambridge University Press.

Nagy, J. 1992. Environmental significance of foraminiferal morphogroups in Jurassic North-Sea deltas. *Palaeogeography Palaeoclimatology Palaeoecology* 95 (1-2), 111-134.

Nagy, J. 2005. Delta-influenced foraminiferal facies and sequence stratigraphy of Paleocene deposits in Spitsbergen. *Palaeogeography Palaeoclimatology Palaeoecology* 222 (1-2), 161-179.

Nagy, J. 2007. *Microfossils. Facies and Stratigraphy*. *In* Nagy, J. (ed). GEO4220 Depositional environments and stratigraphy. Oslo: Unipub AS, 3-26.

Nagy, J., Kaminski, M.A., Kuhnt, W. and Bremer, M.A. 2000. *Agglutinated Foraminifera from Neritic to Bathyal Facies in the Palaeogene of Spitsbergen and the Barents Sea*. *In* Hart, M.B., Kaminski, M.A. and Smart, C.W. (eds). Proceedings of the Fifth International Workshop on Agglutinated Foraminifera: Grzybowski Foundation Special Publication, 7, 333-361.

Nagy, J., Pilskog, B. and Wilhelmsen, R. 1990. *Facies controlled distribution of foraminifera in the Jurassic North Sea Basin*. *In* Hemleben, C. and et al. (eds). Paleoecology, Biostratigraphy, Paleoceanography and Taxonomy of Agglutinated Foraminifera. Dordrecht: Kluwer Academic Publishers, 969-1015.

Pagani, M., Caldeira, K., Archer, D. and Zachos, J.C. 2006. An ancient carbon mystery. *Science* 314 (5805), 1556-1557.

Petracca, A.N. 1972. Tertiary microfauna, Mackenzie delta area, arctic Canada. *Micropaleontology* 18 (3), 355-368.

Plink-Björklund, P. 2005. Stacked fluvial and tide-dominated estuarine deposits in high-frequency (fourth-order) sequences of the Eocene Central Basin, Spitsbergen. *Sedimentology* 52 (2), 391-428.

Plink-Björklund, P. and Steel, R.J. 2004. Initiation of turbidity currents: outcrop evidence for Eocene hyperpycnal flow turbidites. *Sedimentary Geology* 165, 29-52.

Podobina, V.M. 2000. *Palaeogene agglutinated foraminifera of the West Siberian biogeographical province*. *In* Hart, M.B., Kaminski, M.A. and Smart, C.W. (eds). Proceedings of the Fifth International Workshop on Agglutinated Foraminifera: Grzybowski Foundation Special Publication, 7, 387-396.

Reading, H.G. 1996. *Sedimentary environments: processes, facies, and stratigraphy*. 3rd ed, Oxford: Blackwell Science Ltd.

Sanders, H.L. 1960. Benthic studies in Buzzards Bay III: The structure of the soft-bottom community. *Limnology and Oceanography* 5, 138-153.

Schröder-Adams, C.J. and McNeil, D.H. 1994. *Oligocene to Miocene Agglutinated Foraminifera in deltaic and deep-water facies of the Beaufort-Mackenzie Basin*. Bulletin 477, Ottawa/ Calgary: Geological Survey of Canada. 66 pp.

Schweitzer, H.-J. 1980. Environment and climate in the Early Tertiary of Spitsbergen. *Palaeogeography Palaeoclimatology Palaeoecology* 30, 297-311.

Shipboard Scientific Party. 2004. *Leg 208 summary*. *In* Zachos, J.C., Kroon, D. and Blum, P. (eds). Proceedings of the Ocean Drilling Program, Initial Reports. College Station: RX (Ocean Drilling Program), 208.

Sluijs, A., Schouten, S., Pagani, M., Woltering, M., Brinkhuis, H., Sinninghe Damsté, J.S., Dickens, G.R., Huber, M., Reichart, G.-J., Stein, R., Matthiessen, J., Lourens, L.J., Pedentchouk, N., Backman, J., Moran, K. and the Expedition 302 Scientists. 2006. Subtropical Arctic Ocean temperatures during the Palaeocene/Eocene thermal maximum. *Nature* 441 (1 June 2006), 610-613.

Steel, R.J., Dalland, A., Kalgraff, K. and Larsen, V. 1981. *The central Tertiary basin of Spitsbergen: sedimentary development in a sheared margin basin*. *In* Kerr, J.W. and Fergusson, A.J. (eds). Geology of the North Atlantic Borderlands: Canadian Society of Petroleum Geologists, Memoir 7, 647-664.

Steel, R.J., Gjelberg, J., Helland-Hansen, W., Kleinspehn, K., Nøttvedt, A. and Rye-Larsen, M. 1985. The Tertiary strike-slip basins and orogenic belt of Spitsbergen. *The Society of Economic Paleontologists and Mineralogists* Special Publication 37, 339-360.

Walther, J. 1893-1894. *Einleitung in die Geologie als historische Wissenschaft*. 3 vol, Jena: Gustav Fischer Verlag. 1055 pp.

Williamson, W.C. 1858. *On the Recent Foraminifera of Great Britain*, London: Ray Society. 107 pp.

Wright, C.A. and Murray, J.W. 1972. Comparisons of modern and Palaeogene foraminiferid distributions and their environmental implications. *Mém BRGM* 79, 87-96.

Zachos, J.C., Bohaty, S.M., John, C.M., McCarren, H., Kelly, D.C. and Nielsen, T. 2007. The Palaeocene-Eocene carbon isotope excursion: constraints from individual shell planktonic foraminifer records. *Philosophical Transactions of the Royal Society a-Mathematical Physical and Engineering Sciences* 365 (1856), 1829-1842.

Zachos, J.C., Lohmann, K.C., Walker, J.C.G. and Wise, S.W. 1993. Abrupt climate change and transient climates during the Paleogene: A marine perspective. *Journal of Geology* 101, 191-213.

Zachos, J.C., Schouten, S., Bohaty, S., Quattlebaum, T., Sluijs, A., Brinkhuis, H., Gibbs, S.J. and Bralower, T.J. 2006. Extreme warming of mid-latitude coastal ocean during the Paleocene-Eocene Thermal Maximum: Inferences from TEX86 and isotope data. *Geology* 34 (9), 737-740.

PLATE 1

PLATE 1 – LEGEND

1. *Bathysiphon* sp.: length 370µm, sample n11.
2. *Hyperammina* aff. *elongata* Brady, 1878: length 510µm, sample n21.
3. *Psammosphaera* aff. *fusca* Schulze, 1875: diameter 340µm, sample n17.
4. *Thurammina* aff. *papillata* Brady, 1879: diameter 430µm, sample n6.
5. *Crithionina* sp.: longest diameter 460µm, sample n14.
6. *Labrospira turbida* Schröder-Adams and McNeil, 1994: 430µm, sample n14.
7. *Labrospira turpicula* McNeil, 1997: 360µm, sample n6.
8. *Labrospira* sp.: 120µm, sample n10.
9. *Ammobaculitis* sp.1: length 390µm, sample n21.
10. *Ammobaculitis* sp.2: length 830µm, sample n21.
11. *Ammodiscus tenuissimus* Grzybowski, 1898: diameter 180µm, sample n8.
12. *Trochammina mellariolum* Eicher, 1965: diameter 140µm, sample n19.
13. *Trochammina perlevis* McNeil, 1997: diameter 230µm, sample n19.
14. *Haplophragmoides multicubiculus* McNeil, 1997: 700µm, sample n8.
15. *Reticulophragmium borealis* (Petracca, 1972) : 1490µm, sample n12.
16. *Reticulophragmium arcticum* (Petracca, 1972) : 610µm, sample n12.
17. *Reticulophragmium ministicoogense* McNeil, 1997: 460µm, sample n10.
18. *Cyclammina* aff. *cyclops* McNeil, 1988: 530µm, sample n10.
19. *Verneuilinoides exvadum* McNeil, 1997: length 430µm, sample n6.
20. *Verneuilinoides durus* McNeil, 1997: length 470µm, sample n8.
21. *Convallina elongata* McNeil, 1997: length 720µm, sample n8.
22. *Convallina* aff. *logani* McNeil, 1997: length 530µm, sample n14.

PLATE 1

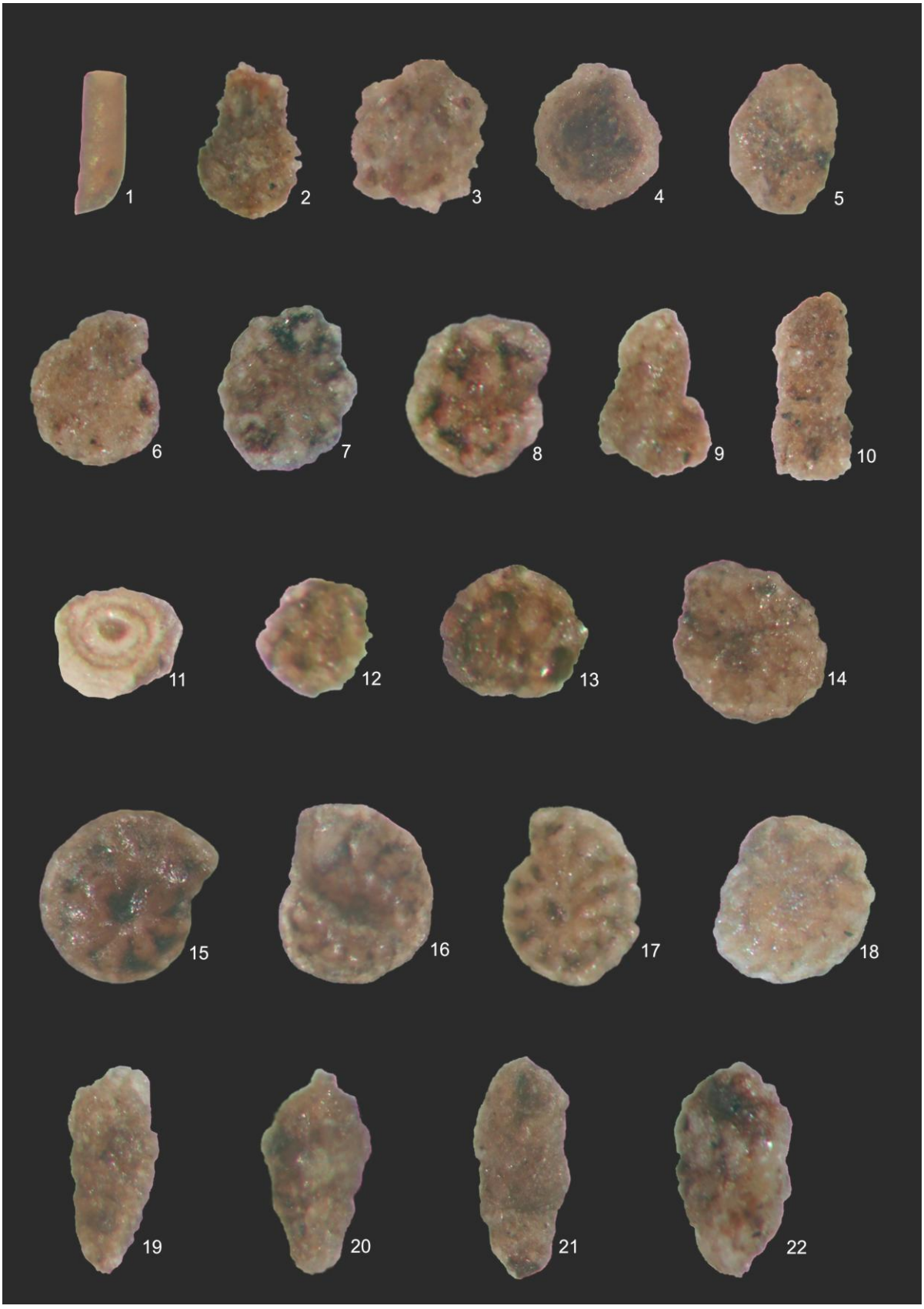

APPENDICES 1-10

APPENDIX 1: LOGGING SHEET

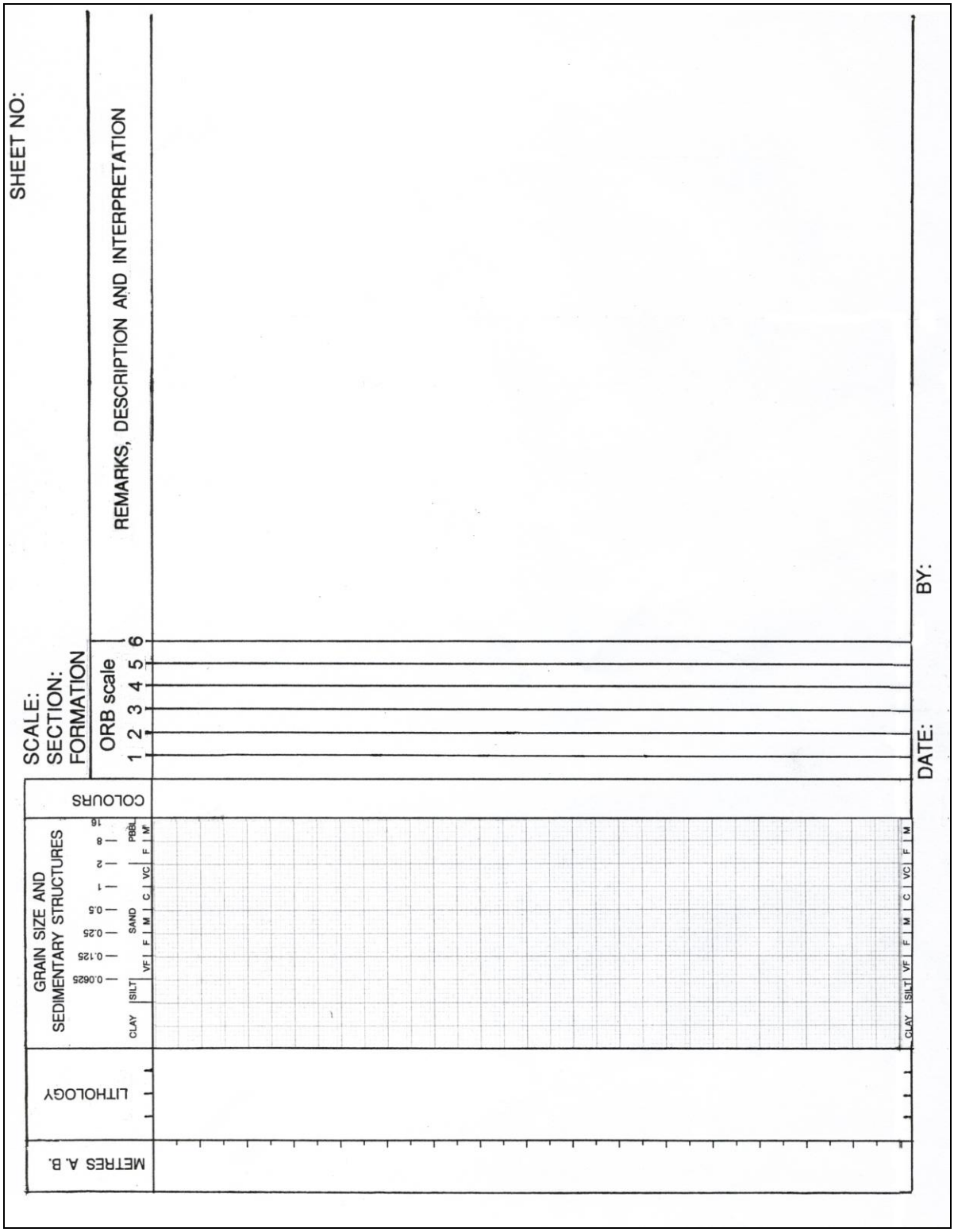

APPENDIX 2: RENAMING OF SAMPLES

short IDs	IDs of 1997 samples
n1	N-1-2-97
n2	N-1-4-97
n3	N-1-5-97
n4	N-1-6-97
n5	N-1-7-97
n6	N-1-9-97
n7	N-1-11-97
n8	N-1-13-97
n9	N-1-15-97
n10	N-1-17-97
n11	N-1-19-97
n12	N-1-21-97
n13	N-1-24-97
n14	N-1-26-97
n15	N-2-2-97
n16	N-1-28-97
n17	N-2-3-97
n18	N-2-6-97
n19	N-2-8-97
n20	N-2-10-97
n21	N-2-11-97
n22	N-2-12-97

short IDs	IDs of 2007 samples
s0	N-3-0-07
s1	N-3-1-07
s2	N-3-2-07
s3	N-3-3-07
s4	N-3-4-07
s5	N-3-5-07
s6	N-3-6-07
s7	N-3-7-07
s8	N-3-8-07
s9	N-3-9-07
s10	N-3-10-07
s11	N-3-11-07
s12	N-3-12-07
s13	N-3-13-07
s14	N-3-14-07
s15	N-3-15-07
s16	N-3-16-07
s17	N-3-17-07
s18	N-3-18-07
s19	N-3-19-07
s20	N-3-20-07
s21	N-3-21-07
s22	N-3-22-07
s23	N-3-23-07
s24	N-3-24-07
s25	N-3-25-07
s26	N-3-26-07
s27	N-3-27-07
s28	N-3-28-07
s29	N-3-29-07

APPENDIX 3: BORON

Sample	Boron (ppm)	Boron (g)
n22	123	0.593
n21	154	0.559
n20	158	0.543
n19	99.2	0.505
n18	93	0.516
n17	122	0.523
n16	106	0.52
n15	91.7	0.502
n14	106	0.547
n13	128	0.537
n12	144	0.522
n11	122	0.584
n10	128	0.566
n9	101	0.535
n8	91.9	0.55
n7	80	0.594
n6	96.2	0.524
n5	73.8	0.526
n4	77.1	0.554
n3	77.8	0.534
n2	74.7	0.556
n1	58.9	0.54
Min	58.9	0.502
Max	158	0.594
Mean	104.8	0.542
StdD	27.1	0.026

APPENDIX 4: TOTAL ORGANIC CARBON, TOTAL INORGANIC CARBON AND CALCIUM CARBONATE

Sample	TC (%)	std error	TOC (%)	std error	TIC (%)	std error	$CaCO_3$ (%)	std error
n22	1.53	± 0.02	1.53	± 0.02	0	± 0.000	0.00	± 0.00
n21	1.42	± 0.01	1.47	± 0.01	-0.05	± 0.001	-0.40	± 0.05
n20	1.17	± 0.01	1.13	± 0.01	0.04	± 0.001	0.33	± 0.04
n19	2.56	± 0.03	2.38	± 0.02	0.18	± 0.003	1.50	± 0.18
n18	2.39	± 0.02	2.4	± 0.02	-0.01	± 0.000	-0.08	± 0.01
n17	0.83	± 0.01	0.82	± 0.01	0.01	± 0.000	0.08	± 0.01
n16	1.05	± 0.01	1.04	± 0.01	0.01	± 0.000	0.08	± 0.01
n15	0.87	± 0.01	0.81	± 0.01	0.06	± 0.001	0.50	± 0.06
n14	1.44	± 0.01	1.44	± 0.01	0	± 0.000	0.00	± 0.00
n13	2.04	± 0.02	2.04	± 0.02	0	± 0.000	0.00	± 0.00
n12	1.16	± 0.01	1.14	± 0.01	0.02	± 0.000	0.17	± 0.02
n11	1.42	± 0.01	1.35	± 0.01	0.07	± 0.001	0.58	± 0.07
n10	1.32	± 0.01	1.32	± 0.01	0	± 0.000	0.00	± 0.00
n9	1.25	± 0.01	1.27	± 0.01	-0.02	± 0.000	-0.17	± 0.02
n8	1.11	± 0.01	1.08	± 0.01	0.03	± 0.000	0.25	± 0.03
n7	0.76	± 0.01	0.77	± 0.01	-0.01	± 0.000	-0.08	± 0.01
n6	0.89	± 0.01	0.89	± 0.01	0	± 0.000	0.00	± 0.00
n5	0.65	± 0.01	0.63	± 0.01	0.02	± 0.000	0.17	± 0.02
n4	0.74	± 0.01	0.71	± 0.01	0.03	± 0.000	0.25	± 0.03
n3	0.69	± 0.01	0.68	± 0.01	0.01	± 0.000	0.08	± 0.01
n2	0.65	± 0.01	0.65	± 0.01	0	± 0.000	0.00	± 0.00
n1	0.54	± 0.01	0.53	± 0.01	0.01	± 0.000	0.08	± 0.01
Min	0.54		0.53		-0.05		-0.40	
Max	2.56		2.40		0.18		1.50	
Mean	1.20		1.19		0.02		0.15	
StdD	0.55		0.54		0.04		0.37	

APPENDIX 5: NOMINAL COUNTS OF FORAMINIFERAL SPECIES

Sample	*Hyperammina* aff. *elongata*	*Bathysiphon* sp.	*Rhizammina* sp.	*Thurammina* aff.*papillata*	*Saccammina* sp.	*Psammosphaera* aff. *fusca*	*Ammodiscus tenuissimus*	*Ammobaculitis* sp.1	*Ammobaculitis* sp.2	*Crithionina* sp.	*Ammotium* sp.	*Reophax* aff. *fusiformis*	*Haplophragmoides richardsensis*	*Haplophragmoides multicubiculus*	*Haplophragmoides* sp.	*Haplophragmoides perexilis*	*Labrospira turbida*	*Labrospira turpicula*	*Labrospira* sp.1	*Reticulophragmium ministicoogense*	*Reticulophragmium arcticum*	*Reticulophragmium borealis*	*Cyclammina cyclops*	*Verneuilinoides exvadum*	*Verneuilinoides durus*	*Verneuilinoides distentus*	*Convallina elongata*	*Convallina* aff.*logani*	*Trochammina mellariolum*	*Trochammina perlevis*	*Textulariina genus indet*	SUM without *Textulariina genus indet*	total SUM
n21	4			3		2	6	2	2	38							19		1				1	7	9		11		30	48	17	183	200
n19			1	1		3				1						14	43				12	10		17	37		1		41	19	14	200	214
n17						11				23											6	49		11					72	40	4	212	216
n14			4					4		14	5						92				7	41		13	9				31	8	1	228	229
n12		1	1							3							42		2		4	86		9	7				23	23	8	201	209
n11		1	1							2			5						15	16		13	12	66	12			4	20	25	8	192	200
n10	1					1				3		1							18	31			16	69	33			3	11	6	10	193	203
n8			8			8	2							13	4				7					78	15	62	9		23	9	9	238	247
n6			1	3	1	15						2		17			9	5				2		52	40				33	2	20	182	202

APPENDIX 6: PERCENTAGES OF FORAMINIFERAL SPECIES

Sample	*Hyperammina* aff. *elongata*	*Bathysiphon* sp.	*Rhizammina* sp.	*Thurammina* aff.*papillata*	*Saccammina* sp.	*Psammosphaera* aff. *fusca*	*Ammodiscus tenuissimus*	*Ammobaculitis* sp.1	*Ammobaculitis* sp.2	*Crithionina* sp.	*Ammotium* sp.	*Reophax* aff. *fusiformis*	*Haplophragmoides richardsensis*	*Haplophragmoides multicubiculus*	*Haplophragmoides* sp.	*Haplophragmoides perexilis*	*Labrospira turbida*	*Labrospira turpicula*	*Labrospira* sp.1	*Reticulophragmium ministicoogense*	*Reticulophragmium arciticum*	*Reticulophragmium borealis*	*Cyclammina cyclops*	*Verneuilinoides exvadum*	*Verneuilinoides durus*	*Verneuilinoides distentus*	*Convallina elongata*	*Convallina* aff.*logani*	*Trochammina mellariolum*	*Trochammina perlevis*	*Textulariina genus indet*
n21	2.2			1.6		1.1	3.3	1.1	1.1	20.8							10.4		0.5				0.5	3.8	4.9		6.0		16.4	26.2	8.5
n19			0.5	0.5		1.5				0.5						7.0	21.5				6.0	5.0		8.5	18.5		0.5		20.5	9.5	6.5
n17						5.2				10.8											2.8	23.1		5.2					34.0	18.9	1.9
n14			1.8					1.8		6.1	2.2						40.4				3.1	18.0		5.7	3.9				13.6	3.5	0.4
n12		0.5	0.5							1.5							20.9		1.0		2.0	42.8		4.5	3.5				11.4	11.4	3.8
n11		0.5	0.5							1.0			2.6						7.8	8.3		6.8	6.3	34.4	6.3			2.1	10.4	13.0	4.0
n10	0.5					0.5				1.6		0.5							9.3	16.1			8.3	35.8	17.1			1.6	5.7	3.1	4.9
n8			3.4			3.4	0.8							5.5	1.7				2.9					32.8	6.3	26.1	3.8		9.7	3.8	3.6
n6			0.5	1.6	0.5	8.2						1.1		9.3			4.9	2.7				1.1		28.6	22.0				18.1	1.1	9.9

APPENDIX 7: ABUNDANCE, DOMINANCE AND DIVERSITY

Sample	Abundance (ind/g)	Dominance (%)	Diversity	
			alpha	H(S)
n21	4.14	26.2	4.21	2.14
n19	5.76	21.5	3.11	2.07
n17	4.41	34	1.39	1.67
n14	3.07	40.6	2.98	1.92
n12	3.76	42.8	2.50	1.68
n11	5.50	34.4	3.47	2.10
n10	16.28	35.8	2.83	1.87
n8	7.89	32.8	2.92	2.05
n6	5.28	28.6	3.20	1.95
Min	3.07	21.5	1.39	1.67
Max	16.28	42.8	4.21	2.14
Mean	6.23	33.0	2.96	1.94
StdD	4.02	6.7	0.76	0.17

APPENDIX 8: SIMILARITY INDEX VALUES BASED ON SPECIES OCCURRENCE

	n6	n8	n10	n11	n12	n14	n17	n19	n21
n6	-	0.550	0.535	0.480	0.270	0.309	0.307	0.548	0.339
n8	-	-	0.513	0.559	0.229	0.246	0.220	0.307	0.284
n10	-	-	-	0.744	0.193	0.200	0.161	0.354	0.212
n11	-	-	-	-	0.396	0.319	0.364	0.407	0.343
n12	-	-	-	-	-	0.658	0.540	0.578	0.426
n14	-	-	-	-	-	-	0.492	0.574	0.425
n17	-	-	-	-	-	-	-	0.450	0.510
n19	-	-	-	-	-	-	-	-	0.476
n21	-	-	-	-	-	-	-	-	-

APPENDIX 9: PERCENTAGES OF MORPHOGROUPS

Sample	Morpho-subgroup 1a	Morpho-subgroup 2a	Morpho-subgroup 2b	Morpho-subgroup 3a	Morpho-subgroup 3b	Morpho-subgroup 4a
n21	2.2	23.5	42.6	11.5	16.9	3.3
n19	0.5	2.5	30.0	39.5	27.5	0
n17	0	16.0	52.8	25.9	5.2	0
n14	1.8	6.1	17.1	61.4	13.6	0
n12	1.0	1.5	22.9	66.7	8.0	0
n11	1.0	1.0	23.4	31.8	42.7	0
n10	0.5	2.1	8.8	33.7	54.9	0
n8	3.4	3.4	13.4	10.1	68.9	0.8
n6	0.5	10.4	19.2	18.1	51.6	0

APPENDIX 10: SIMILARITY INDEX VALUES BASED ON MORPHOGROUP OCCURRENCE

	n6	n8	n10	n11	n12	n14	n17	n19	n21
n6	-	0.791	0.812	0.817	0.474	0.555	0.530	0.679	0.586
n8	-	-	0.764	0.683	0.340	0.422	0.321	0.540	0.469
n10	-	-	-	0.848	0.525	0.587	0.420	0.726	0.398
n11	-	-	-	-	0.647	0.646	0.556	0.843	0.539
n12	-	-	-	-	-	0.890	0.555	0.723	0.448
n14	-	-	-	-	-	-	0.544	0.732	0.501
n17	-	-	-	-	-	-	-	0.636	0.753
n19	-	-	-	-	-	-	-	-	0.614
n21	-	-	-	-	-	-	-	-	-

ACKNOWLEDGEMENTS

This master thesis has come into existence under kind supervision of Jenö Nagy and Henning Dypvik at the Department of Geosciences, University of Oslo (UiO).

I would especially like to thank Jenö Nagy who has always been friendly and extremely supportive. Henning Dypvik, presently on his sabbatical, has proven to be the fastest email answerer ever. Takk for at dere gjorde det så trivelig å skrive masteroppgaven!

I appreciated financial support by Worldwide University Networks (WUN) for the fieldwork in Svalbard associated with this master thesis, but most of all I am grateful for the great experience in academic as well as personal terms. Big thanks to Florin Burca for joint field logging and teamwork. Cheers also to Sigurd Nerhus for borrowing of and introduction to his GPS and for a real good time on Svalbard.

I benefited very much from the UNIS course "Sequence Stratigraphy –A Tool for Basin Analysis" in preparation for the field part of my thesis. With respect to the thesis writing, the Endnote course offered by the geology librarians has proven extremely helpful. Furthermore, the equipment for digital photography of the foraminifera has been kindly placed at my disposal by Elisabeth Alve who has also introduced me to its operation.

I enjoyed lunch and coffee breaks with Berenice, Micha, Martin, Ariel, and Egil. The latter were also helpful in gently forcing me to speak Norwegian.

Big thanks to my roomies Silvia Hess and Stefan Rothe who supported me in so many ways, but most of all were extremely enjoyable company! This might be the right occasion to apologize to everyone in our room and corridor for loud laughter, too.

I owe a lot of gratitude to Legolas who had to bear all my displeasure, never let me down, and will surely get a new S now. Last – far from least, thanks to my friends and family: schön, dass es euch gibt und dass ihr skype-sei-dank immer für mich da seid!